Birk F. Lillebo
Lars Fredrik H. Hansen
Markus Hatlo

Investigations of Copper Contamination in Lithium-Ion Batteries Using Non-intrusive Analytical Methods

Bachelor's thesis

◼ NTNU
Norwegian University of
Science and Technology

Birk F. Lillebo
Lars Fredrik H. Hansen
Markus Hatlo

Investigations of Copper Contamination in Lithium-Ion Batteries Using Non-intrusive Analytical Methods

NTNU
Norwegian University of
Science and Technology

NTNU | Faculty of Engineering
Department of Energy
and Process Engineering

Bachelor's Thesis

Report title:	Report title Norwegian:
Investigations of copper contamination in lithium-ion batteries using non-intrusive analytical methods	Undersøkelse av kobber forurensing i litiumionbatterier ved bruk av ikke-inngripende analyse metoder
Given date: 19.12.23 **Submission deadline:** 22.05.24	**Number of pages report / pages attached:** 69 / 21
Project participants: Birk F. Lillebo birk.lillebo@ntnu.no Lars Fredrik H. Hansen lfhansen@ntnu.no Markus Hatlo markhat@ntnu.no	**Internal supervisors:** Odne Stokke Burheim Professor, NTNU odne.s.burheim@ntnu.no Ejikeme Raphael Ezeigwe Postdoctoral Fellow ejikeme.r.ezeigwe@ntnu.no
Field of study: Renewable Energy Engineering	**Project number:** BIFOREN24-08
External company contact: FREYR	**External supervisor:** Daniel Tevik Rogstad Senior Engineer – Cell Design

Freely available: ☑

Available by agreement with the external partner: ☐

The thesis released after: dd/mm/yyyy

Deep šnyt

Preface

This bachelor's thesis is a collaborative project made by three Renewable Energy Engineering students at The Norwegian University of Science and Technology, Trondheim. The bachelor's program is under the department of Energy and Process Engineering, and the report serves as the final thesis in the subject FENT2900 - Bacheloroppgave Fornybar Energi, Spring 2024.

The thesis aims to provide a method to effectively detect metal contamination in batteries at an early stage. The thesis centres on an analytical approach to the voltage data during the first battery cycles. To achieve this, the participants made coin cells from commercially available electrode sheets in the lab at the Department of Energy and Process Engineering. The thesis also explores how battery technology and early contamination detection plays a role in economical saving, demand, and environmental concerns.

The participants have appreciated the work put into this thesis. The project has given a more profound understanding of battery technology. Thereby, its potential role in the future and its limitations. The project was limited to the spring semester. This gave the participants invaluable experience and knowledge, but also proved frustrating and difficult. Throughout the semester, the participants struggled to produce working batteries. As the submission deadline approached, the group had to make several adjustments to their problem definition. Fortunately, the group's co-supervisor was able to make some working batteries, which therefore serves as the data foundation of this thesis.
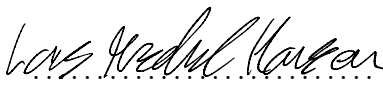
The participants continued to make attempts at battery production and error investigations while analysing the donated batteries. In the final two weeks, the participants discovered that components of their allocated electrolyte had evaporated, rendered the wettability ineffective. The participants were then able to make working batteries when handed another electrolyte with known effectiveness, but the discovery was too late for the data to be included in the final thesis.

Keywords: Lithium-ion batteries, contamination, DVA, ICA

Trondheim, 21.05.2023

Birk Ferdinand Lillebo   Lars Fredrik H. Hansen   Markus Hatlo

Acknowledgements

Abstract

This bachelor's thesis addresses the detection of contamination in lithium-ion batteries during the first cycles. The main goal of this thesis is to discover if analysis methods like differential voltage analysis (DVA) or incremental capacity analysis (ICA) might indicate contamination. For this, both contaminated and non-contaminated NMC111 cells with lithium anodes were created and cycled. The voltage curve of the cells during the cycling was then analysed using DVA and ICA. Due to issues with the electrolyte during the production of cells, the number of results is limited.

The non-contaminated NMC111 cells worked as expected. The lithium anode resulted in stable cells that could be used as a reference for the contaminated cells. The first batch of contaminated cells did not cycle properly and had an erratic voltage curve. The cells were contaminated with 0.4 mg of copper between the separator and the cathode. The hypothesis was that the cells would react away the copper before continuing the charging, resulting in a small stagnation. An issue with the measuring of small amounts of copper limited the amount of research that could be done.

The contaminated cells showed a similar stagnation in voltage at about 3.6 V. After the stagnation, all the cells experienced a voltage drop before turning erratic. A second batch of contaminated cells was created using less contamination. These cells followed the same behaviours, and exemplified the same stagnation as the first contaminated batch. This behaviour is theorised to stem from the creation of metal dendrites on the anode side. These dendrites puncture the separator, causing an internal short circuit. The short circuit causes high-currents, melting the dendrites. This cycle causes continuous fluctuation in the voltage, making the cells unusable.

To analyse the voltage data, a new analysis tool was created. The tool is a plot combining the voltage capacity relation, DVA, an ICA and the reversible potential of possible metal redox reactions. This combination figure allows for easy cross-examination between different kinds of analysis, which makes it easier to discern connections. The plot was not utilized much, due to the lack of working contaminated cells.

Further studies should explore the potential of the combination figure. A larger sample size needs to be made, and different electrode chemistries should be tested. In addition, different C-rates and cycling procedures should be tested. Finally, a new way to introduce an accurate amount of copper must be devised.

Abstract in Norwegian (Sammendrag)

Denne bacheloroppgaven tar for seg oppdagelse av kontaminasjon i litiumionbatterier under de første syklusene. Hovedmålet med oppgaven er å finne ut om analysemetoder som differensiell spenningsanalyse (DVA) eller inkrementell kapasitetsanalyse (ICA) kan indikere kontaminasjon. For dette ble både kontaminerte og ikke-kontaminerte NMC111-celler med litiumanoder laget og testet. Spenningskurven til cellene ble deretter analysert ved hjelp av DVA og ICA. På grunn av problemer med elektrolytten under produksjonen av cellene, er antallet resultater begrenset.

De ikke-kontaminerte NMC111-cellene fungerte som forventet. Litiumanoden resulterte i stabile celler som kunne brukes som referanse for de kontaminerte cellene. Den første runden med kontaminerte celler fungerte ikke som forventet og hadde en ujevn spenningskurve. Cellene var kontaminert med 0,4 mg kobber mellom separatoren og katoden. Hypotesen var at cellene ville reagere bort kobberet før de fortsatte oppladingen, noe som bør resultere i en liten stagnasjon. Vanskeligheter med målingen av små mengder kobber begrenset mengden forskning som kunne utføres.

De kontaminerte cellene viste en lik stagnasjon i spenning ved cirka 3,6 V. Etter stagnasjonen hadde alle cellene et spenningsfall før de ble ujevne. Den andre runden med kontaminerte celler ble laget med mindre kontaminasjon. Disse cellene fulgte samme oppførsel og eksemplifiserte samme stagnasjon som den første kontaminerte runden. Denne oppførselen antas å stamme fra dannelsen av metalldendritter på anodesiden. Disse dendrittene bryter seg gjennom separatoren, noe som forårsaker en intern kortslutning. Kortslutningen fører til høye strømmer som smelter dendrittene. Denne syklusen forårsaker kontinuerlig svingning i spenningen, noe som gjør cellene ubrukelige.

For å analysere spenningsdataene ble det laget et nytt analyseverktøy. Verktøyet er en figur som kombinerer spenningskapasitetsforhold, DVA, en ICA og det reversible potensialet for mulige metallredoksreaksjoner. Denne kombinasjonsfiguren tillater enkel undersøkelse mellom forskjellige typer analyser, noe som gjør det lettere å se sammenhenger. Figuren ble ikke brukt mye, på grunn av manglende fungerende kontaminerte celler.

Videre studier bør utforske potensialet til kombinasjonsfiguren. En større utvalgsstørrelse må lages, og forskjellige elektrodesammensetninger bør testes. I tillegg bør forskjellige C-rater og testprosedyrer testes. Til slutt må en ny måte å introdusere en nøyaktig mengde kobber i cellen utvikles.

Contents

Abbreviations

CO_2e Carbon Dioxide equivalent.

BEP Break Even Point.

DoD Depth of Depletion.

DVA Differential Voltage Analysis.

EC/EMC Ethylene Carbonate/Ethyl Methyl Carbonate.

EV Electric vehicle.

GHG Greenhouse Gas.

ICA Incremental Capacity Analysis.

ICE Internal Combustion Engine.

ISC Internal Short Circuit.

LAM Loss of Active Material.

LCO Lithium Cobolt Oxide.

LFP Lithium Iron Phosphate.

LIB Lithium-Ion Battery.

LLI Loss of Lithium Inventory.

NMC Lithium Nickel Manganese Cobalt Oxides.

NMP N-Methyl-2-pyrrolidone.

OCV Open Circuit Voltage.

SEI Solid Electrolyte Interface.

SoC State of Charge.

SoH State of Health.

List of Tables

List of Figures

1 Introduction

Lithium is the most energy dense metal and is ideal for energy storage due to its light weight and high electrochemical potential. Because of these qualities, the global demand for lithium-ion batteries is at an all-time high. Further, it is expected to grow exponentially in the following years. To handle this level of growth, several companies have started the construction of factories which produce GWh of battery capacity annually, so-called "giga"-factories. [1]

The forecasted growth in capacity demand co-accelerate the growth of waste and mining related emissions. Today, about 5% of all batteries produced are discarded after ageing. Research into more efficient methods to detect faulty batteries is therefore a topic of interest for manufacturers. Lithium-Ion Battery (LIB)s are commonly used in household appliances, phones, and laptops, but also at an increasing rate in vehicles. [2, 3, 4]

The United Nations has developed 17 goals for sustainable development, where the 5 most relevant are pointed out in Figure 1.1. Battery technology can play a major role in reaching these goals. Collaborations between governments and industry aim to safeguard human rights, support the energy transition, and facilitate economic growth. The technology aims to be a game changer and provide the 850 million people, which as of 2017 live without access to electricity, new possibilities. LIBs can help reduce emissions in the form of Electric vehicle (EV)s. Battery packs can also help smooth out the power output of intermittent power sources like solar or wind power. [5, 6]

Figure 1.1: *Relevant United Nations sustainability goals for the subject of the thesis. [6]*

The Paris Agreement has a goal to limit the increase in the average world temperature to 2℃, but ideally no more than 1.5℃. The world is currently not set to reach these goals, and a change in trajectory is vital to avoid disastrous consequences. In 2017, about 40% of the total Greenhouse Gas (GHG) emissions came from the transport and power sector. One of the solutions is to decarbonize these sectors through lithium-ion batteries. [1]

1.1   Economic impact

Today's battery production is a result of skyrocketing demand since 2010. The possibility of clean and renewable energy drove the motivation for the production of EVs and LIB energy storage. Between 2010 and 2018 the battery demand grew 30% annually. This resulted in a demand of 180 GWh in 2018, over 8 times more than in 2010. In 2020, the global battery demand was estimated at 282 GWh, with China having the highest demand of 142 GWh. This equals 50% of the total battery demand. To keep up with the rising demand for batteries, gigafactories with the means to annually produce gigawatt hours of battery capacity are being built. The current biggest EV producer, Tesla, has built five gigafactories with plans to expand the capacity of these factories to over 100 GWh per year. Teslas gigafactory in Nevada produces 37 GWh of their *4680* type of cell annually. The *4680* cells are cylindrical cells with a 44 mm diameter, 80 mm height, and an estimated capacity of 100 Wh. A production of 37 GWh is equivalent to 370 million *4680* cells a year, or about a million a day. One of the biggest issues with gigafactories is the area needed to create them. The Nevada gigafactory has a size of 500 000 m^2. [1, 6, 7, 8, 9]

Battery demand is still expected to grow exponentially. In 2019, the World Economic Forum and the Global Battery Alliance released a report, "A vision for a sustainable battery value chain in 2030", where they predicted the future economic and environmental impact of LIB production. This report estimated the market to continue to grow at 25% annually, resulting in a demand of 2.5 TWh/year by 2030. This is 14 times the total LIB demand in 2018 and is equivalent to 26 billion *4680* cells a year, or 71 million cells a day. The report estimated that this demand growth would bring large economic and societal benefits. The market for battery production will multiply by 15 from 2018 to 2030. The demand growth would provide revenue opportunities of up to $300 billion. The market would create 10 million jobs and provide 600 million people access to electricity. Further, the creation of electricity grids for off-grid communities would contribute to solutions for other issues like hunger, health, and sanitation. [1]
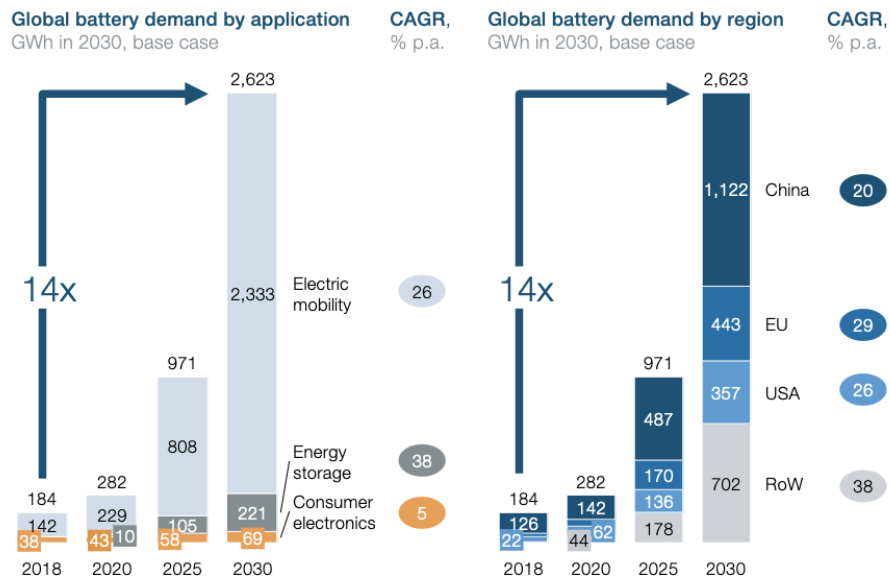
Figure 1.2: *Estimated global battery demand 2018-2030.* [1]

One of the biggest difficulties of battery production is the storage space needed during formation and ageing. As mentioned earlier, Tesla's gigafactory in Nevada produces over 1 million cells a day. This means that the factory needs the storage space for 14-21 million cells for an ageing time of 2–3 weeks. In the USA, the floor space is estimated at \$3,000/m^2 per year. This means that the gigafactory in Nevada, with a size of 500,000 m^2, costs \$1.5 billion per year. [1, 7]

Argonne National Library created a model for calculating the cost of the different manufacturing processes, known as the BatPac model. Table 1.1 and Figure 1.3 shows the BatPac model for a factory producing 100,000 EV battery packs per year. As presented, the formation/ageing process takes 33% of the total manufacturing cost. Together with coating and drying, these processes take up 48% of total cost. In turn, these are the areas most needing study and research. [10]
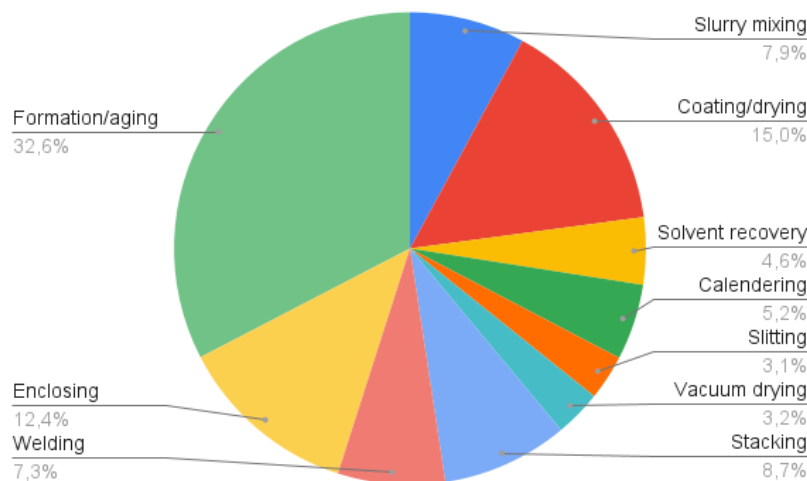
Figure 1.3: *Cost of LIB manufacturing processes, visualized in percentages. Numbers are taken from Table 1.1*

Formation and ageing take up almost the entire throughput of the process, as seen in Table 1.1. The throughput is closely related to the process cost. As ageing leaves the cell resting for 1.5 - 3 weeks, the process itself is not costly, but the energy and storage is. An acceleration of this process could save millions of monies in cost and would be welcomed by the industry.

Table 1.1: *Cost and throughput for a LIB manufacturing process, model based on 67 Ah NMC622/AG cell, 6,320,000 cells/year or 100,000 EV battery packs/year. [10] Inspired by [5]*

Manufacturing process	Cost [$/year]	Cost [%]	Throughput	Space [m^2]
Slurry mixing	7,396,000	7.91%	30 min - 5 h	1,200
Coating/drying	13,984,000	14.96%	35 - 80 m/min	1,500
Solvent recovery	4,296,000	4.60%	NA	225
Calendering	4,849,000	5.19%	60 - 100 m/min	225
Slitting	2,891,000	3.09%	80 - 150 m/min	300
Vacuum drying	2,990,000	3.20%	12 - 30 h	300
Stacking	8,086,000	8.65%	NA	600
Welding	6,864,000	7.34%	NA	600
Enclosing	11,636,000	12.45%	Design dependent	600
Formation/ageing	30,482,750	32.61%	1.5 - 3 weeks	3,550
Total process	93,447,750	100%	1.5 - 3 weeks	15,425

*Floor space cost is based on $3,000 /m^2 per year, and labour cost at $15 /h. [5, 10]

*The manufacturing cost includes equipment, labour, and plant floor cost.

1.2   Environmental impact

Batteries are considered the future for a low-carbon solutions. Electrifying transport, and smoothing an electrical grid based upon intermittent renewable energy. In the last decade, significant progress in LIBs has made it a reliable technology. An exponential increase in battery density, has resulted in 82% of new car sales in Norway are electric. This rapid technological shift promises a greener future, but still has challenges in meeting the predicted demand. [1, 11]

By using cars as an example, the average petrol car has lower production emissions, but a higher lifetime emission output. Breaking down each of these cycles is necessary to show how these vehicles compare. Figure 1.4 shows a breakdown of both electric and Internal Combustion Engine (ICE) vehicles. It establishes that 40-60% of the total EV emissions come from the battery. As the battery stands for such a large part of the production emissions, the total Carbon Dioxide equivalent (CO_2e) for an EV is nearly double that of an ICE vehicle, depending on its size. [2]

Typical upstream battery-electric-vehicle emissions,[1] %

Electric vehicle

40–60	~10
15–20	10–20	~5

ICE[3] vehicle

25–35	20–30
20–25	15–20

- ■ Battery
- ■ Steel
- ■ Aluminum
- ■ Plastics
- ■ Other[2]
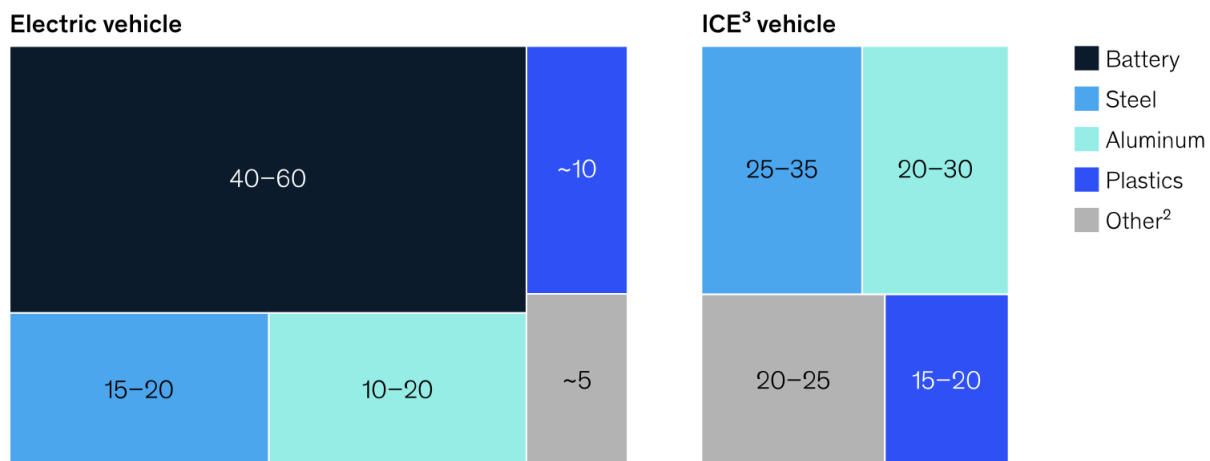
[1]Including all upstream emissions from raw material extraction to the OEM, including logistics.
[2]Including glass, copper, electronics, textiles, and logistics.
[3]Internal-combustion engine.
Source: McKinsey analysis

Figure 1.4: *Percentage of emissions connected to EV and ICE vehicle production.* *[2]*

Researchers still believe LIBs are the key to a sustainable future where GHG emissions are limited. A comparison made by Reuters in 2021, presented in table 1.2, compares a petrol driven mid-size saloon and a mid-size SUV to equal sized Tesla models. This comparison shows that on 100% hydroelectric energy, the Break Even Point (BEP) for each comparison is about 13,500 km for a mid-size saloon and 14,800 km for a mid-size SUV. This range is about equivalent to the average annual driving distance for passengers cars in Norway, which in 2016 was 12,390 km. Statistics indicate that all passenger cars in Norway on average drive between 15,000 and 12,000 km annually from their first, to 14th year. [12, 13]

Table 1.2: *Table showing a mid-sized saloon and a mid-size SUV compared to a Tesla EV equivalent, and when each in 3 scenarios reach their BEP in GHG emissions. [12] *23% coal-fired, plus other fossil fuels and renewables.*

Power scenario	Tesla 3 vs. Toyota Corolla	Tesla Y vs. Honda CR-V
100% hydroelectric	13,500 km	14,800 km
U.S. energy mix*	21,700 km	23,800 km
100% coal-fired	126,700 km	143,200 km

These statistics give life to LIBs both in the automotive industry, and in the energy market. The World Economic Forum highlighted LIBs as a key technology to achieve goals connected to both the Paris Agreement and the United Nations Sustainable Development Goals. Numbers from 2017 report that the annual global GHG emission is 50 $GtCO_2e$. About 40% of this is connected to power and transport. Road transport alone accounts for 5.8 $GtCO_2e$, where 4 $GtCO_2e$ stands for passenger road transport. EVs currently generate 30-60% less emission compared to ICE vehicles, depending on the power mix. A by-product of such a change is the improvement of local air quality, avoiding the release of toxic emissions such as nitrogen oxide or particulate matter. Decarbonizing energy and transport can provide access to clean city air and energy. This can also provide access to basic modern energy infrastructure for 850 million people, which today live without access to electricity. These features greatly improve health, standards of living, and productivity. [1]

Lithium can be found in brines and hard rocks. For rocks, lithium is found in pegmatites, which is a complex aluminium silicate deposit. The most important pegmatite in economic terms is spodumene, containing 8% Li_2O. This is considered a high lithium content, and the rock is found in relative abundance. On the other hand, there are brines found in underground reservoirs. Extracting lithium from brine is a straightforward process. This makes it stand for the majority of the world lithium extraction. The salt-rich brine is pumped to the surface and spread to evaporate over several months. Over this period, the concentration of lithium is increasing. The brine is then purified, removing contaminants and undesired elements. Other by-products are filtered out, and lithium carbonate is extracted. It is then washed and dried into the final product. [14, 4]

In 2021, 74% of the about 106 tonnes of lithium produced was exclusively used in batteries. LIBs are mineral intensive and depend on other rare minerals such as nickel, manganese, cobalt, and graphite. Several of these are notorious for bad working conditions. In terms of emissions, the main sources are: mining, active-material production, logistics, and cell production. Especially rock mining operations emit substantial emissions. However, this can be reduced heavily by utilizing renewable energy. An example of this can be observed in the difference between China's and Sweden's emission value chain. Sweden achieves a 45 CO_2e/kWh, while China falls short with 108 CO_2e/kWh. This feat stems from the use of renewable energy and mineral sourcing. In Figure 1.5, a map of major mining locations for each mineral is shown. [2, 3, 4]
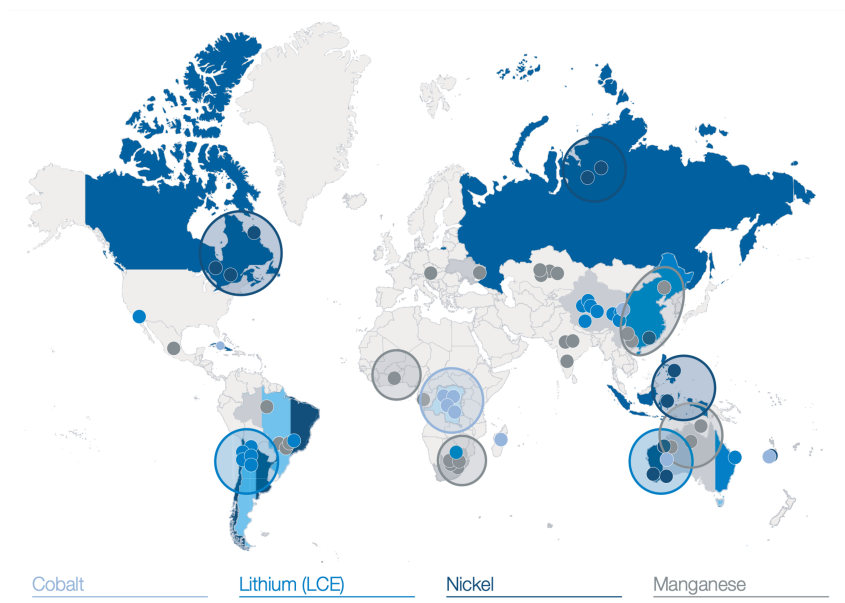
Figure 1.5: *Major mining locations for Cobalt, Lithium, Nickel, and Manganese.* [1]

To improve production line emissions, studies suggest that recycling LIBs can save up to 51% of the resources used in production. This number includes the reduction of fossil fuels in the extraction and production processes.This can be done by recycling materials such as cobalt, lithium, nickel, and manganese. To achieve this reduction, early detection could prove essential to prevent economic losses and environmental harm. [2, 3, 4]

1.3 Outline and problem formulation

This thesis focuses on non-intrusive analytical methods to bring forth new models for detecting defective batteries. These methods could be used to identify contamination in a timely and effective way. Such research gains relevance, especially as the demand for LIBs grows and the need for economic efficiency is paramount. Being able to identify faulty cells at an early stage insures that companies are more efficient. This frees up storage space and production capacity for good cells. The application of such research is relevant for all battery manufacturers and can have immense effects on storage and energy. A less energy intense production, in combination with a recycling system for important materials, can thus heavily reduce GHG emissions.

The work presented in this thesis is done by experimentally analysing lithium-ion cells with a constant charging rate, with special focus on the first cycles. Data is compared to see if similar patterns can be detected for contaminated batteries. To analyse the data, analytical methods including Incremental Capacity Analysis (ICA) and Differential Voltage Analysis (DVA) are utilized. In addition, cell voltage compared with reversible potentials for possible contaminants are considered in the attempt to make contamination estimations.

2   Theory

This section will focus on the underlying theory relevant for this thesis. Important aspects such as battery production, lithium-ion battery chemistry, contamination in batteries and different analysis methods will be explained. This theory will be the basis for the investigation of contamination detection in lithium-ion batteries.

2.1   Primary vs. Secondary Batteries

A battery is a container that stores chemical energy and can convert it to electrical energy. Batteries work by utilizing redox reactions by separating the reactants and thereby redirecting the electrons, generating a current. [15]

Batteries can be divided into two categories, primary and secondary. The difference between primary and secondary batteries is that primary batteries can only be discharged once. Secondary batteries are rechargeable and can be used multiple times. Common primary batteries are alkaline batteries, for example AA and AAA batteries used in households. Alkaline batteries often use potassium hydroxide as an electrolyte. Potassium hydroxide is a basic solution with a pH over 7, resulting in the name alkaline. A common alkaline battery chemistry is Zinc — Manganese dioxide. Table 2.1 shows the half cell and total reaction for a Zinc — Manganese dioxide battery. [15, 16]

Table 2.1: *The half cell reactions and total reaction for an alkaline primary battery.* [16]

Electrode	Discharge reaction
Anode:	$Zn_{(s)} + 2OH^- \rightarrow ZnO_{(s)} + H_2O_{(l)} + 2e^-$
Cathode:	$2MnO_{2,(s)} + 2H_2O_{(l)} + 2e^- \rightarrow 2MnO(OH)_{(s)} + 2OH^-$
Total:	$Zn_{(s)} + 2MnO_{2,(s)} \leftrightarrow ZnO_{(s)} + Mn_2O_{3,(s)}$

Common examples of secondary batteries are lead acid batteries and lithium-ion batteries. Lead acid batteries are commonly found in petrol cars and consist of lead and lead dioxide plates submersed in sulphuric acid. Table 2.2 shows the half cell and total reaction for a Lead acid battery. [15, 17]

Table 2.2: *The half cell reactions and total reaction for a lead acid secondary battery. [15]*

Electrode	Discharge reaction
Anode:	$Pb_{(s)} + H_2SO_4 \rightleftharpoons PbSO_{4,(s)} + 2H^+ + 2e^-$
Cathode:	$PbO_{2,(s)} + H_2SO_4 + 2H^+ + 2e^- \rightleftharpoons PbSO_{4,(s)} + 2H_2O_{(l)}$
Total:	$Pb_{(s)} + PbO_{2,(s)} + 2H_2SO_4 \rightleftharpoons 2PbSO_{4,(s)} + 2H_2O_{(l)}$

The reason secondary batteries can be recharged, is because the redox reaction occurring is reversible. The chemistry and thermodynamics that determine this will be explained in chapter 2.3. Primary batteries utilize reactions that can't be reversed easily, and that would take extra steps to reverse. In contrast, secondary batteries use redox reactions that can be reversed by applying a sufficient current. [15, 17]

2.2 Battery Terminology

To have a more meaningful discussion of batteries and to decrease confusion, the meaning of certain terms should be defined. Firstly, when describing battery capacity and charging, the term State of Charge (SoC) is used. SoC describes how much of the total capacity the battery is charged to, given as a percentage. For example, if a battery has a total capacity of 4 mAh, and it is charged to 2 mAh, the SoC is 50%. Other times, it is more relevant to describe how much of a battery has been discharged. Here, Depth of Depletion (DoD) is used. DoD is related to SoC as shown in Equation 2.1. DoD can also be in referance to how much of the battery's capacity that is usually in use. [15, 18]

$$SoC = 100\% - DoD \tag{2.1}$$

The charging rate of a battery is often described using C-rates. C-rate is presented in equation 2.2. The C-rate is defined as the change in SoC divided by the time it takes for the change to happen, in hours. A charge from 0% to 100% in half an hour would require a charge with a C-rate of 2C. A definition of C-rate is presented in Equation 2.2. [15]

$$C_{rate} = \frac{\Delta SoC}{t} = \frac{SoC_{max} - SoC_{min}}{t} \tag{2.2}$$

The maximum capacity of a battery will degrade over time, both due to calendar ageing and cycle ageing. To describe the degradation of a battery, State of Health (SoH) is used. SoH is defined as the present maximum capacity divided by the original maximum capacity, as presented in Equation 2.3. [15]

$$SoH = \frac{Q_{max,present}}{Q_{max,original}} \tag{2.3}$$

Finally, it is important to clarify what is meant when by the terms anode and cathode. It is usually taught that the oxidation occurs at the anode and that the reduction occurs at the cathode. However, this becomes a problem with secondary batteries, since they both charge and discharge. This means that each electrode both reduces and oxidises. This would mean that the anode and cathode would switch place, when going from discharging to charging. It has therefore become custom to call the electrodes by how they react during discharge. The anode is the electrode that is oxidised during discharge and reduces during charging. Table 2.3 show an overview of this, in addition to which polarity the electrodes have. [15]

Table 2.3: *Charge and discharge cycle electrode polarity. Inspired by [19].*

Half-cycle	Polarity	Electrode	Process
Discharge	-	Anode	Oxidation
	+	Cathode	Reduction
Charge	-	Cathode	Reduction
	+	Anode	Oxidation

2.3   Reversible potential

It is necessary to have an understanding of the terms energy and voltage when working with batteries. The energy of any system is defined as the sum of potential, kinetic and internal energy. The change of energy in a system is defined by the heat and work that is applied on, or performed by the system. When considering a battery, kinetic and potential energy is ignored. This is because it does not affect the chemical or electrical energy. Assuming an open and steady state system, the total change of energy in a battery is defined as the change of enthalpy (ΔH). Enthalpy in thermodynamics is the sum of the internal energy (U) and the product of pressure (P) and volume (V), as seen in equation 2.4. [15, 20]

$$H = U + P \cdot V \tag{2.4}$$

The change of enthalpy, and therefore the change of energy in a battery, can be expressed by subtracting the reversible heat (Q_{rev}) from the reversible work (W_{rev}). In chemistry, the enthalpy change is equal to the sum of the of Gibbs free energy change (ΔG), and the product of entropy change (ΔS) and temperature (T). The relation between enthalpy change and Gibbs free energy change is presented in Equation 2.5. [15, 20]

$$\Delta H = W_{rev} - Q_{rev} = \Delta G + T\Delta S \tag{2.5}$$

In chemistry, it is more interesting to look at the molar energy than the total energy. This is because the reactions happen per mol, and the molar Gibbs free energy is therefore more related to the reactions. In Equation 2.6 this is noted using lower case letters and a line above ($\bar{g}$). With molar Gibbs free energy, the reversible cell potential can be found as shown in Equation 2.6. [15, 20]

$$\Delta\bar{g} = \Delta\bar{h} - T\Delta\bar{s} = -zFE^{rev} \tag{2.6}$$

In Equation 2.6 molar Gibbs free energy is expressed as the product of the number of electrons transferring per reactant in the reaction (z), Faraday's constant (F) and the reversible cell potential (E^{rev}). Rewriting the equation by dividing the entire equation by -zF, gives an equation for the cell potential, shown in equation 2.7. [15, 20]

$$E^{rev} = -\frac{\Delta\bar{g}}{zF} \tag{2.7}$$

The Gibbs free energy is dependent upon the concentration ratio (Q), as seen in Equation 2.9. This is the only variable for the reversible potential, therefore, at standard conditions, Gibbs free energy has a constant value. Consequently, this results in constant half cell potentials, and allows for the creation of the Galvanic series. The galvanic series is a collection of half cell reaction potentials, calculated at standard conditions ($Q=K_{equilibrium}$). The Galvanic series uses the reduction of hydrogen ions into hydrogen gas as a reference potential. This collection of half cell potentials allows for simple calculations of the total cell potential in a reaction. This is done by subtracting the anode reduction potential from the cathode reduction potential, as presented in Equation 2.8. However, not all half cell reactions usually appear in the Galvanic series, as there are many reactions that occur infrequently. The Galvanic series usually includes the most common reactions. [15]

$$E^o_{cell} = E^o_{cathode} - E^o_{anode} \tag{2.8}$$

Until now, standard conditions for the reaction have been assumed. For real-world calculations, the impact of concentration and temperature needs to be accounted for. Equation 2.9 shows the relationship between the standard Gibbs free energy ($\bar{g}^o$), the gas constant ($\bar{R}$), temperature (T) and the natural logarithm of the concentration ratio between products and reactants (ln(Q)). [15]

$$\Delta\bar{g} = \Delta\bar{g}^o + \bar{R}Tln(Q) \tag{2.9}$$

$$\Delta\bar{g} = \Delta\bar{g}^o + \bar{R}Tln\left(\frac{[Product]}{[Reactant]}\right)$$

Substituting Gibbs free energy for the reversible potential using Equation 2.7 a new formula for cell potential is made. This equation is known as Nernst equation and is shown in Equation 2.10. Nernst equation is the most commonly used equation when calculating cell potential. Assuming standard room temperature (298K), leaves only z as a variable, since R and F are respectively the gas constant and Faraday's constant. Inserting the constant values into Equation 2.10 gives Equation 2.11. However, using the natural logarithm is unpractical. Multiplying the natural logarithm with 2.303 gives an approximation to the decimal logarithm, logarithm base 10, and gives Equation 2.12, which will be used further. [15]

$$E_{cell} = E^o - \frac{RT}{zF}ln(Q) \tag{2.10}$$

$$E_{cell} = E^o - \frac{0.0257}{z}ln(Q) \tag{2.11}$$

$$E_{cell} = E^o - \frac{0.0592}{z}log(Q) \tag{2.12}$$

Nernst equation is a good approximation for the reversible potential of the cell. However, Nernst equation does not account for losses in the cell. These losses are for example from ohmic resistances and concentration diffusion. The next chapter will discuss these losses. [15]

2.4   Potential losses

When the cell reaction begins, the cell is no longer in equilibrium, and this leads to irreversibilities and potential losses. Nernst equation gives an accurate chemical representation of the cell's potential. However, there are more physical factors to account for, namely ohmic resistances (rj), reaction overpotentials (η_r) and concentration overpotentials (η_c). These losses are represented in equation 2.13, first for charging then discharging. Resistances and overpotentials (η) represent energy lost during discharging and extra energy needed during charging. [15, 21]

$$E^{rev}_{charge} = E^{rev}_{spont.} + rj + \eta \tag{2.13}$$

$$E^{rev}_{discharge} = E^{rev}_{spont.} - rj - \eta$$

2.4.1   Ohmic resistance

When the cell is no longer in equilibrium, a current passes between the electrodes through the electrolyte. The potential loss from this current is called ohmic resistance losses (η_{ohmic}). Usually, this would be expressed using ohm's law. However, to make the formula more general it is advantages to represent the loss as the product of current density (j) and ohmic resistivity (r), as shown in Equation 2.14. [15]

$$U = RI \tag{2.14}$$

$$\eta_{ohmic} = rj$$

Current density is the current divided by the cross-sectional area (A_c), and ohmic resistivity is the ohmic resistance multiplied by the cross-sectional area of the cell. The ohmic resistivity can also be found as the product of the conductivity of the electrolyte (κ) and the distance between the two electrodes (δ), as shown in Equation 2.15. [15]

$$r = \frac{\delta}{\kappa} \tag{2.15}$$

The conductivity of the electrolyte, is a measure of how easily the electrons can travel through the electrolyte, and it is not constant. The conductivity of the electrolyte is dependent on the molar concentration ($\bar{c}$) and on its molar specific conductivity (Λ). This relation is shown in Equation 2.16. [15]

$$\kappa = \Lambda \bar{c} \tag{2.16}$$

There are two different ways to determine the molar specific conductivity. Firstly, there is the Debye-Hückel-Onsager relation presented in Equation 2.17. The molar specific conductivity is equal to the standard molar specific conductivity minus the product of the material constant (S) and the square root of the concentration (c). [15, 22]

$$\Lambda = \Lambda_0 - S\sqrt{c} \tag{2.17}$$

The second way to calculate the molar specific conductivity is the Vogel-Fulcher-Tammann equation presented in Equation 2.18. This equation is dependent on multiple material constants (A, E_a) and the temperature (T). [15, 23]

$$\kappa = \frac{A}{\sqrt{T}} exp\left(-\frac{E_a}{R}\frac{1}{T - T_0}\right) \tag{2.18}$$

2.4.2 Reaction overpotential

As mentioned earlier, when a reaction is not at equilibrium, there is a current in the battery. With this current, there is a loss called the reaction overpotential that is the product of the activation energy. The activation energy is the energy needed for a reaction to occur. The relation between reaction overpotential (η_r) and the current density is named the Butler-Volmer equation presented in Equation 2.19. [15, 24, 21]

$$j = j_0 \left(exp\left[\frac{(1-\alpha)zF}{\bar{R}T}\eta_r\right] - exp\left[-\frac{\alpha zF}{\bar{R}T}\eta_r\right]\right) \tag{2.19}$$

Using Equation 2.19 to find the reaction overpotential is challenging. This is because of the two exponential functions, requiring iteration to find the overpotential. However, inspecting the equation reveals that at high overpotentials the right half of the reaction becomes smaller. Most batteries have a high enough overpotential to make the right side negligible. Therefore, the equation can be simplified to Equation 2.20. Now the equation can be rewritten to be the overpotential as a function of current density. [15, 21]

$$j = j_0 exp\left[\frac{(1-\alpha)zF}{\bar{R}T}\eta_r\right] \tag{2.20}$$

$$\eta_r = \frac{\bar{R}T}{(1-\alpha)zF}ln\left(\frac{j}{j_0}\right)$$

$$\eta_r = -\frac{2.303\bar{R}T}{(1-\alpha)zF}log(j_0) + \frac{2.303\bar{R}T}{(1-\alpha)zF}log(j)$$

Finally, the equation can be written as Equation 2.21, which is called the Tafel equation. The Tafel equation is a linearisation of the Butler-Volmer equation, and a more practical equation for calculating the reaction over potential. An advantage with rewriting the constants as a and b, is that these values can be found in tables for known cells. [15, 21]

$$\eta_r = a + b \cdot log(j) \tag{2.21}$$

$$a = -\frac{\bar{R}T}{(1-\alpha)zF}log(j_0), \qquad b = \frac{\bar{R}T}{(1-\alpha)zF}$$

2.4.3   Concentration polarization overpotential

Lastly, there is the concentration polarization overpotential. This overpotential stems from the limits of diffusion. When a current is applied, the ions in the electrolyte have to move to the electrode to react. However, when the current density becomes high, not enough reactants reach the electrolyte and an overpotential is created. The amount of overpotential is given by Equation 2.22. [15]

$$\eta_c = \frac{\bar{R}T}{zF}\left|ln\frac{\bar{c}_{surf}}{\bar{c}_{bulk}}\right| \tag{2.22}$$

Equation 2.22 has two concentrations. The bulk concentration ($\bar{c}_{bulk}$) is the concentration that the majority of the electrolyte has. The second concentration is the surface concentration ($\bar{c}_{surf}$). When the reaction occurs, the substance at the surface of the electrode reacts, reducing the concentration on the surface. This difference produces the overpotential. [15]

2.5 Lithium-ion Battery Components

LIBs have the highest capacities of the secondary batteries. Furthermore, because of lithium's high negative reduction potential, they also have some of the highest cell potentials. LIBs work by transferring lithium ions and electrons between electrodes. When the battery is charging, the lithium ions move to the anode, and when it is discharging, the ions move to the cathode. Only about 55% of the lithium ions travel from the cathode to the anode. If more than 55% of the ions were transferred, it would cause structural degradation. This limit is known as the Inaccessible lithium problem. When the lithium ions move to the cathode and the ions are inserted into lithiated metal oxide or lithiated metal phosphate molecules. A simplification of this is shown in Figure 2.1. [15]
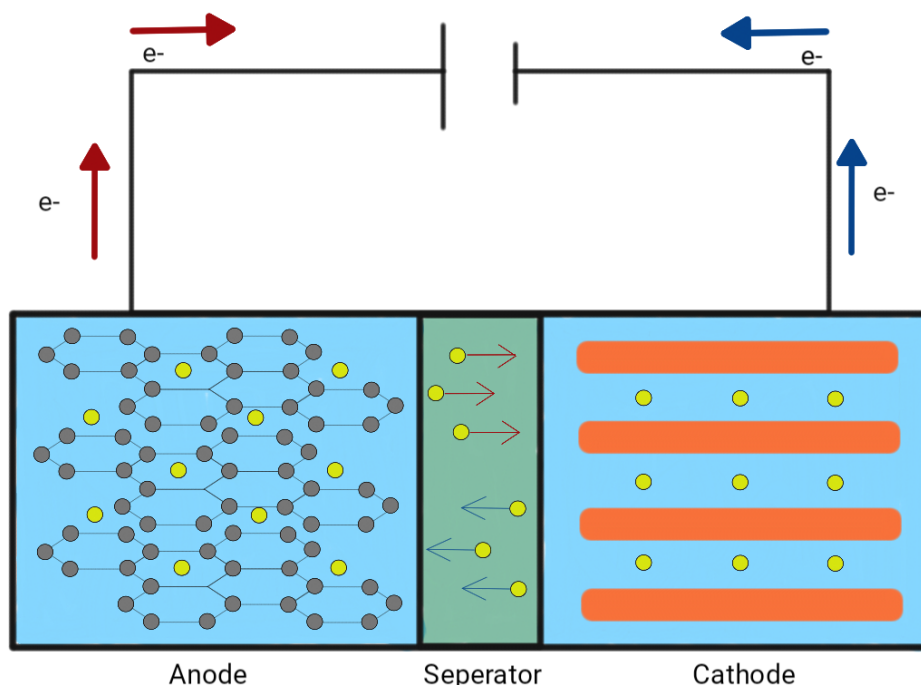
Figure 2.1: *A simplification of how a LIB charges and discharges. Figure made by author, inspired by [25, 26]*

The anode in a LIB usually uses a graphite based active material, which is attached to the copper current collector with a binder. A lithium metal anode is sometimes used in research as a reference electrode. This because of its stable and known potential, making it easier to distinguish the cathode potential. For the cathode, different lithium chemistries are used, typically with an aluminium current collector. The most used chemistries are Lithium Iron Phosphate (LFP), Lithium Cobolt Oxide (LCO) and Lithium Nickel Manganese Cobalt Oxides (NMC). In 2015, LCO, LFP, and NMC shared equal parts of the marked and comprised about 80% of batteries in use. [27]

The cathode material is built up by crystal structures, which form under production, when enough heat is applied. The structure is described by the smallest repeatable unit in the crystal. There are three main structures for lithium-ion batteries, Layered, Spinel and Olivine crystal structure. Layered crystal structure is made up of plates of cathode material stacked on top of each other in layers. Then the lithium ions can be placed between these layers. The Spinel structure is a bit more complicated. The structure is a form of repeating lattice structure, where the lithium ions can fit in the tunnels that are made. Lastly, there is the Olivine structure. In the book, Lithium-ion Battery Chemistry A Primer, the author explains the Olivine structure as follows " ...the olivine structure consists of hexagonal close packed array of oxygen atoms in half of the octagonal empty spaces with iron (Fe) and phosphorus (P) in a complex structure" [27]. In the Olivine structure, the lithium ions are inserted in between the molecules. All of these structures can be seen in Figure 2.2. To the left is the layered crystal structure, in the middle is the Spinel crystal structure and to the right is the Olivine crystal structure. [27, 28]

Layered crystal structure   Spinel crystal structure   Olivine crystal structure
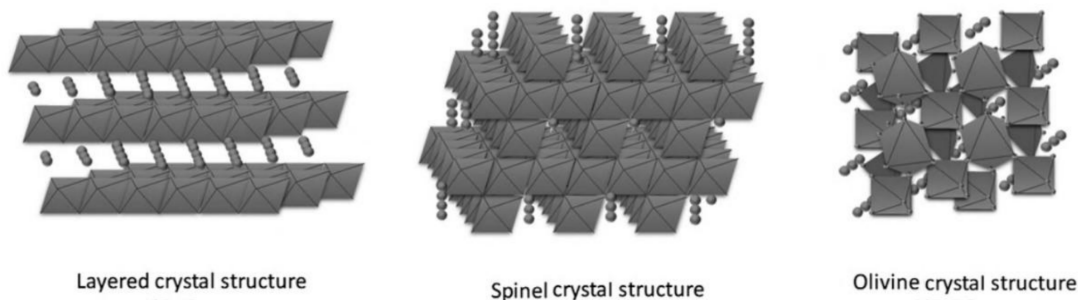
Figure 2.2: *Different crystal structures for lithium-ion cathode materials. From left to right: Layered, Spinel and Olivine crystal structure.[27]*

2.5.1   Cathode

The cathode material is usually how the battery is categorized. Meaning, if the battery uses an LFP cathode, it is called an LFP battery. As mentioned earlier, there is more diversity in the cathode materials. This section will describe the three most common, LCO, LFP and NMC.

Lithium cobalt oxide - LCO

Lithium cobalt oxide was the first commercially produced lithium-ion battery. It was developed in the 1980 by John Goodenough, and in 1991 Sony had commercialized LCO. Today it is mostly used in smaller applications like phones or computers. LCO forms a layered crystal structure, and its half cell and total reactions are given in Table 2.4. It is suited for smaller applications because of its high energy density and voltage, which is at about 3.8 V. One of the reason for its high voltage is its high ion conductivity. [27, 29]

Table 2.4: *The half cell reactions and total reaction for a LCO battery with graphite anode. [15]*

Electrode	Discharge reaction
Anode:	$Li_xC_{6,(s)} \rightleftharpoons xLi^+ + C_{6,(s)} + xe^-$
Cathode:	$Li_{1-x}CoO_{2,(s)} + xLi^+ + e^- \rightleftharpoons LiCoO_{2,(s)}$
Total:	$Li_{1-x}CoO_{2,(s)} + Li_xC_{6,(s)} \rightleftharpoons LiCoO_{2,(s)} + C_{6,(s)}$

LCO is rarely used for large applications because of the high cost of cobalt. Cobalt is an uncommon metal which is expensive to mine. In larger applications, the cobalt amounts make the battery cost inefficient. LCO also does not have a good life cycle compared to the other LIB cathodes. Meaning the battery has to be changed out more often. Additionally, it is not as safe as other batteries due to its thermal instability. At about 150℃ LCO can start to experience thermal runway and at 200℃ LCO reaches total thermal runaway. [27, 30]

Lithium iron phosphate - LFP

LFP is one of the most commonly used lithium cathode chemistries. It forms an Olivine crystal structure and its half cell reactions and total reaction is presented in Table 2.5. LFP is most commonly used in EVs. This is both because LFP is a low-cost chemistry and because it is one of the safest lithium cathode materials. These properties have made LFP the leading cathode material in the market. Many of these advantages stem from the use of iron. Firstly, the low cost of iron makes the production of LFP less expensive. Further, iron is non-toxic and is not harmful to the environment, making LFP more sustainable. [27]

There are two main reasons why LFP one of the safest cathode materials. Firstly, phosphate and oxygen have a strong bond together, meaning they are unlikely to react with other substances. The second reason is that LFP needs to reach about 350℃ to react destructively with the electrolyte, meaning it can be classified as highly thermally stable. In addition, LFP has smaller particle sizes than other lithium cathode materials. This allows for better lithium-ion transportation and therefore faster charge/discharge of the battery. [27, 30]

Table 2.5: *The half cell reactions and total reaction for an LFP battery with graphite anode. [28]*

Electrode	Discharge reaction
Anode:	$Li_xC_{6,(s)} \rightleftharpoons xLi^+ + C_{6,(s)} + xe^-$
Cathode:	$Li_{1-x}FePO_{4,(s)} + xLi^+ + xe^- \rightleftharpoons Li_1FePO_{4,(s)}$
Total:	$Li_xC_{6,(s)} + Li_{1-x}FePO_{4,(s)} \rightleftharpoons C_{6,(s)} + Li_1FePO_{4,(s)}$

Some negative aspects of the LFP is that it has a lower voltage than other lithium cathode materials, at around 3.3 V. This also results in a lower energy density of about 90-120 Wh/kg. To achieve the desired voltage or total energy, more cells of LFP usually have to be used. [27]

Nickel manganese cobalt - NMC

NMC is the last of the three most common cathode materials, and it is expected to be the most used cathode chemistry in the future. NMC forms a layered crystal structure and its half cell reactions and total reaction is presented in Table 2.6. NMC has a high voltage, resulting in a high energy density. NMC is also thermally stable, and has a long life span. Some batteries can endure up to 6000 full cycles, making it ideal for long-term usage. And NMC generally has a low cost, but this will be described more later. [27, 30]

Table 2.6: *The half cell reactions and total reaction for a NMC(y, z, 1-y-z) battery with graphite anode. Here, 1-y-z is between 0 and 1. [28]*

Electrode	Discharge reaction
Anode:	$Li_xC_{6,(s)} \rightleftharpoons xLi^+ + C_{6,(s)} + xe^-$
Cathode:	$Li_{1-x}(Ni_yMx_zCo_{1-y-z})O_{2,(s)} + xLi^+ + xe^- \rightleftharpoons Li_1(Ni_yMx_zCo_{1-y-z})O_{2,(s)}$
Total:	$Li_xC_{6,(s)} + Li_{1-x}(Ni_yMx_zCo_{1-y-z})O_{2,(s)} \rightleftharpoons C_{6,(s)} + Li_1(Ni_yMx_zCo_{1-y-z})O_{2,(s)}$

Unlike other cathode chemistries, NMC has different variants based on the ratios between its elements. This is because the different elements have different traits, and thus the ratios can be changed to adapt the battery to specific situations. A larger ratio of nickel gives a higher discharge capacity. However, this increases structural degradation, which in turn reduces the life span of the battery. A larger ratio of manganese gives better cycle life and more thermal stability. Conversely, this reduces capacity, and reduces energy density. Lastly, a larger ratio of cobalt result in better rate capability, resulting in a high power output. As described in the LFP section, cobalt is expensive. Cobalt also increases some safety risks in the cell. All of these traits are summarized in Table 2.7. [27, 28, 30]

Table 2.7: *The advantages and disadvantages of Nickel, Manganese, and Cobalt, when used in a NMC cathode.*

Element	Advantages	Disadvantages
Nickel	Higher discharge capacity	Increased structural degradation
Manganese	Better cycle life	Reduced capacity
	More thermal stability	Better energy density
Cobalt	Better rate capability	Expensive
	Higher power out put	Lower safety

Because of these different traits, many variations of NMC have been created. The first NMC batteries were called NMC111/NMC333 meaning that the there were equal parts of each element. All the parts have to add up to 1, to make the charge of the material equal to 1. According to the formula in Table 2.6, the chemical formula for NMC333 would be $LiNi_{0.3}Mo_{0.3}Co_{0.3}$. Today, it is more common to use NMC532. NMC622 and NMC811 are being researched and may become more used in the future. The common trend among these new variants is that the ratio of nickel goes up, while especially the ratio of cobalt goes down. This is mainly because of two reasons. The first reason is cost, as nickel is much cheaper than cobalt. Reducing the amount of cobalt thereby reduces the overall cost of the battery. Secondly, the increase in nickel improves the energy density of the battery. In contrast, manganese is cheaper than nickel, but does not improve the energy density. USA and China both have a goal of making batteries that have an energy density of 350 Wh/kg by 2030. As the biggest battery producers, increasing the energy density is an important aspect. As an example, NMC111 has a capacity of about 158 mAh/g. In contrast, NMC622 has a capacity of around 180 mAh/g. [1, 27, 30]

2.5.2 Separator and electrolyte

A separator is used between the electrodes to prevent a short circuit. The separator not only prevents a short circuit, but is a key component for ionic conductivity. To enable good ionic conductivity, a uniform and porous separator is used. Other key characteristics are a strong wettability, chemical stability, and low electric conductivity. Depending on the situation, qualities, and compositions vary. The most utilized separators are made of non-woven materials. However, fabricating non-woven layers thinner than 25 µm is difficult. Because of this, polymeric separators are also widely used. [4]

Commercial separators are made of microporous polyolefin membranes, such as polypropylene and polyethylene. In fluorinated polymers, PVDF and copolymers are used. Studies in the field of separators is heavily focusing on sustainability, especially separators made of eco-friendly materials. Natural polymers such as cellulose and silk are therefore being investigated. Other highly researched areas revolve around improving the previously mentioned characteristics. [4]

Electrolyte is essential for reactions to occur at the electrodes. The electrolyte should enable high ionic conductivity, wettability, and sustain a high electrochemical window. A good electrolyte typically also possesses a low viscosity and a high flash point. In addition, it ideally should be environmentally friendly, be easy to process and be cost-effective. There are multiple forms of electrolyte, both liquid and solid. Liquid electrolyte is the most common, while solid electrolyte is in its early stages, being researched for its high safety and mechanical stability. Liquid electrolytes are usually a lithium salt dissolved in carbonate solvents, such as ethylene carbonate / dimethyl carbonate (EC/DMC). Reactions of the electrolyte can facilitate the growth of an irregular SEI layer compared to an ideal formation. An irregular SEI layer decomposes the electrode. Therefore, other additives are being investigated to prevent this degradation. The SEI layer will be explained further in *Production of Lithium-ion batteries*. [4]

2.5.3 Anode

Since lithium-ion batteries were developed and commercialised in the 1980s, carbon-based anodes have been the standard. The most commonly used carbon-based anodes are artificial or natural graphite. In 2015, 93% of produced batteries used a graphite anode. Other anodes like lithium metal or silicon alloys can be used. These anodes have about 10 times the capacity of the graphite anode. However, these anodes are not common because of their drawbacks. For example, lithium is too reactive with oxygen, which creates safety issues. Even though these anodes have higher capacities, it does not impact the battery's total capacity. This is because the cathode is the limiting factor in determining the battery's capacity. A natural graphite anode has a capacity over 300 mAh/g. Compared to NMC622, which has a capacity of about 180 mAh/g. As a result, increasing the anode capacity does not improve the battery capacity. Therefore, graphite is often chosen for its other qualities. [27, 31]

Carbon Anodes

Carbon used in anodes can be divided into 4 categories: Natural/Artificial graphite, Porous/soft carbon, Graphene and Hard carbon. Graphite is commonly found and easy to produce, making it a low-cost material. Graphite forms a stable SEI layer in its first cycle, compared to other materials which require more cycles. A stable SEI layer leads to good intercalation and deintercalation of lithium-ions. As shown in Figure 2.3, graphite forms a crystal structure that is made of hexagons. Lithium-ions are inserted into these hexagons, between the layers. [27, 31]

Hard carbon is another less used anode material. It is a more structurally disordered version of graphite's structure. What differentiates hard carbon from graphite is its higher theoretical capacity and lower reversibility. This means that hard carbon in theory has a higher capacity, but looses this over time. In addition, the disordered structure results in a lower voltage of about 4.1 V. This makes graphite more suitable as an anode. [27, 31]
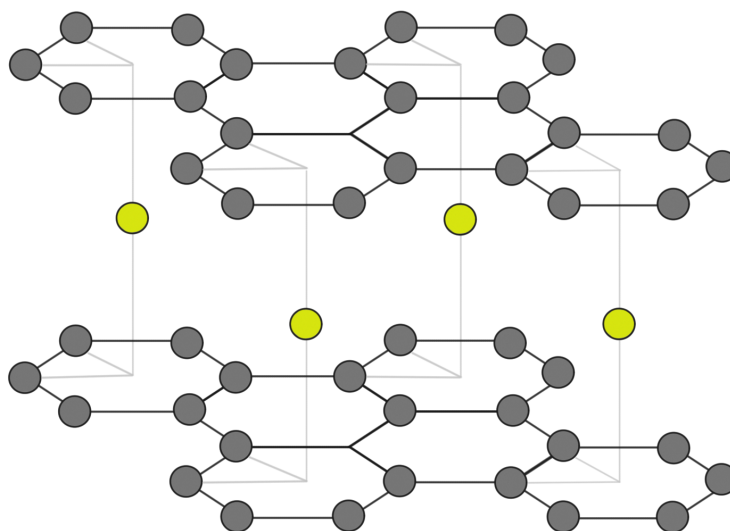
Figure 2.3: *The layered crystal structure of graphite. The carbon atoms form hexagons, which is graphite's repeatable unit. Lithium ions are inserted into the hexagons between the layers. Figure made by author, inspired by [27, 32, 33]*

Other forms of carbon are mostly used as additives in graphite. Additives are added to the anode to improve specific properties of the material. An example is Carbon black, which is a soft carbon. Carbon black is used as an additive to increase electric conductivity. Additionally, carbon black is low cost, costing around 10-20% of graphite. Another form of carbon additive is graphene. Most manufacturers do not use graphene when producing batteries. However, graphene is being researched for use in metal alloy anodes. [27, 31]

Metallic Anodes

Other than carbon anodes, there are metallic alloy anodes and Lithium titanium oxide (LTO). LTO has a market share of about 0.7%, but is being researched by companies for its qualities. Similarly to metal lithium anodes, LTO does not form an SEI layer, meaning no lithium is lost to the formation of this SEI layer. It also has a high voltage against lithium, decreasing the amount of dendrite formation. Dendrites are metal spikes forming on the anode. However, LTO has a low energy density and a low operating voltage, causing it to be less popular than carbon. [27, 31]

Silicon alloy anodes have been experiencing an increase in use. About 1.4% of produced batteries use silicon alloy anodes. Silicon forms covalent bonds, sharing electrons and having a +4 charge. This means that 4 lithium ions can be stored by one silicon atom, compared to 1 lithium-ion needing 6 carbon atoms. Silicon also has a much higher volumetric and gravimeter density than graphite. Silicon is one of the most common elements in the earths crust, leading to silicon being low cost. However, silicone's biggest drawback is its volumetric expansion. When lithium is inserted into silicon, it forms a lithium-silicon alloy. During this process, silicon experiences a 320% volumetric increase. This leads to multiple failures in the anode. Therefore, anodes with high degrees of silicon have very low life spans. [27, 31]

2.6   Production of Lithium-ion batteries

Lithium battery production is a well established practise that follows distinct steps. This part will go through the theory behind commercial, non-commercial battery production, and coin cell assembly. and contamination factors. This establishes the background for the methodology.

2.6.1   Commercial production of lithium-ion batteries

Battery production can be divided into 6 different main steps. The first step is called slurry mixing, where the active material, slurry solvent, and binder are combined into a slurry. An example of a slurry could be, LFP as the active material, N-Methyl-2-pyrrolidone (NMP) as the slurry solvent, and a CMC binder. Next, the slurry is coated onto the current collector. The current collector is normally copper for the anode and aluminium for the cathode. Then the current collector with the wet active material slurry is vacuumed dried, to remove the liquid solvent. Further, the strip is calendared to acquire the right thickness. Calendaring is the process of smoothing out the strip by passing it through two metal cylinders. This makes the slurry more dense, improving the volumetric power and energy density. After this, the current collector is cut into the appropriate size and the battery is assembled. There are two main ways to assemble a battery. Either stack the strip into many layers and make a pouch cell, or the strip can be rolled into a cylinder. All of these steps are summarized in Figure 2.4. [34]
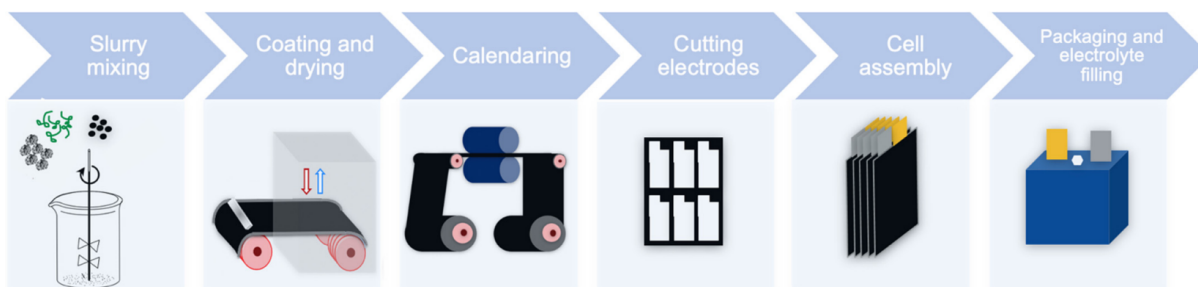
Figure 2.4: Slurry mixing: Active material, solvent, and binder are mixed. Coating and drying: The slurry is coated on a current collector and is dried to remove liquid. Calendaring: The current collector is pressed to smooth out the slurry and improve energy density. Cutting electrodes: The current collector is cut into the right size strips. Cell assembly: The electrodes are stacked with the separator. Packaging and electrolyte filling: The cells are placed in a container and filled with electrolyte.[34]

The last steps of LIB manufacturing consists of wetting, formation and ageing. These steps are the subject of much study due to high-cost and time consumption. Formation and ageing makes up 32% of total production cost and takes 3–4 weeks to complete. Before the formation cycling can begin, the electrolyte needs to be evenly distributed throughout the battery in close contact with the active materials. To ensure this, the cell needs to be left for 3–4 days after the electrolyte is introduced to the cell. This process is called wetting and can be done at a temperature between 40-60℃to provide the electrolyte better access to the electrodes. Without a sufficient wetting period, the Solid Electrolyte Interface (SEI) formation will be flawed and result in capacity loss and a higher self discharge rate. [5, 35, 36]

When cycling a LIB with a graphite anode, the SEI layer will form. Electrolyte will react with lithium ions on the anode of the battery. This reaction will result in the decomposing and solidifying of the electrolyte, creating the SEI layer on the surface of the anode. This reaction occurs because of the electrolyte's reduction potential is larger than that of the graphite anode. Graphite has a reduction potential of 0-0.25 V versus Li^+/Li, while the electrolyte has about 1 V versus Li^+/Li. [5, 37]

The resulting SEI layer has a positive effect on the battery. The layer serves as a protection for the anode, keeping the electrolyte and the electrode separated. It prevents further decomposing of the electrolyte and improves on the lithium-ion flow in the battery. This is because of the SEI layer's insulating and ion conductive properties. In addition, the SEI layer increases the stability and safety of the cell. This makes the formation one of the most critical stages of the battery production. To ensure the composition and stability of the SEI layer, the cell usually requires multiple low charge rate cycles. An example of a formation process can consist of a first electrode wetting for 6-24 h at room temperature, 1-2 formation cycles at C/10-C/5 charge/discharge rates. A second electrode wetting for 12-24 h at room temperature, 1-2 formation cycles at C/5-C/2. And finally, a third electrode wetting for 12-24 h at 40-60℃. However, most battery manufacturers keep their SEI formation process secret. [38, 39, 40]

After the wetting and formation, the batteries go through ageing. This process can take up to 4 weeks to complete. The procedure verifies stability and quality of the cell. Ageing can be divided into two main types of ageing, calendar and cycle ageing. Calendar ageing consists of resting the battery, without applying any current, to check the cell for self discharging. Cycle ageing usually consists of charging and discharging the batteries for multiple cycles at high C-rate and temperature. [5, 34]

2.6.2 Non-commercial production of lithium-ion batteries

Non-commercial batteries are highly aimed at research purposes. Lithium-ion batteries for research can be created just the same way as commercial ones, but in a more laborious manner. Non-commercial production is void of industry machines, as the production number is not a priority. The slurry mixing, calendering, cutting and assembly are therefore manual processes, where researchers examine every part of the production for improvements. This manual labour can hardly match the accuracy of commercial production, and is the reason many research cells are built from commercially produced pouch cells and electrode sheets. Research oriented commercial cells are often dry, meaning they are shipped without electrolyte. Using commercial pouch cells or electrode sheets to research new electrode materials or other aspects of batteries gives high-quality and reproducible results. [19]

Another consideration of non-commercial batteries is cost. Creating large pouch cell batteries, is the most similar to commercial cells. However, the cost and material usage is typically too high. Therefore, it is most common to use coin cell batteries to research characteristics. Coin cells produced properly can give similar results as pouch cell, but at a reduced cost. One big draw back of coin cells is that they are assembled by hand, unlike machine made pouch cells. Coin cell production requires training and good documentation to account for differences from the human factor. [41]

2.6.3 Coin cells

There are six key steps to make high-quality research oriented cells. These steps are: slurry mixing, slurry cooling, porosity control, sufficient wetting, N/P ratio control, and electrode alignment. Slurry mixing is emphasized as an important step to ensure uniformity. Uniformity is the most important factor for consistent and quality cells, as it has a big impact on the final cell performance. An inconsistent slurry carries over into the calendering process, where the unevenness can be emphasized with an uneven spread or thickness. Therefore, carefully calibrated equipment is necessary to make uniform electrodes. [42]

Another key factor is the dryness of the used components. Moisture can cause instability in the active material, such as gas evolution and other safety risks. Before introduction to a glove box, all components should be dried. This can be done in a vacuum oven. For especially vulnerable components such as the separator, this step is extra critical towards cell performance because of its porous structure. As the separator membrane is deformable and can melt under high heat, low-temperature drying is the recommended process. Here, it is advised to follow the manufacturer's drying instructions. Before drying, the metal components should be cleaned. These parts can contain metal or organic contamination, and pose a great performance risk to the final cell. [42]

The assembly is a likewise important step to ensure quality cells. In figure 2.5, a common setup is presented. This assembly ensures good contact between the layers. When assembling, careful placement of the electrodes is required to insure alignment. A misalignment has a big impact on cell capacity. In some studies, the use of a slightly wider anode has been used to minimize this issue and stably produce high-capacity cells. Another concern is the separator. A piercing of the separator can cause a short circuit, deeming the cell unusable. Therefore, careful handling of the separator is required. [41, 42, 43]

Positive cell casing

Stainless steel spring

Stainless steel spacer

Positive electrode

Seperator

Negative electrode

Negative cell casing
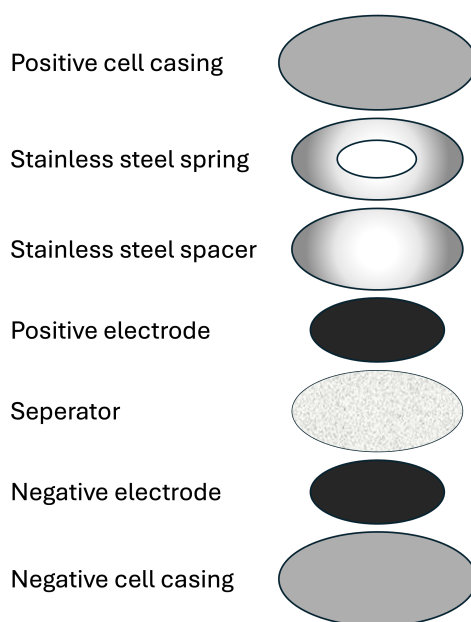
Figure 2.5: *The parts of a coin cell and the order they are assembled. Figure made by author, inspired by [41]*

The last component of the coin cell is the electrolyte. There are many papers proposing different methods or calculations of how much electrolyte to use. The use of too much electrolyte in a cell, can leave the cell "flooded". This overflows the pores of the electrodes and separator. In turn, leaving the cell unable to soak up all the electrolyte. The opposite can happen with too little electrolyte. The electrodes remain dry and the formation of the SEI layer is compromised and therefore suboptimal for the performance of the cell. In equation 2.23, a pore volume-based equation is proposed to calculate the necessary amount of electrolyte. [41, 43]

$$Pore\ volume = Area \cdot Thickness \cdot Porosity \tag{2.23}$$

The equation assumes that the separator porosity is known, while the porosities of the cathode and anode are estimated based on the known densities of the active materials. To get the total amount of electrolyte, the calculated pore volumes of anode, cathode, and separator are added up.[43]

2.7   Metal contamination

Metal is one of the most dangerous types of contamination in a battery. When a current is applied, the metal reacts into ions. These ions can then react with lithium on an electrode, forming metal spikes called dendrites. The dendrites can grow through the separator and cause an Internal Short Circuit (ISC), causing thermal runaway and high internal resistance. Even if the dendrite does not puncture the separator, the effects of metal contamination are largely noticeable in the battery performance. Performance issues like this can be spotted through erratic cells, where contaminated batteries have a higher self-discharge and capacity loss. This is due to the metal-ions finding their way into the cathode structure, creating a dissolution of transition-metal-ions. This dissolution is known to cause higher rates of degradation. [44]

The most common metal contaminations are copper, iron, aluminium, and nickel. Contamination from these metals can occur at several steps along the production line. Particles in the air from the assembly process can contaminate the shells, slurry and other parts of the battery. Paired with lithium, their respective reduction potentials are listed in Table 2.8. [44, 45]

Table 2.8: *Reversible potentials of selected contamination metals versus lithium and their half cell reaction.* [20]

Element	Reaction	E° [V]	E° vs. Li/Li$^+$ [V]
Copper	$Cu^{2+} + e^- \rightleftharpoons Cu^+$	0.16	3.20
	$Cu^+ + e^- \rightleftharpoons Cu_{(s)}$	0.52	3.56
	$Cu^{2+} + e^- \rightleftharpoons Cu_{(s)}$	0.34	3.38
Iron	$Fe^{3+} + e^- \rightleftharpoons Fe^{2+}$	0.77	3.81
	$Fe^{3+} + 3e^- \rightleftharpoons Fe_{(s)}$	-0.04	3.00
	$Fe^{2+} + 2e^- \rightleftharpoons Fe_{(s)}$	-0.44	2.60
Aluminium	$Al^{3+} + 3e^- \rightleftharpoons Al_{(s)}$	-1.68	1.36
Nickel	$Ni^{2+} + 2e^- \rightleftharpoons Ni_{(s)}$	-0.24	2.80

By adding electrolyte to the cell, the cell can facilitate electrolysis. The amount of substance that has reacted in the cell can be calculated by Faraday's second law of electrolysis, shown in Equation 2.24. This law determines that the amount of chemical change brought about by the same supply of current in substances is proportional to their respective amount of substance. [46]

$$n = \frac{Q}{zF} \tag{2.24}$$

In Faraday's law, the amount of substance (n), in mol, is the amount that has reacted at the electrode. Total electric charge (Q) is transferred to or from the electrode in Coulombs, which can be calculated by $I \cdot t$, Current in Ampere and time in seconds. The amount of substance that has reacted is equal to the total electric charge divided by Faradays constant (F), and the number of electrons per reaction (z). [46]

2.8   Self discharge in lithium-ion batteries

A battery at rest with full or partial SoC will lose capacity over time. This phenomenon is called self discharge and happens as a natural degradation of the battery. After time, this results in the battery's end of life. The unwanted capacity loss is mostly attributed to the relationship between the electrodes and the electrolyte. When a battery is new, the cell reaction works at max capacity given a certain amount of active material. As the cell is cycled, active material is lost due to unwanted reactions and the capacity is decreased. Some lost capacity will be recovered when charging the battery, this being the reversible self discharge. There is much study done on this subject, as a battery's self discharge rate is a large indicator of the battery's performance. A reason for LIBs wide usage is because of its low self discharge rate, about 2% of capacity per month. [47, 48, 49, 50]

There are multiple factors contributing to self discharge in batteries. The most prominent reasons are Loss of Lithium Inventory (LLI), Loss of Active Material (LAM) and lithium plating. LLI is due to reactions between the electrodes and the electrolyte, or impurities within the cell. During the formation of the SEI layer, lithium ions are consumed to create a thin solid interphase between the electrolyte and the anode. The SEI layer has a positive impact on the battery, yet is a source of delithiation and self discharge. Delithiation makes lithium-ions unavailable to intercalate into the electrodes, decreasing SoH. The SEI layer can increase in size during the battery's life, causing more delithiation and self discharge. The lithium-ions can also react with impurities within the electrolyte. Metal contamination contributes to delithiation and an increase in self discharge by reacting with the available lithium-ions. [48, 51, 49, 50]

LAM and isolation from current collectors are also factors for self discharge. Similarly to lithium ions, active material can react with contaminants and electrolyte reducing SoH. In addition, the lithium can become solid, causing lithium plating between the anode and the SEI layer. In turn, this can cause a disconnect and increase self discharge. Self discharge can also come from the leakage of electrons. Short circuits and electrolyte conductivity can cause stray electrons, resulting in a loss of capacity. [48, 51, 50, 52]

Determining the self discharge rate is important for deciding the performance of the battery. However, the measurement of the self discharge rate is difficult and time-consuming, considering how small the self discharge is. One method of measuring the self discharge rate is to directly measure the lost capacity. This involves charging the battery to a specific SoC and allowing it to rest and self discharge for a sufficient time. Then discharging the battery and seeing lost capacity. This method requires careful characterization of the cell to separate the reversible and irreversible losses. [53]

Another method is to measure the charge needed to hold the SoC. The cell is charged to a specified SoC, then a current is applied to hold the voltage in place. The needed current will be equal to the self discharge rate. [53]

A final method of measuring self discharge rate is to monitor the voltage decrease. Cell capacity can be determined by the relationship between cell voltage and SoC. Subsequently, the self discharge rate can be determined from the capacity. This in turn means that at any time, the voltage decrease can indicate the self discharge rate. The voltage should be measured for at least a week to produce stable results. [53]

2.9   Relation between open circuit voltage and state of charge

Open Circuit Voltage (OCV) and SoC are closely related, and their relationship behaves the same for most LIBs. The relation can be found from the Nernst equation from Equation 2.7. If considering a discharging battery, the total reaction is shifted to the right, increasing the amount of product and decreasing the amount of reactants. This results in a total decrease in the voltage as the SoC is decreased. When charging, this is reversed. When the battery moves toward 0% or 100% SoC, the voltage acceleration spikes. Considering 0% SoC, the concentration of lithium ions on the anode is minimal. Since the relation is based on the logarithm of the concentration ratio, a small increase in this concentration will result in a rapid acceleration of voltage. When moving toward 100% SoC, the concentration of lithium-ions on the cathode side becomes small, resulting in another rapid acceleration of voltage. An illustration of this relation is presented in Figure 2.6. [54, 55, 56]
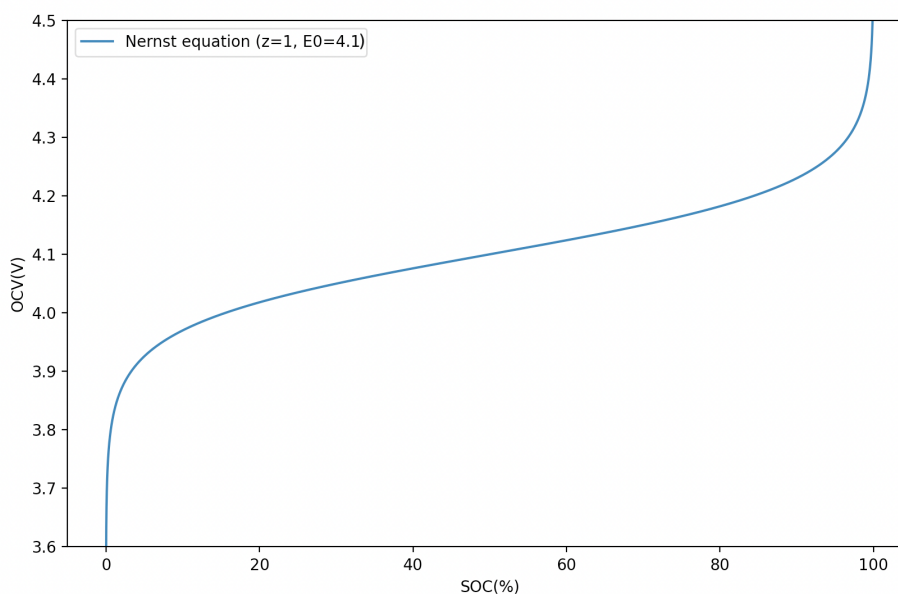
Figure 2.6: *Nernst equation gives an approximation of how a cell's voltage curve will behave during charging and discharging.*

When the Nernst equation is presented as a function of SoC, it becomes a non-linear function consisting of the difference between two logarithmic functions. This is presented in Figure 2.6. This relation is affected by the type of battery, temperature, and C-rate. However, the shape stays mostly the same. Small alterations in the slope of this curve might indicate faults like contaminants and electron leaks. By analysing these alterations, some characterization of the battery can be made. These types of analysis are known as ICA, and DVA. [54, 55, 56]

2.10 Differential Voltage Analysis and Incremental Capacity Analysis

Differential voltage analysis and incremental capacity analysis are based on voltage measurements under constant current charge or discharge. These are used to discover and analyse degradation and capacity loss in LIBs. DVA and ICA inspect the derivative of voltage over capacity (dV/dQ) and capacity over voltage (dQ/dV), respectively. When batteries degrade because of LLI, LAM or impedance increase, the battery experiences capacity loss. In turn, this affects the voltage capacity relation. This can happen at very specific voltages and is difficult to spot on the voltage capacity curve. However, when analysing the derivative, troves, and peaks are easily detected. An example of DVA is depicted in Figure 2.7. [57, 58, 59, 52]
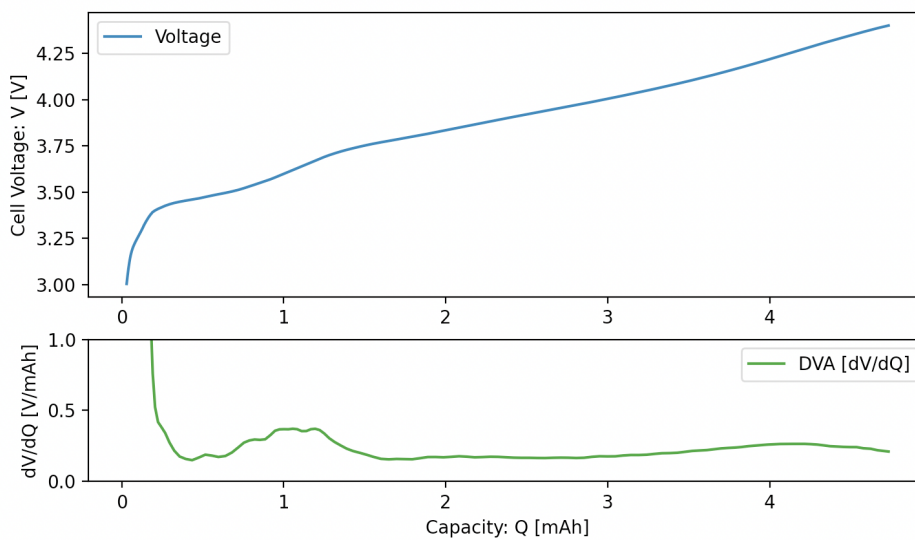
Figure 2.7: *An example of a DVA comparing the voltage capacity relation to the voltage differential.*

The ICA is more complicated to analyse than the DVA. When presented alone, the ICA is difficult to connect to the different points on the voltage capacity. This, contrasts with DVA, where any point on the voltage curve can be connected vertically to any point on the differential curve. However, if the ICA is rotated 90°counter clockwise, as presented in Figure 2.8, similar connections between the voltage curve can be done horizontally. [58, 59, 60]
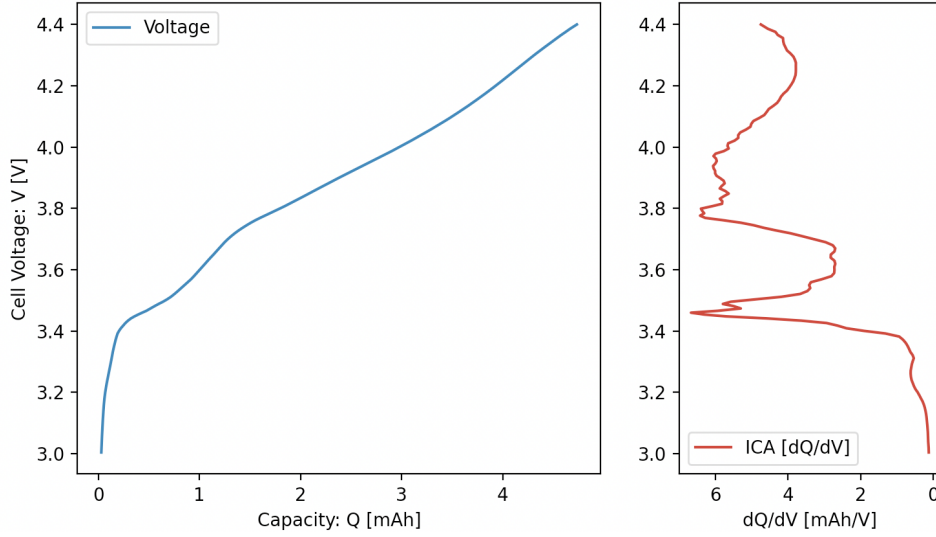
Figure 2.8: *An example of an ICA comparing the voltage capacity relation to the capacity differential.*

The methods are non-destructive and can be utilized during the formation process without any additional resource loss. Mathematically, the DVA curve is derived as the voltage gradient divided by the capacity gradient, presented in Equation 2.25. While the ICA curve is derived as the capacity gradient divided by the voltage gradient, presented in Equation 2.26. [61, 59, 60]

$$dV/dQ = \frac{\Delta V}{\Delta Q} \tag{2.25}$$

$$dQ/dV = \frac{\Delta Q}{\Delta V} \tag{2.26}$$

To create high-quality DVA and ICA curves, the measured potential should be close to the OCV. This is due to the SoC-OCV relation. Currents in the range of C/10 or lower is recommended. [58, 59, 60]

3   Methodology

This section of the thesis is dedicated to explaining the methodology of the lab work. The aim is to provide insight into the processes of coin cell production from commercially available electrodes. This way the experiments can be repeated, and further studies can be preformed. The goal of this work is to first create high quality, comparable batteries, which can be analysed using DVA and ICA. Using these cells as a reference point, a batch of contaminated batteries can be created and compared. Via voltage curve data from the formation cycle, methods to easily spot faulty batteries. Discovering these deficiencies at an early stage can contribute to reducing cost and storage time. The methodology will therefore go through the steps this project takes to achieve these goals.

3.1   Coin cell production

This part of the methodology will present the key stages of research oriented coin cell production. For this project, a standard NMC111 electrode with known parameters was used. Parameters for this electrode are known from the supplier and presented in attachment B. Using factory electrodes ensures accuracy and quality by removing variations connected to making them from scratch.

a   b   c   d   e
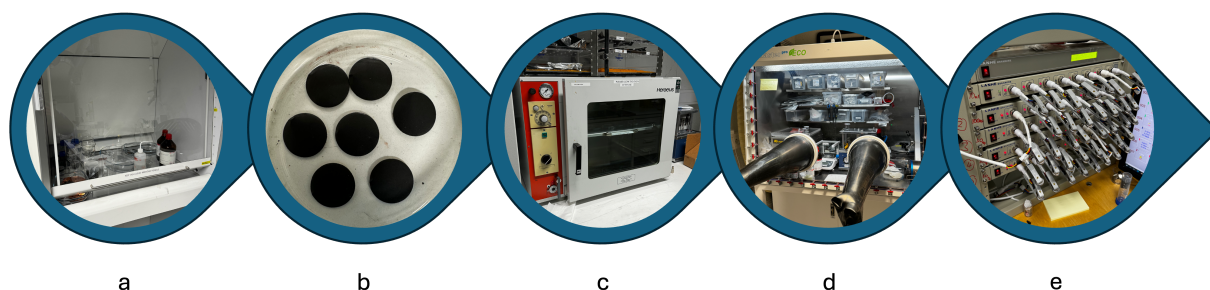
Figure 3.1: *The sequence shows the steps of coin cell production. a) The fume box is used to wash electrodes. b) The electrodes are punched into adequate size. c) The electrodes are dried in a vacuum oven, d) The glove box is used to assemble the coin cell. e) Finished cells are tested.*

The five steps used for coin cell production are displayed in Figure 3.1. First, the electrodes have to be prepared. They will then be punched out to the appropriate size for the coin cell. Afterwards, all components go through a drying process, before going into the glovebox. The coin cells are assembled, wetted, and cycled. Key difficulties connected to each step will also be presented.

3.1.1   Equipment list

The equipment needed for coin cell production is stated in Table 3.1. The equipment list ensures that all needed equipment is known and present. Another reason for the list is to include safety equipment. This is to ensure that handling of chemical components and machines is done safely. The table is divided into the key steps of coin cell production and could be used as a checklist.

Table 3.1: *Table over the equipment used making batteries from electrodes. Note that the washing equipment is only applicable when making one-sided electrodes from two-sided sheets.*

Equipment				
Washing	**Punching**	**Drying**	**Glove box**	**Formation and ageing**
Fume box	Cutting board	Vacuum oven	Glove box	LAHNE battery test system
Plastic gloves	Hammer	Glass plates	Plastic gloves	
Protective glasses	15 mm punch		Plastic tweezers	
Glass beaker	17 mm punch		Pneumatic press	
Pipette	Paper		Tissue	
Scissors	Plastic tweezers			
Tissue				

It is important to note that the equipment list does not include battery components. The table addresses safety equipment, and tools which make processes and components easier to handle. Components such as electrodes, separators, and electrolyte are components which can be independently adjusted to the use case or research interest.

3.1.2   Electrode preparation

The project used two ways to prepare the electrodes for coin cells. Either washing electrodes from commercial pouch cells, or using one-sided commercial electrode sheets. Commercial NMC111 electrodes from LIFUN technologies were used. The pouch cells are dry cells, meaning they were manufactured without electrolyte. The dry cells are cut open, and the electrodes are taken out. After this, the electrodes are washed. By washing off the active material on one side of each electrode, and the current collector are exposed. This allows electrical conductivity between the coin cell casing and the active material in the finished battery. For NMC111, NMP is used as a solvent. Carefully wetting tissue and swiping at the active material slowly dissolves it, without damaging the electrode. At this stage, it is important to minimize the creation of bends to the cleaned electrode, as this will increase the chance of a faulty battery. An alternative to this method is to use commercial one-sided electrode sheets. When using one-sided sheets, the previous steps are skipped. These one-sided sheets became the preferred choice for this project.

3.1.3   Punching

With a clean electrode sheet, the electrodes are ready to be punched out. For this, a 15 mm circular punch is used. This is a good fit for the standard LIR2032 casing. After this, the separators are also punched out. These are punched with a 17 mm punch. To get everything ready for the glove box, electrodes, glassware and metal parts have to be dried.

3.1.4   Drying

Drying takes place in a vacuum oven where the aforementioned parts are dried. This is done at 65℃ for a minimum of 3 hours, but preferably overnight. This step ensures that the contents going into the glove box contains minimal amounts of moisture. This protects the glove box atmosphere and the batteries from moisture contamination. Once the contents are dried, the vacuum oven is slowly filled with air to prevent the electrode and separator pieces flying inside. All components can then be brought over to the glove box for assembly.

3.1.5   Glove box

The assembly of the battery is done inside a glove box. A glove box has a separate atmosphere, in this case made of argon gas. Some hazardous chemicals are especially sensitive to air and water vapour. Especially lithium, which is highly reactive with O_2, is prevented from combustion. The separated workspace therefore allows workers to safely handle these chemicals. The glove box is then a contamination free space to assemble the battery. When introducing the battery components to the glove box, an intermediate antechamber is used. This chamber should be filled and evacuated 3 times before opening from the inside of the glove box. This is to ensure minimal O_2 content in the introduced air.

The cell is then assembled. The assembly layers are presented in the theory in Figure 2.5. The assembly begins with the negative cell casing. After this, the anode is placed with its current collector facing the cell casing. Both electrodes are weighed before placement in the battery, as to later calculate the capacity and C-rate for cycling. Before and after the separator, a 20 µL solution of Ethylene Carbonate/Ethyl Methyl Carbonate (EC/EMC) is placed. For the contaminated batches, this is where the contamination is inserted. Then the cathode is placed with the current collector facing the positive cell casing. To make sure the parts have good contact, two spacers and a spring are placed inside. Then the positive cell casing is placed on top and the cell is sealed with a pneumatic press. The resulting battery is then taken out of the glove box and wetted for 2–3 days before formation cycling.

3.1.6   Contamination

Some batches were injected with copper contamination. To insert an accurate amount of contamination, a dispersion was made with EC/EMC electrolyte and 99.7% pure dendritic copper powder with a particle size of <45 µm. The dispersion was made up of 400 µL of EC/EMC and 4 mg of copper, resulting in a 10 µg/µL. The desired amount of copper was calculated using Faraday's law. The dispersion was then placed within the battery in ratios with clean electrolyte to get the desired amount in each case.

3.1.7   Cycling

Following wetting, the batteries are tested. For batteries with graphite anodes, a SEI layer is to be formed. For batteries with lithium anodes, the cycling is mainly to collect data and ensure working batteries. To cycle the batteries, a LAHNE testing station, and LAND battery test system is used. These test systems record time, voltage, and current with high precision. This allows for the creation and calculation of other variables, such as dV/dQ or dQ/dV, for every data point. First, a cycle fitting the project goals had to be created.

The cycling procedure used is different from typical procedures. As the goal is to analyse the first cycles of the batteries, a shorter procedure adjusted for this purpose is created. The procedure, presented in Figure 3.2, shows the cycles used for NMC111 batteries with lithium anodes. This procedure consists of two charge and discharge cycles. For NMC111, the battery is charged to 4.2 V and discharged to 2.4 V. The cell is charged with a C-rate of C/20 until the battery reaches its upper voltage parameter. The battery is then held at constant voltage for 50 min to ensure stability, then discharged to its lower voltage parameter. These limits are defined in the accompanying datasheet B, and adjusted for a lithium anode. After two cycles of charge and discharge, the battery is charged 50% SoC and the rested for 200 hours. After 200 hours, the difference in voltage can help indicate self-discharge or contamination, and can be analysed further in conjuncture with the formation data.
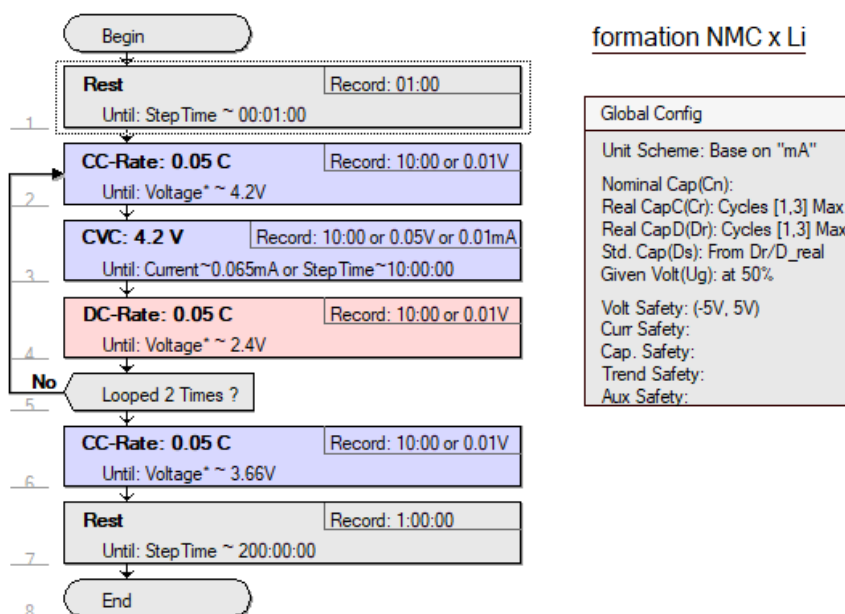
Figure 3.2: *The formation cycle used for NMC111 cathode with lithium anode.*

To cycle the batteries, the correct capacity has to be found. One cell is cycled using the specific capacity from the datasheet in combination with the active material cathode weight. This lets the program calculate the capacity of the battery, subsequently the current needed to achieve the assigned C-rate. During the cycling, the program calculates the practical capacity of the battery, using current and time data. Subsequently, the actual specific capacity can be calculated and used for the subsequent batteries to get the correct charging time and current.

3.2   Data treatment

To analyse the data received from LAND, a python code was produced to present the data in an organized, clear, and comprehensible manner. The script consists of multiple functions with different purposes. To read the data csv file, the code uses panda library to create a dictionary to work with. The following functions are simple in how they plot figures based on two values, one x-axis and one y-axis.

Among these functions are the noise remover. This function averages any list of values to a chosen degree. The purpose of this is to limit the noise of a plot, making it easier to interpret. The way the function averages the lists is by creating a bracket that moves with the integer of the list, changing the value to the average of the bracket. The size of the bracket is determined by the chosen degree. For example, with a degree of 5 the bracket would have a size of 11, including the 5 previous integers, the integer itself, and the 5 next. The result is much cleaner slopes in the plotted figures. An example of this is presented in Figure 3.3. In the figure, a dV/dQ plot is presented with and without the noise remover. The noise remover introduces change to the data, but this is minimal, and the data is much more understandable.
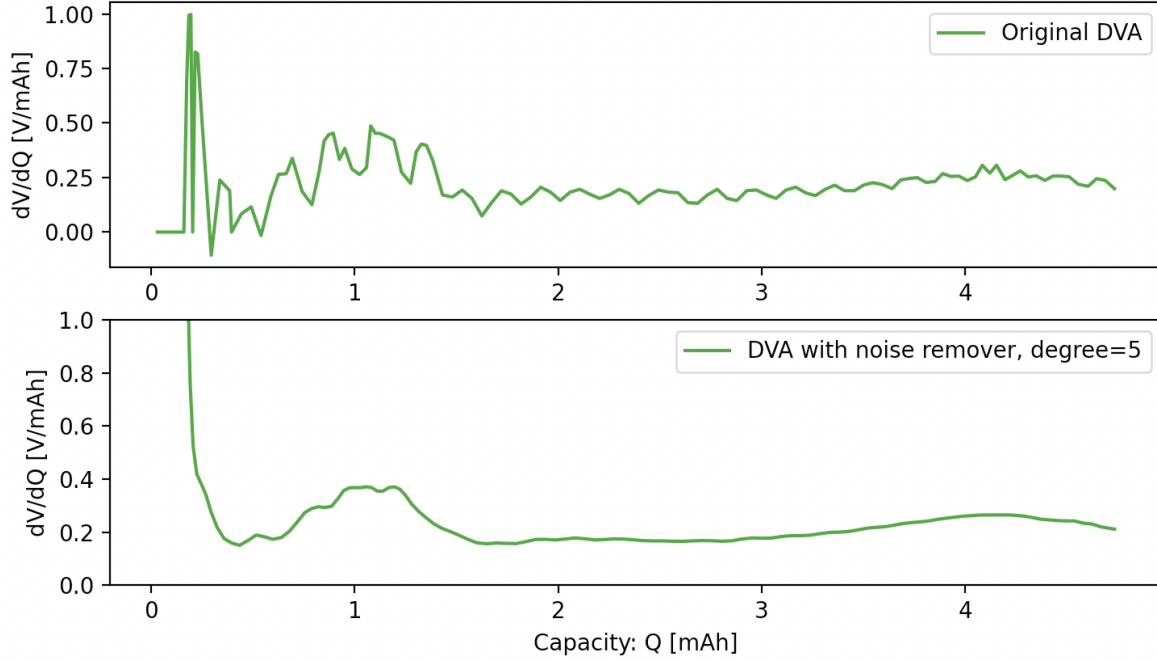
Figure 3.3: *The difference in noise between a calculated differential using the noise remover and derivative function, and the directly calculated differential from the data.*

The LAND data automatically calculates values for dV/dQ and dQ/dV. However, this data is noisy and cluttered. When the land system calculates a differential, it takes every value and subtracts the previous value to gain the slope at that exact point. With already noisy data, this differential becomes very cluttered, to fix this, a derivative function was made. The derivative function in Equation 3.1 makes a similar averaging to the noise remover, only with a bracket of two. Instead of averaging the values, it averages the differential of the current and the last integer with the differential of the current and the next.

$$\Delta f(i) = \frac{\sum_{i=-1}^{2} f(i) - f(i-1)}{4} \tag{3.1}$$

4   Results and discussion

This section of the thesis will present the collected data, and the results from the practical work in the battery lab. Further, these results will be compared and discussed. Finally, the findings from this research will be presented.

4.1   Experimental results

Twelve NMC111 cells were made with a lithium anode. This section will divide the results into two categories, non-contaminated cells and contaminated cells. The non-contaminated cells will serve has a reference for the further discussion of the contaminated cells. These cells will be called *NMC 1*, *NMC 2*, and *NMC 3*.

4.1.1   Reference cell

The non-contaminated NMC111 cells turned out to be stable throughout the study. For simplicity, the following paragraphs will use the *NMC 1* cell. In Figure 4.1, the voltage and current during the cycling procedure is presented. The voltage is very stable, with clean and smooth curves. During the first charge, the voltage experiences a bump after about 7 hours. This is somewhat expected, as the first cycles of a battery are often less stable. A reason for the overall stability could be the lithium anode. The creation of the SEI layer causes LLI, which affects the stability of the voltage curve. Considering how lithium anodes do not create an SEI layer, the effects of SEI formation are eliminated.
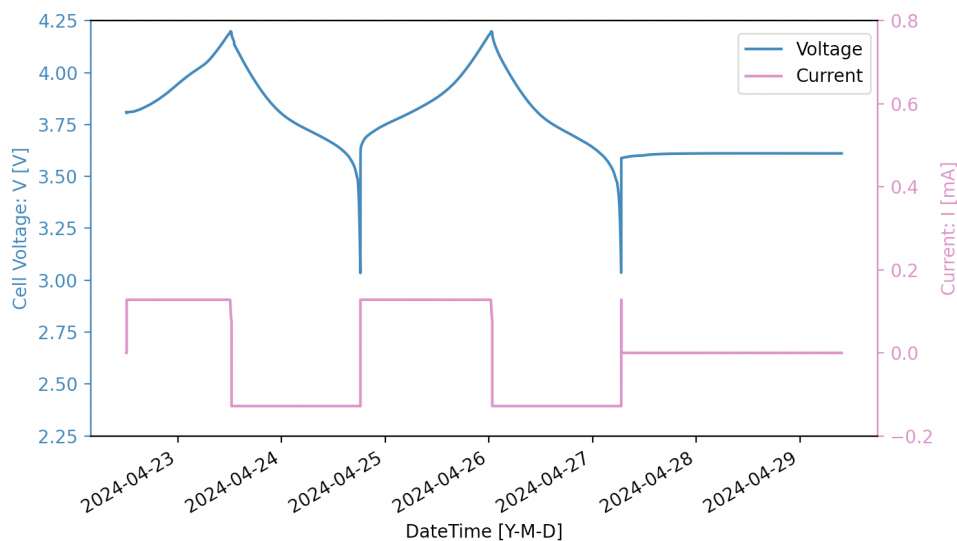
Figure 4.1: *The voltage and current of* NMC 1 *during the cycling test. Noise reduction 5.*

The procedure consisted of two cycles of C/20 charge and discharge. This was to improve on the stability of the voltage. The C-rate however was too low, in relation to the parameters. The C-rate should be C/20, but in Figure 4.1 it is about C/30. This is most likely due to an error in the capacity calculation. The manufacturer of the electrodes states that the cathode has a specific capacity of 200 mAh/g. Using the discharge capacity, the actual specific capacity was calculated to be about 140 mAh/g.

The voltage capacity relation for the non-contaminated NMC111 cells is close to the theoretical Nernst equation 2.10. In Figure 4.2 the second charging cycle is presented. Comparing this to the Nernst function in Figure 2.6, a likeness can be observed. The voltage of the cell behaves almost perfectly like the Nernst equation predicts. As mentioned in the theory, the voltage will never reach the end of the Nernst function because not all the lithium can be removed from the cathode. The result is a voltage capacity relation that behaves close to theoretically perfect.
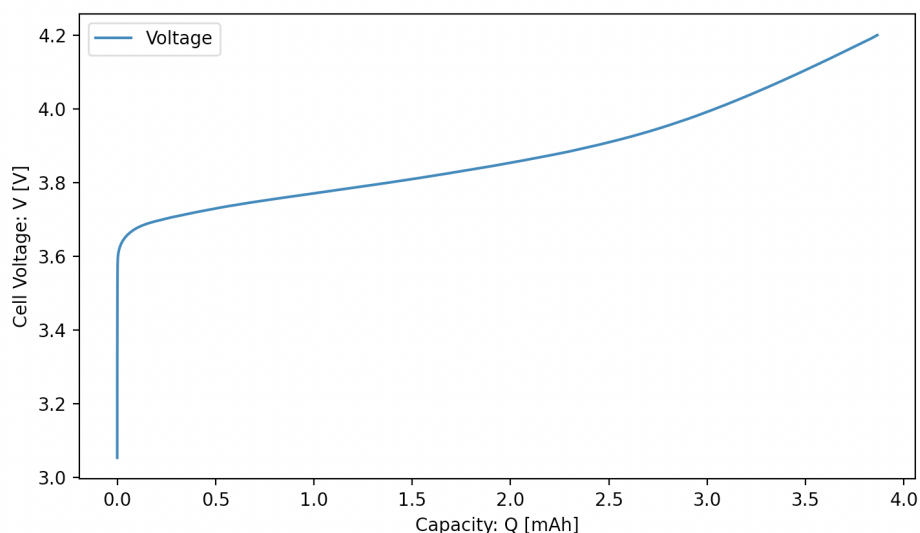
Figure 4.2: *Voltage capacity relation for* NMC 1 *during the second charge. Noise reduction 5.*

Because of the stable voltage curves, the DVA and ICA are also close to ideal. Figure 4.3 presents an analysis of the second charging cycle of *NMC 1*. The analysis is a combination of the voltage-capacity relation, an ICA to the right, a DVA on the bottom, and a plot of the reversible potential for the contamination reactions on the left. This setup makes analysis of any point on the curve easier.
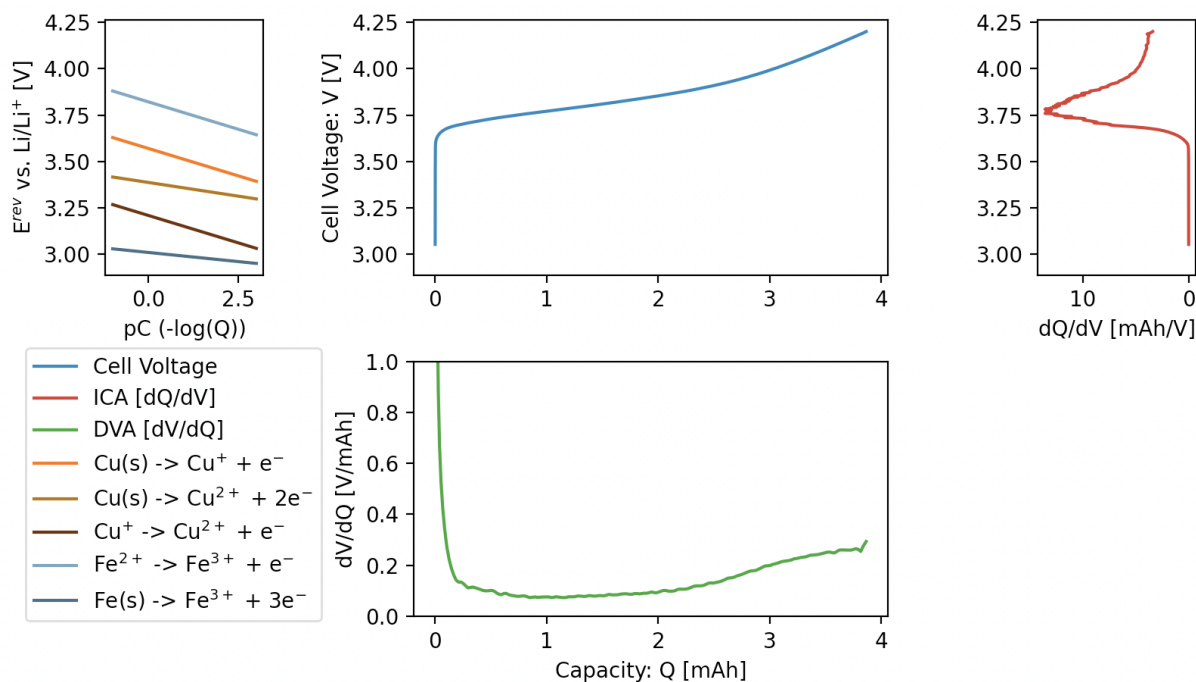
Figure 4.3: *The combination figure for* NMC 1*. The plot contains the voltage capacity relation in the middle. To the right is a ICA and on the bottom is a DVA. To the left is the reversible potential of possible contamination reactions listed. Noise reduction 5*

Since all the plots share either the capacity axis or the voltage axis, vertical and horizontal lines can be drawn to analyse any point. An example of this is presented in Figure 4.4. When the growth of the voltage curve becomes more gradual, the capacity grows at an increased rate. This is shown in the ICA plot with peaks or troughs. However, when the voltage curve accelerates, the DVA shows peaks and troughs. The contamination figure on the left allows for checking possible reactions, occurring at different concentrations of metal contamination. In theory, if a functioning battery was contaminated with copper, the voltage should stagnate at a reaction voltage before continuing. This in turn would indicate the copper reacting into ions. At this point, the reversible potentials could indicate what reaction could be happening, and the concentration of said contaminate. This combination of analysis allows for a more detailed understanding of what happens inside the cell during cycling.
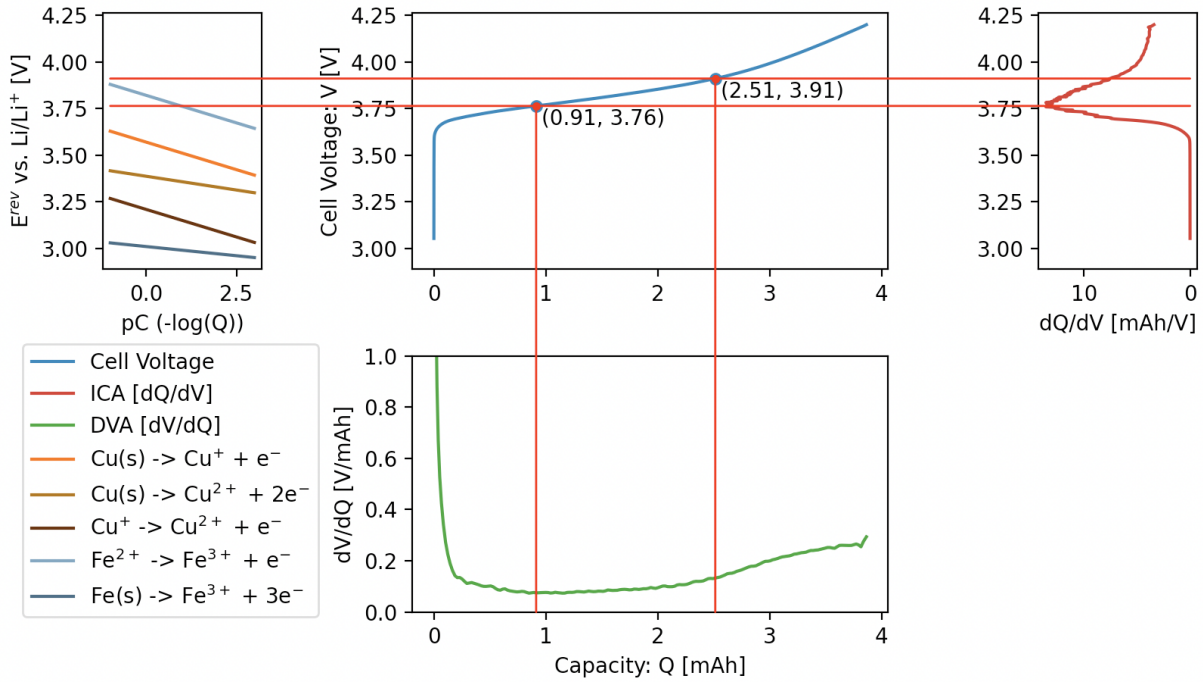
Figure 4.4: *The combination figure for* NMC 1, *with red lines to indicate relations between different plots. Noise reduction 5.*

Figure 4.4 shows the analysis of *NMC 1* with markers on interesting capacities. In the ICA, a peak is visible at 3.76 V. This correlates to a capacity of 0.91 mAh, about one quarter of maximum capacity. This peak indicates a change in acceleration, the voltage changes from decelerating to accelerating. In the DVA, it can be observed how after reaching a capacity of 2.5 mAh, an increase occurs. This increase indicates how the voltage has a sudden increase in acceleration at 2.5 mAh before stabilizing at an increase of 0.2 V/mAh. Neither of the points indicate any contamination or faults. However, this example shows how useful this combined plot can be in analysing cell data. The combined plot makes it easier to determine relations between different analysis methods.

The rest of the non-contaminated NMC111 cells are very similar to *NMC 1*. In Figure 4.5 the three NMC111 cells are presented. The cells are analysed using the combined plot, without the reversible potentials plot. In these plots, *NMC 1* and *NMC 2* have had an arbitrary offset value α and β added to the voltage and DVA plots respectably. The offset is to separate the curves, making it clearer to see each curve. Because of this offset, the reversible potentials would no longer have any correlation to voltage curves.
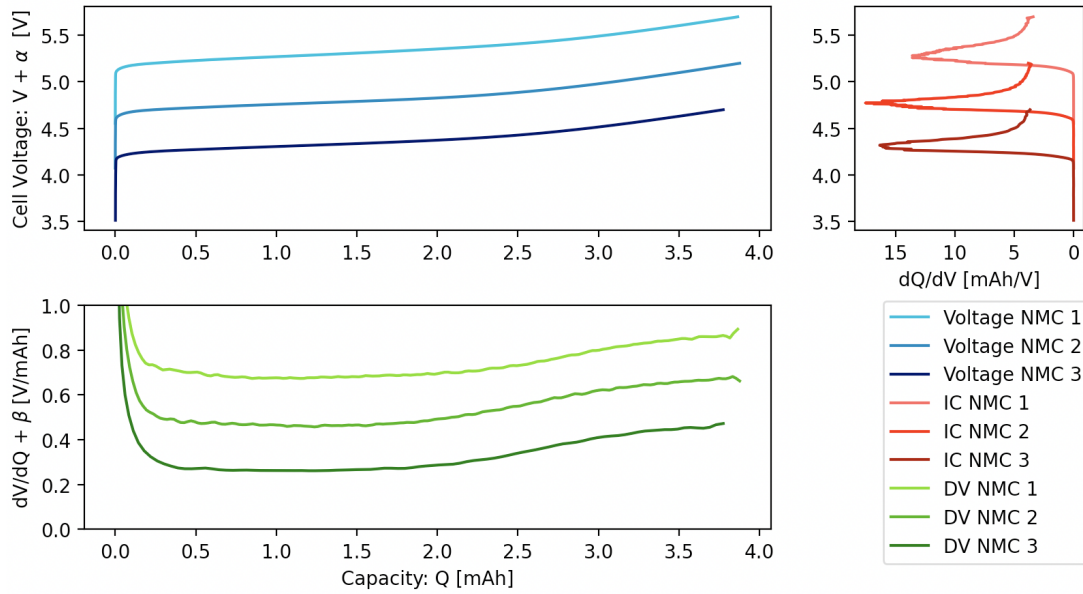
Figure 4.5: *A figure combining DVA and ICA for the three non-contaminated NMC111 cells. An arbitrary offset α of 0.5 V has been added to each curve in the ICA and voltage plot, for clarity. An arbitrary offset β of 0.2 mAh has been added to each curve in the DVA for clarity. Noise reduction 5*

From Figure 4.5 it is clearly observed that the curves have similar characteristics. Of these cells, it is apparent that *NMC 1* and *NMC 2* have different maximum peaks in the ICA. This reveals a slight variation in stagnation at the centre of the voltage capacity plot. When analysing the voltage capacity relation, this difference is difficult to spot. This highlights the effectiveness of ICA and DVA.

The non-contaminated NMC111 cells are stable cells. Therefore, these can be used as a reference for how the voltage of the contaminated cells should appear. Since the non-contaminated cells behave so similar, *NMC 1* will continue to represent the non-contaminated cells moving forward.

4.1.2   Contaminated batteries

Batteries inserted with copper powder as a contaminant were made in two batches. The first batch introduced copper into the batteries using a small metal spatula. The amount of copper was determined using Faraday's law, shown in Equation 2.24, and the specific capacity given by the battery manufacturer of 200 mAh/g. For the first batch, the amount of copper was calculated from 5% of the cathode capacity. This was approximately 400 µg of copper. Using Equation 4.1, an estimated amount of copper particles was calculated to be 935 particles.

$$Particles = \frac{m_{cu}}{\rho V_{particle}} = \frac{3m_{cu}}{4\rho \pi r_{particle}} \tag{4.1}$$

An overview of all the contaminated cells and the amount of copper used in each is presented in Table 4.1. In the second batch, the dispersion method explained in the methodology was used to insert the copper.

Table 4.1: *An overview of the contaminated cells, including which batch the battery belongs to, the battery's name and the amount of copper powder contamination used in the battery.*

Batch	Name	Amount of copper	Copper particles
1	400 cont. 1	400 µg	935
	400 cont. 2	400 µg	935
	400 cont. 3	400 µg	935
	400 cont. 4	400 µg	935
2	70 cont.	70 µg	163
	78 cont.	78 µg	181
	40 cont.	40 µg	94
	<40 cont. 1	< 40 µg	<94
	<40 cont. 2	< 40 µg	<94

Using the spatula to manually measure copper contamination meant the exact amount became uncertain. Cell *400 cont. 1* and *400 cont. 2* are presented in Figure 4.6. The pictures were taken right after the copper was introduced, after the second round of electrolyte. In *400 cont. 1* the contaminant was spread out, while in *400 cont. 2* the contaminant was concentrated on one point. This was done to observe if the placement of the copper would affect the cells in any way. The amounts in Figure 4.6a and Figure 4.6b are visually different. *400 cont. 1* looks to have significantly more copper than *400 cont. 2*. This might just be due to the perspective of the picture, or the spread of the copper in *400 cont. 1*. Since there is no way to know if *400 cont. 1* or *400 cont. 2* are closer to the specified amount of copper, both are assumed to contain 400 µg. *400 cont. 3* and *400 cont. 4* had amounts visually closer to *400 cont. 2*.

(a) *Contaminated NMC111 400 cont. 1.*

(b) *Contaminated NMC111 400 cont. 2.*
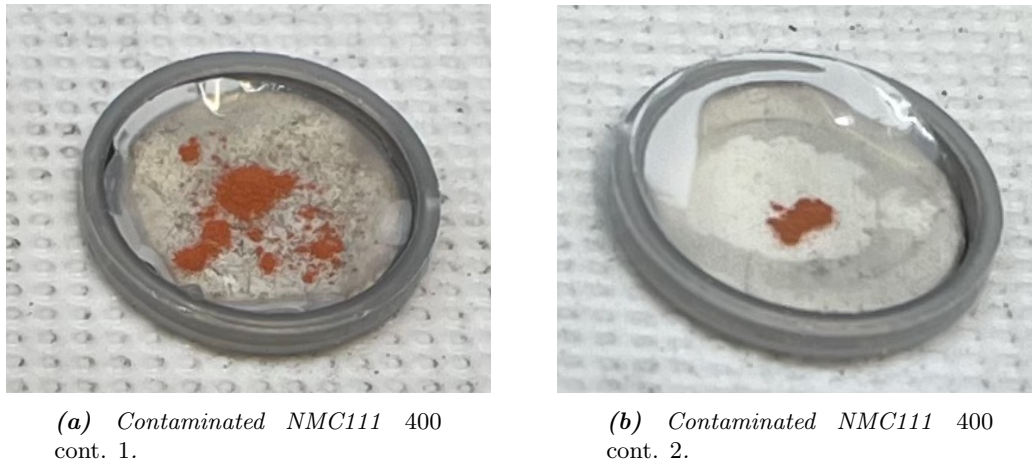
Figure 4.6: *Picture of contaminated cells* 400 cont. 1 *and* 400 cont. 2 *during implementation of copper contaminant.*

Figure 4.7 shows the voltage curve for *400 cont. 1.* It can be observed that this voltage curve does not resemble the reference curve presented in Figure 4.1. The contaminated cell curve is much more random and erratic. The cell starts off by quickly increasing its voltage. Thereafter, the voltage drops to about 1.3 V, then continues to fluctuate between 2 V and 2.5 V. After this, the voltage becomes less erratic and rises slowly, with voltage spikes appearing at seemingly random intervals. These behaviours are characteristic of all the contaminated cells.
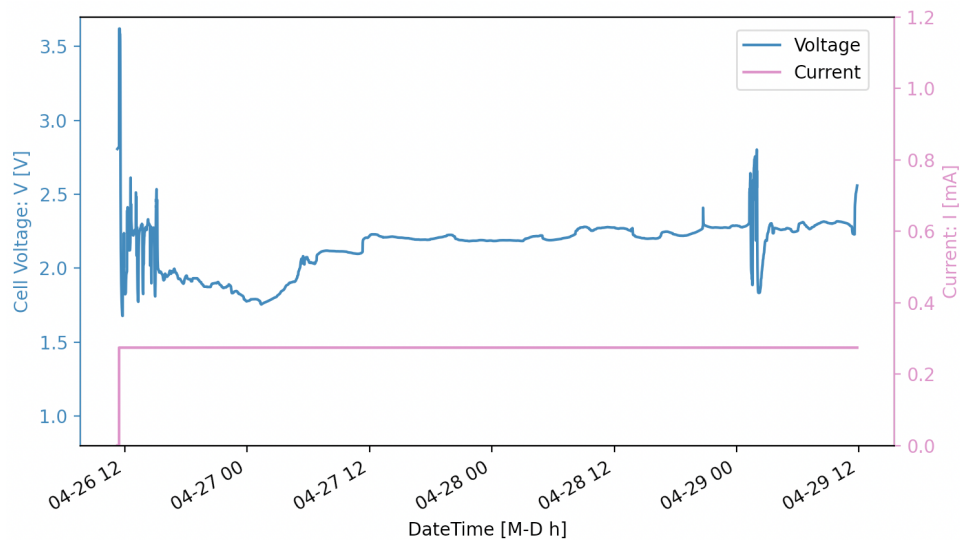
Figure 4.7: *The voltage and current of* 400 cont. 4 *during the cycling test. Noise reduction 5*

The erratic voltage of the first batch was hypothesised to be caused by too much added copper. Therefore, a second batch of cells was made with a smaller amount of copper contamination. This batch used the dispersion method described in the Methodology. Firstly, the calculation percentage was reduced to 1% of the cathode capacity. Secondly, the capacity value was changed. Using the discharge capacity from the reference cell, the actual specific capacity was calculated to be about 140 mAh/g. Using the updated values, the new amounts of copper contamination were calculated. Additionally, the second batch introduced more variations in the amount of copper used in each cell. This was done to observe how different amounts affected the cells. The amounts are summarised in Table 4.1. The second batch had similar voltage curves to the first contaminated batch. Even though the voltage curves are more or less random and difficult to explain, there are some parts of the curve that share similar characteristics.

Further discussion will focus on the first batch of contaminated cells. The first batch was chosen because it has similar amounts of copper, they therefore have more similar curves. The second batch of contaminated cells proved more random, making it harder to make connections and explanations. Still, comparisons with the second batch will be done when possible. Figure 4.8 shows the complete voltage curve for *400 cont. 4* along with smaller highlighted areas.
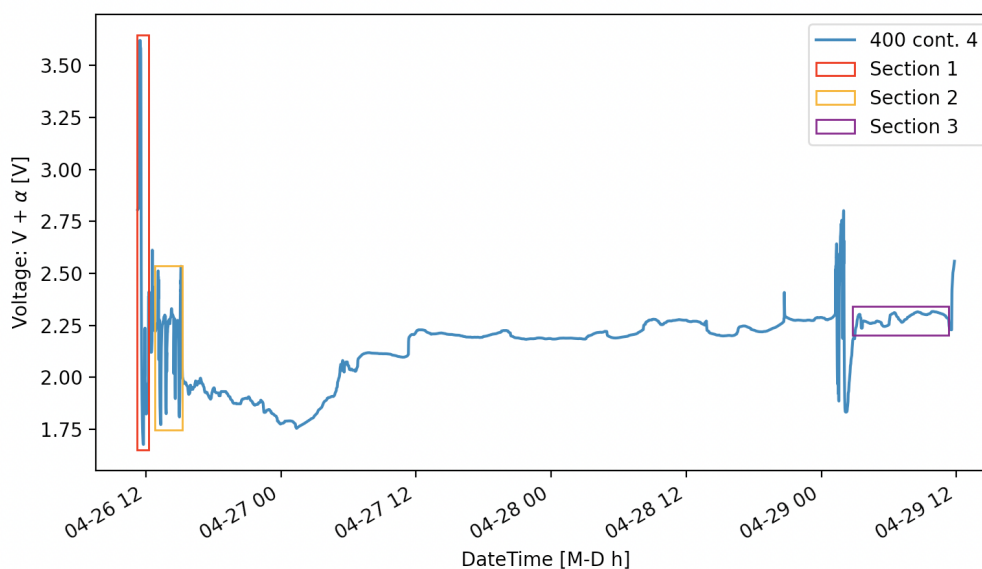
(a) Whole voltage curve for 400 cont. 4
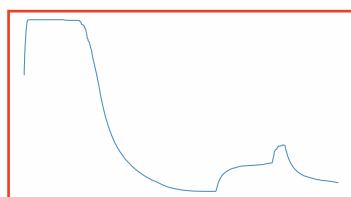
(b) Section 1
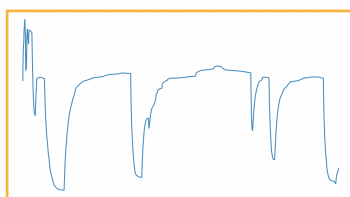
(c) Section 2
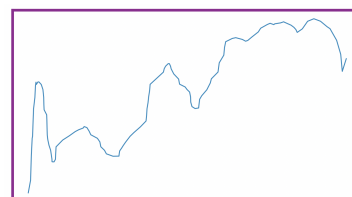
(d) Section 3

Figure 4.8: *A complete figure which dissects the whole voltage curve into sections and presents these sections for further analysis.*

Figure 4.8a shows the sections of the voltage curves that are the most interesting. Figure 4.8b, 4.8c and 4.8d are enhanced plots from the marked sections in Figure 4.8a. These sections will be discussed separately in the following chapters.

4.1.3   Section 1 - The first slope

Analysing the voltage curve of the first batch, similar patterns can be observed. In particular, the first 0.03 mAh of the cycling showed similar behaviours. This segment is highlighted by Section 1 in Figure 4.8. This first segment for the entire batch is combined and presented in Figure 4.9. The figure also includes the reversible potential for the different copper reactions against lithium.
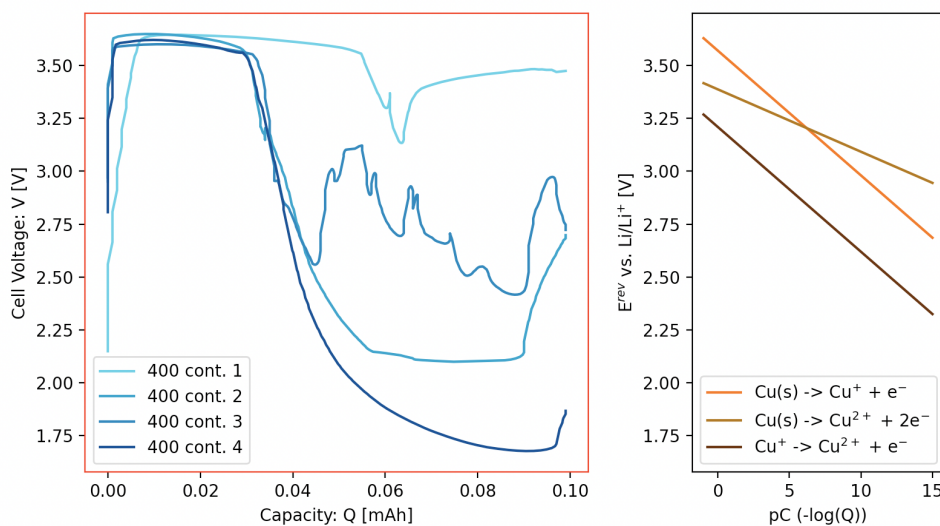
Figure 4.9: *Section 1 of the voltage of batch 1 during the cycling test. The right plot is the reversible potentials of copper reactions versus lithium. Noise reduction 5.*

It can be difficult to differentiate between the different curves in Figure 4.9. Therefore, an alpha value has been added similarly to earlier plots. The separated curves are presented in Figure 4.10. However, Figure 4.9 is still necessary to find the correlation between the voltage and the copper reactions.
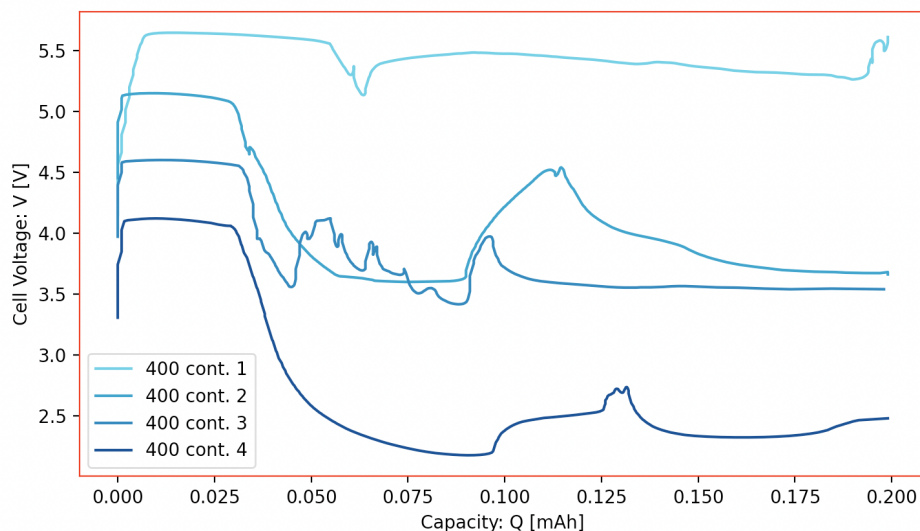
Figure 4.10: *Section 1 of the voltage of batch 1 during the cycling test. An arbitrary offset α of 0.5 V has been added to each curve for clarity. Noise reduction 5.*

What stands out the most in the Figure 4.10, is the plateau after the initial increase in voltage. When the cells reach about 3.6 V the voltage becomes approximately constant until the capacity reaches about 0.03 mAh. This is except for *400 cont. 1* which has a constant voltage to about 0.06 mAh. The section of this plateau is highlighted with red lines in Figure 4.11. After this plateau, the cells experience a drastic voltage drop. The voltage drop is different in length and magnitude for each cell. After this, all the cells start charging again, but after accumulating voltage the cells experience another drop. Furthermore, it is clear that the voltage of the cells becomes more erratic after the first drop.
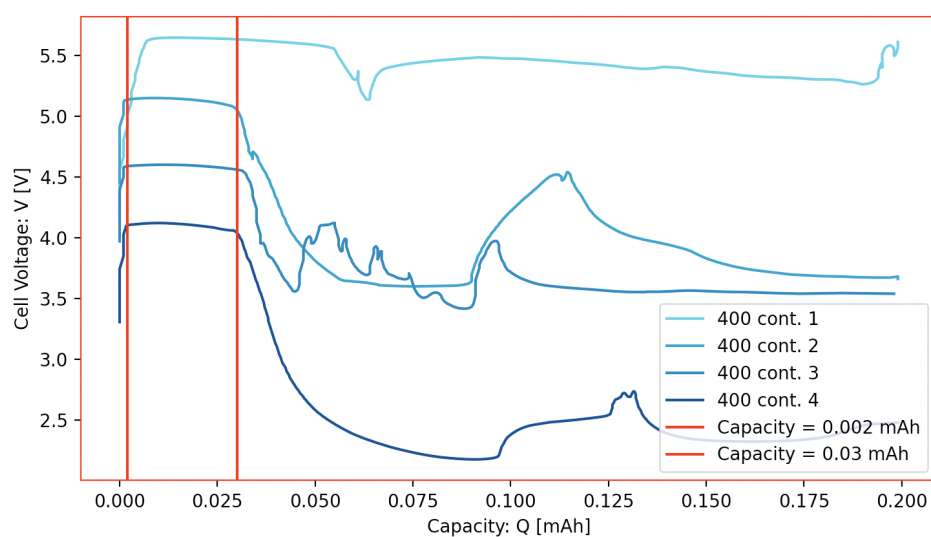
Figure 4.11: *Section 1 of the voltage of 400 cont. 1 during the cycling test. Red lines have been added to mark the plateau. An arbitrary offset α of 0.5 V has been added to each curve for clarity. Noise reduction 5.*

This plateau occurs at around 3.6 V, which is close to the voltage that copper reacts with lithium ions. Faraday's law was used with a total 0.03 mAh of electric charges transferred, two electrons per reaction and the copper molar mass of 63.55 g/mol. According to this calculation, about 35.5 µg of copper should have reacted. This is only about 9% of the total copper introduced into the cell.

This pattern can also be observed in the second batch of contaminated cells. As seen in Figure 4.12a the reaction occurs at a similar voltage of 3.6 V. However, the cut-off is about 0.015 mAh for at least three of the cells. *<40 cont. 3* starts to drop off at about 0.05 mAh, while *78 cont.* does not have a drop in voltage like the other cells. 0.015 mAh is about half of the electric charge applied to the first batch before a change happened. This might be because the total amount of copper powder contamination in batch two also is lower. With 0.015 mAh applied, only 17.8 µg could have reacted, which is less than the total copper contamination in all the cells. The change in voltage is therefore not caused by a depletion of available copper. Rather, it seems that after this amount of electric charge is applied to the battery, the number of copper ions in the cell reaches a critical point where a new reaction can occur.
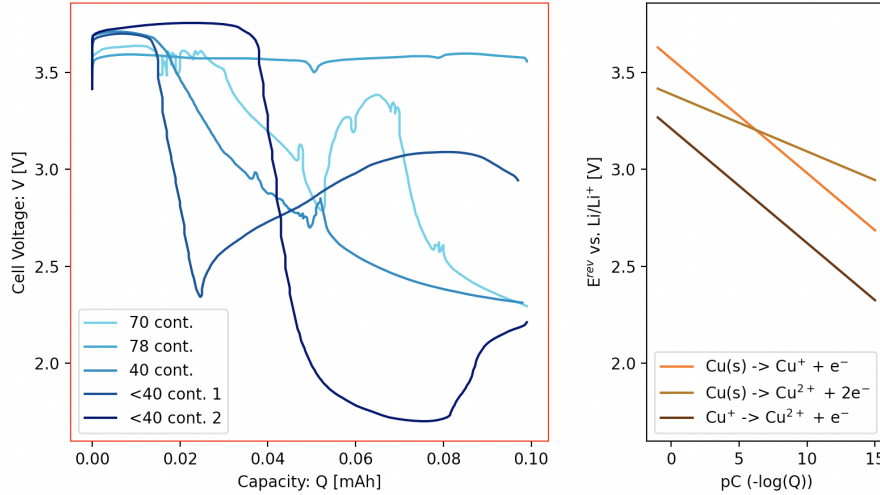
(a) *Section 1 of the voltage of batch 2 during the cycling test. The right plot is the reversible potentials of copper reactions versus lithium. Noise reduction 5.*
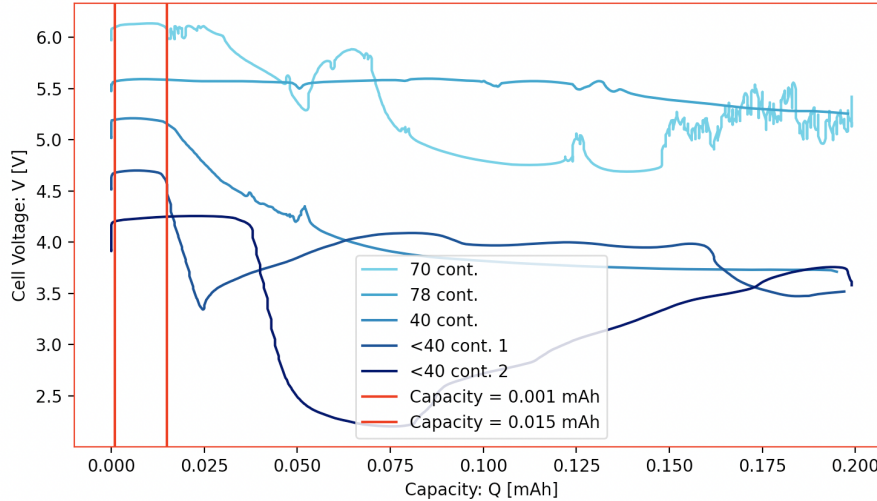
(b) *[Section 1 of the voltage of batch 2 with an α value]Section 1 of the voltage of batch 2 during the cycling test. An arbitrary offset α of 0.5 V has been added to each curve for clarity. Noise reduction 5.*

Figure 4.12: *Plots used to analyse batch 2*

The start of each contaminated cell follows a similar pattern. A plausible theory for this behaviour is dendrite growth. The copper powder is introduced into the cell on the cathode side. When the cell reaches a critical voltage of 3.6 V, the copper reacts and is oxidised to copper ions. These ions travel through the separator. The copper ions can then reach the lithium metal, where they almost instantly react back into copper metal. This occurs because lithium metal is highly reactive. When copper reacts back into metal, small spikes or pillars of copper can be created, these are called dendrites. If these dendrites reach a certain size, they could puncture through the separator and cause an ISC. The ISC causes the cell's voltage to rapidly decline, which would explain the drop. Though, knowing exactly what reaction occurs inside the battery would require a more advanced form of analysis.

4.1.4   Section 2 - Following the first slope

After the initial voltage drop, the voltage in the cells starts to differ. Looking closer at section 2 for *400 cont. 4*, presented in Figure 4.13, this behaviour is observed. At 0.3 mAh the voltage spikes towards 2.5-2.6 V before decreasing. The cell's voltage again spikes at 0.45 mAh and ultimately drops to about 1.8 V. Between 0.5 mAh and 1 mAh the voltage behave similarly, but at a lower voltage and over larger capacity spans. Here the voltage appears to have more of the stagnation that appeared in section one before dropping in voltage. The voltage drop after the spikes is very similar to the voltage drop appearing in section 1. However, considering that the cell does not reach 3.6 V, the copper contaminant might be reacting with something apart from lithium.
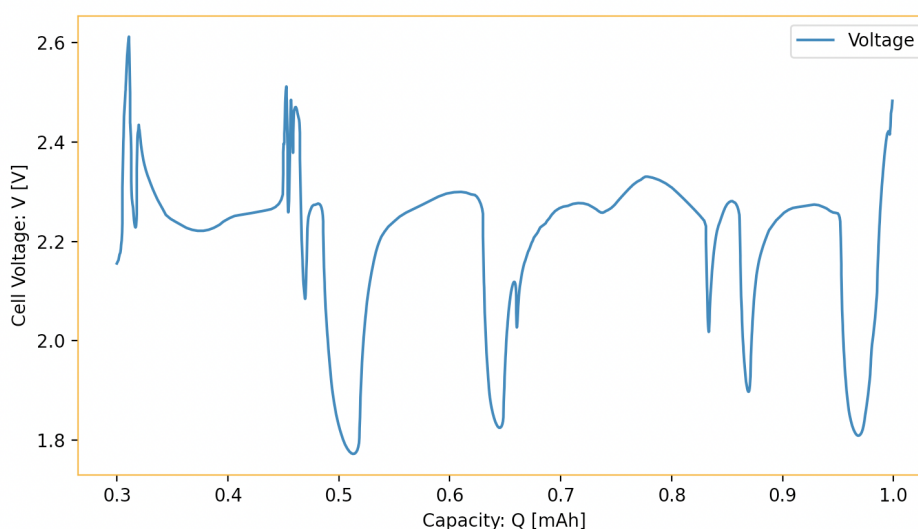
Figure 4.13: *Section 2 of the voltage of* 400 cont. 1 *during the cycling test. Noise reduction 5.*

This fluctuation can be related to other redox reactions occurring at lower potentials. After the primary reaction, the cell accumulates copper ions. These ions could react with other metals like nickel, iron, aluminium, or lithium. These reactions are spontaneous and should only release their energy as heat. However, if the reaction occurs from one side of the separator to the other, it would cause the reaction to release its energy as a current instead. This way, the reaction would act like a discharge, since electrons cannot pass through the separator.

Another possibility is the formation of dendrites. When the first dendrites from section 1 cause an ISC, large amounts of current pass through it. This would release large amounts of heat and will melt the dendrites. When the dendrite has melted, the copper can react into ions and start the formation of dendrites again. The cycle of dendrite formation, ISC, and melting matches the continues fluctuation and could explain the erratic behaviour.

4.1.5   Section 3 - End of the curve

Figure 4.14 presents all the full voltage curve data for the first batch of cells. The previous chapter discussed the second section of these curves, and thereafter, the curves look mostly random. However, towards the end of the curves they seem to stabilise between 2.1 V to 2.3 V. Zooming in on section 3 presents a clearer picture, and is presented in Figure 4.15.
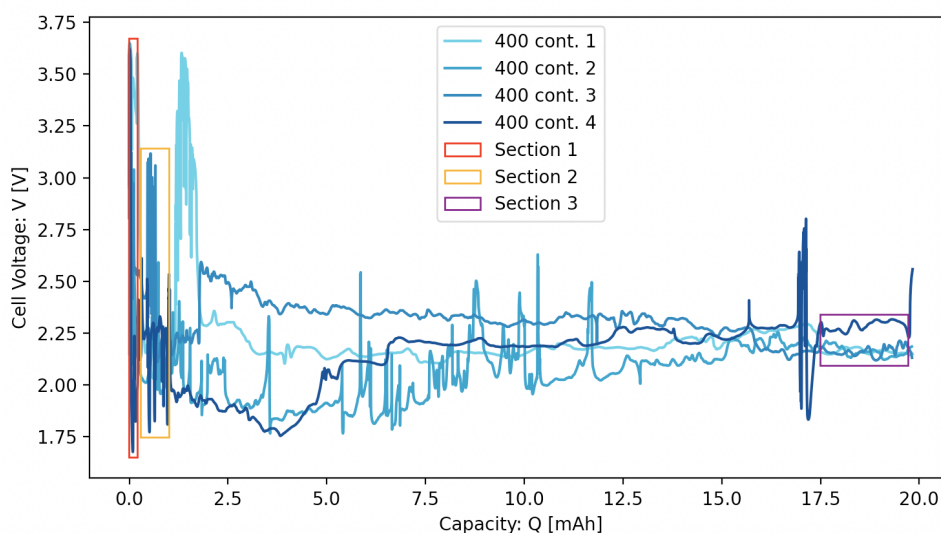
Figure 4.14: *The whole voltage curve of batch 1 during the cycling test. The same sections are highlighted. Noise reduction 5*

The curves in Figure 4.15 still experience fluctuations, but they seem to have calmed down. The fluctuations are still believed to be caused by either the formation and melting of dendrites, or by other redox reactions occurring in the cell. But these fluctuations are not as severe any more. The reason for this could potentially be that the reactions are reaching an equilibrium. Meaning that the redox reactions reach their chemical equilibrium. At the same time, the dendrites reach a state where they melt away immediately after being formed. This makes the effect of an ISC minimal. Even though the cell has a current applied to it, these equilibriums hinder the cell from increasing in voltage, making the cell unusable.
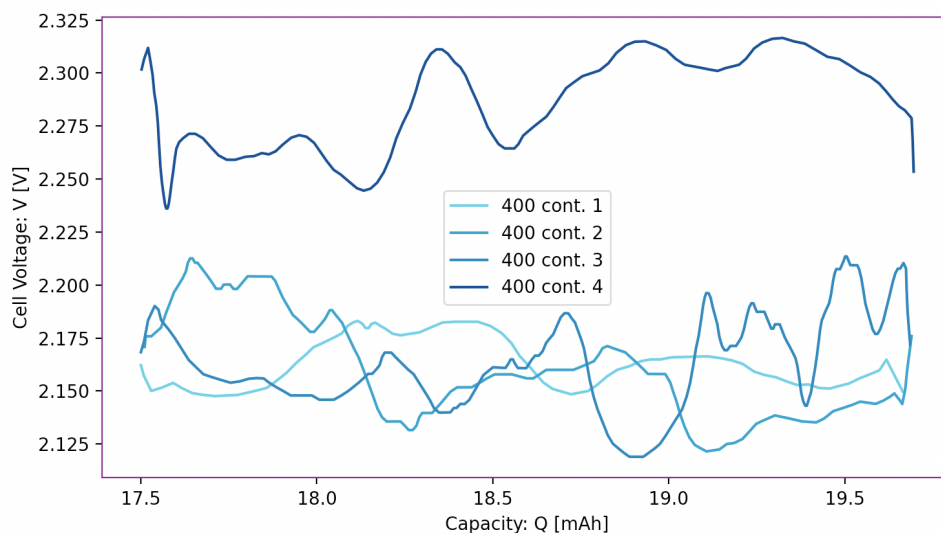
Figure 4.15: *Section 3 of the voltage of batch 1 during the cycling test. Noise reduction 5.*

The three sections are widely different, but can be attributed to the same cause. The first section described a common plateau and a subsequent ISC for all the contaminated cells. The second section is where the cells started to differentiate, and the voltage became erratic and unpredictable. Dendrite growth and ISC is theorized to be the main contributor to this behaviour. Continuing on into the last section, the voltage extremities seem to have shrunk and the reactions grow less erratic. A causation for this could be that the reactions reach an equilibrium.

4.2   Error analysis

The contaminated batteries did not behave as expected. The hypothesised behaviour was voltage curves with a stagnation in growth at around 3.6 V. The plateau would be the contaminant reacting with lithium ions to create copper ions. This would last until all the copper had reacted, before continuing the cycling. These copper ions would then move through the separator before reacting with the solid lithium at the anode and stabilizing. However, this is not happening. Instead, as discussed earlier, a short-circuit occurs. The following section will discuss potential reasons for this.

Too much contaminant is the most likely error. In the first batch of contaminated cells, 400 µg of copper was implemented. The reasoning for this amount was an article on "The influence of metallic contaminants on the electrochemical and thermal behavior of Li-ion batteries" [45]. Here they experienced good results with contaminants equal to 1% of the cathode weight. When the first batch short-circuited, the second batch was created with smaller amounts. The smallest amount of copper implemented in the cells was about 40 µg. This is a tiny amount of copper, but as witnessed from the results, the cells short circuit and fail. After revisiting the article on metallic contaminants, the method of implementing the copper stood out. This article had mixed the copper into the slurry of the cathode. Since this experiment did not involve creating electrodes, this method could not be tried. In a different article, "Life-cycle evolution and failure of metal contaminant defects in lithium-ion batteries" [44], they experienced good results with 5 to 20 particles of contaminant. Due to the lack of high accuracy instruments, this amount was not realistic to implement.

When creating the cells, the process of measuring small amounts of contaminant was a limiting factor. The scale inside the glovebox was unable to register any weight smaller than 3-4 mg. With this limitation, different methods of estimating weight were used. In the first contaminated batch, the spatula was used to repeatedly measure a small amount until the weight registered 4 mg. Dividing this on the number of measured amounts, the weight of each amount could be estimated. The result was a spatula amount of about 0.4 mg. This method of measuring is inaccurate. Assuming an uncertainty of 0.1 mg, the combination of amounts during the measuring becomes very uncertain. During the creation of the second batch, the copper was mixed with the electrolyte. This method involved creating a dispersion with a known concentration of 10 g/L. Then pipette different amounts of the contaminated electrolyte in combination with non-contaminated electrolyte. The problem with this method was not being certain of the amount of copper in the pipette. Since copper does not dissolve in the electrolyte, the particle distribution can become uneven. One pipette might have few particles, while another could have many. The amounts calculated in Table 4.1, assumes an even distribution of copper particles in the electrolyte.

A general source of uncertainty about these results is the number of batteries. The preface explains that a large portion of the produced batteries did not work, due to a faulty electrolyte. This was discovered too late into the project to correct for. The consequent of this is that the results presented in this thesis are not fully reliable. The results found might be outliers. Thus, a larger dataset is required to assess the certainty of the results.

4.3 Economic Aspects

The formation and ageing take up 32.6% of manufacturing cost. The reason for the large process cost is floor space. In the BatPac model presented in the introduction, floor space cost is estimated at $3,000/m^2 per year. It can also be observed that the floor space needed for the formation and ageing is 3,550 m^2, 23% of the total manufacturing space. The resulting annual cost of floor space is calculated to $10.65 million. This is 35% of the total annual process cost. The large necessary floor space is due to each cell needing their own module for formation, before being left for a 2-week ageing process to check self discharge. The ageing itself is a simple process, and does not require much labour or equipment. If this process could be expedited, or if the space needed could be limited, millions of monies could be saved.

Earlier detection of contaminants could have great implications for the LIB economy. The most common battery analysis methods are conducted post-production. Checking self discharge after ageing gives a good indicator of battery performance, and if a cell has been contaminated it is likely to show an abnormal amount of self discharge. However, this can result in many contaminated batteries needing to be recycled after the ageing is finished. DVA and ICA could have a great impact on this. Considering that these methods are non-destructive and able to be applied during the formation. If programs are created that use DVA and ICA to look for contamination, faulty batteries could be recycled before ageing. The result would be minimal wasted floor space for contaminated cells during formation and ageing.

The BatPac model estimated that about 5% of cells are rejected after ageing. For calculation purposes, 10% of the discarded cells were assumed to be recycled because of contamination. This means 0.5% of the entire production would go through ageing unnecessarily. In the BatPac this is equivalent to 17.75 m^2, or $53,250 /year wasted on contaminated cells. Scaling the BatPac model up to that of Teslas gigafactory in Nevada, the potential savings become clear. With a size of 500,000 m^2, assuming a floor space percentage equal to the BatPac model, 115,000 m^2 are allocated to formation and ageing. With 0.5% contaminated cells, 575 m^2 or $1.725 million per year are wasted. With the planned expansion of the gigafactory to 100 GWh, $4.66 million would be wasted every year. This is an assumed scenario, but the potential of early contamination detection is clear.

4.4   Environmental Aspects

As the demand for battery capacity grows, so does the space needed for battery manufacturing. In the economic theory, a 500,000 m^2 Tesla Gigafactory producing about 40 GWh/year worth of battery capacity is presented. Using these parameters combined with the expected capacity need of 2.5TWh by 2030, a calculated area of 31,500,000 m^2 is needed. Comparably, this amounts to a 157,500 m long, 200 m wide strip of 63 gigafactories. This equates to the distance between Oslo and Geilo, Norway, or San Diego and Los Angeles, USA. This will have a significant environmental footprint. And as the demand is expected to grow by 25% every year, this stretch of factories needs to be much longer or produce batteries at a much higher capacity. This goes without considering the environmental aspects of such demand. There are no guaranties that the world can sustain a decarbonized transport and energy sector. The changes needed are undauntedly challenging, as developing countries do not have the same starting point as developed ones. Accordingly, it would be problematic to assume that these can effectively conform to the same infrastructural changes.

Developing countries are often the sources for minerals, such as lithium and cobalt. As demand grows, these countries will both gain and struggle the most. The difference between using renewable energy is vital for reducing GHG emissions. Developed countries have this option, but developing countries in Africa and South America do not. This results in a lesser evil on the total emission scale. A decarbonized energy and transport sector for the developed countries, but more emissions stemming from mineral mining and treatment. As lower standards are used, the risk of child labour, toxic waste disposal in nature, and GHG emissions are the main areas of concern. In the coming decades, developing and developed countries will have to address these issues, to not only prevent environmental damage, but to help developing countries thrive.

Batteries are a significant contributor to decarbonization, and proves this through electric vehicles and as a stabilizing factor in the energy grid. The only fault with this example is that it is often taken from countries with a highly renewable energy mix. Here, great efforts have been made to build the necessary infrastructure to support electrical transportation. The problem then moves to fossil fuelled countries, which want to transition to energy sources such as wind and solar energy. These intermittent energy sources depend on weather, deeming them incomplete elements in a power grid. If a grid is to depend on these power sources, large-scale energy storage is imperative. This energy storage needs to support hours of high load and make up for reduced power production caused by weather fluctuations. In such a case, lithium-ion batteries can be a part of the solution to provide a complete and reliable power grid.

Withholding from a plan to build and use battery solutions is likely to be an impactful threat to the Paris Agreement's goals. A battery storage solution based upon lithium-ion batteries is highly researched and known as a stable energy storage solution. For the world to decarbonize the energy and transport sector, global cooperation is required. The change of equipment, power grid, and regulating power systems is necessary. This change seems to be the biggest hurdle for government regulators to overcome, as the cost versus gain is still considered too high.

With a growing demand for minerals, alternative methods of mineral extraction need to be considered. Recycling is one of these possibilities and has the potential to change how we produce batteries. Ultimately, these minerals can be sourced from the batteries that are detected with contamination. An early detection of this contamination lets the minerals re-enter the production cycle without wasting energy on formation and ageing. As studies suggest a resource saving of 51% by recycling, the argument for such a solution is clear. However, the recycling of LIBs is a tedious and costly process. Consequently, recycling will likely not be a reality unless it is economically viable.

⊡ NTNU

5 Conclusion

Batteries are a significant contributor to stopping the global climate crisis. LIBs part in transforming the transport and energy sectors is essential. Therefore, making battery manufacturing more efficient and sustainable is equally important. This thesis has focused on improving the detection of metal contamination as early into the production phase as possible.

The most significant discovery in this research has been the creation of a new analysis tool, in the form of the combined figure. This plot combines the voltage capacity relation, with a DVA plot, an ICA plot, and the reversible potential of metal contaminants over a range of concentrations. This combination allows for multiple analysis forms at the same time, while enhancing the possibility of determining relations between these different forms.

Three uncontaminated NMC111 cells were assembled and cycled. These cells behaved as expected and therefore served as reference cells for the contaminated cells. Nine contaminated cells with different amounts of contamination were made. These cells had less fortunate results. Nonetheless, these cells were analysed. A similar pattern at the start of the cycling was discovered. The cell's voltage stagnates at around 3.6 V where it plateaus, before the voltage drops. The length of this plateau differed with the amount of contamination.

This behaviour is theorised to be copper reacting to ions, forming dendrites and subsequently short-circuiting the cell. Because of the high current, the dendrites then melt away. Thereafter, the cell turn more erratic. This is believed to be caused by the same dendrite growth, causing ISCs of smaller magnitudes. This causes the cell's voltage to fluctuate continuously. This fluctuation eventually becomes less intense, and the voltage of the cells stabilise between 2.1-2.3 V.

The limited number of cells used in the thesis was caused by faulty electrolyte. This greatly hindered battery production. The defect was discovered too late into the project to be rectified.

The formation and ageing step is responsible for the largest share of the battery manufacturing cost. This is shown in an economic analysis utilizing the BatPac model. The model assumes 5% of batteries are discarded after formation. For calculation purposes, 10% of discarded batteries were assumed to be discarded because of metal contamination. This means that about 0.5% of manufactured batteries are contaminated with metal. If this contamination could be discovered earlier, approximately 572 m^2 of floor space and \$1.725 million could be saved each year per gigafactory.

Further studies should explore the potential of the combination figure. A larger sample size needs to be made, and different chemistries should be tested. In addition, different C-rates and cycling procedures should be tested. Finally, a new way to introduce an accurate amount of copper must be devised.

6 Further work

This bachelor's thesis is limited both in time and in the number of working cells available to study. Making new cells can take up to a week, depending on wetting time and C rate. Further work should therefor start with making working contaminated cells.

A problem identified in this paper was that the amount of copper used probably was too high. This was mostly due to the methods for introducing copper were too inaccurate. Therefore new methods of measuring and inserting copper should be investigated. One example of a new method would be to insert the copper into the slurry before mix, and in that way the amount of copper introduced could be accurately determined.

With working copper contaminated cells, what actually happens inside the cells could studied more closely. Firstly opening the cell and visually assessing them might be interesting. Further more advanced analysis methods could be applied, an example of this would be SEM. Another experiment would be to take out the contaminated cathode after cycling and reuse it with a new anode, separator and electrolyte. Additionally, self discharge could be measured to study the effect of contaminants and if the self discharge could be predicted.

In addition, cells with different electrode chemistries should also be studied. Most importantly using a graphite anode should be tested, since graphite is less reactive than lithium metal and might decrease dendrite creation. Firstly a graphite reference cell should be made to show the formation. Then a contaminated cell could be made and the effect of copper on the formation of the SEI could be studied, as it might help to detect the copper contamination. Different cathode chemistries could also be interesting to try and see if they react differently to copper.

More experimentation with the cycle parameters should also be done. This paper mainly used a C/20 rate when cycling the cells. Higher C rates should be tested to see if similar voltage curves are created. This would be more comparable to how commercial batteries are cycled. In addition a longer CVC step should be used to charge the battery fully. A complete charging of the battery is needed to determine the actual capacity of the battery.

Further analysis of the voltage curves could also be preformed. Looking at the vertical displacement of the voltage could indicate the ohmic resistance in the cell and a quicker increase in voltage could be caused by the concentration losses.

References

[1] *A Vision for a Sustainable Battery Value Chain in 2030.* [Online; accessed 23. Apr. 2024]. Sept. 2019. URL: https://www3.weforum.org/docs/WEF_A_Vision_for_a_Sustainable_Battery_Value_Chain_in_2030_Report.pdf?fbclid=IwAR0c9kVo1o7sHVxLI7_Da3GF-9-QsuaGBVOgmKjvWeeyG1O7FOpV_-U5AGo.

[2] Martin Linder et al. *The race to decarbonize electric-vehicle batteries.* Feb. 2023. URL: https://www.mckinsey.com/industries/automotive-and-assembly/our-insights/the-race-to-decarbonize-electric-vehicle-batteries.

[3] *This chart shows which countries produce the most lithium.* [Online; accessed 23. Apr. 2024]. Jan. 2023. URL: https://www.weforum.org/agenda/2023/01/chart-countries-produce-lithium-world.

[4] C.M. Costa et al. "Recycling and environmental issues of lithium-ion batteries: Advances, challenges and opportunities". In: *Energy Storage Materials* 37 (2021), pp. 433–465. URL: https://www.sciencedirect.com/science/article/pii/S2405829721000829.

[5] Yangtao Liu et al. "Current and future lithium-ion battery manufacturing". In: *IScience* 24.4 (2021).

[6] *The 17 Goals to Sustainable Development.* [Online; accessed 24. Apr. 2024]. Apr. 2024. URL: https://sdgs.un.org/goals.

[7] The Tesla Team. *Continuing Our Investment in Nevada.* 2023. URL: https://www.tesla.com/blog/continuing-our-investment-nevada.

[8] Evlithium. *Everything You Need to Know About the 4680 Battery.* 2023. URL: https://www.evlithium.com/Blog/4680-battery-power-innovation.html.

[9] Fred Lambert. *Tesla announces 4680 battery cell production breakthrough.* 2023. URL: https://electrek.co/2023/10/11/tesla-4680-battery-cell-production-breakthrough/.

[10] Paul A Nelson et al. *Modeling the performance and cost of lithium-ion batteries for electric-drive vehicles.* Tech. rep. Argonne National Lab.(ANL), Argonne, IL (United States), 2019.

[11] Victoria Klesty. "Tesla extends lead in Norway sales, EVs take 82% market share". In: *Reuters* (Jan. 2024). URL: https://www.reuters.com/business/autos-transportation/tesla-extends-lead-norway-evs-take-record-82-market-share-2024-01-02.

[12] Reuters. "Lifetime carbon emissions of electric vehicles vs gasoline cars". In: *Reuters* (July 2021). URL: https://www.reuters.com/business/autos-transportation/lifetime-carbon-emissions-electric-vehicles-vs-gasoline-cars-2021-06-29.

[13]   *Car numbers and mileage up*. [Online; accessed 24. Apr. 2024]. Apr. 2024. URL: `https://www.ssb.no/en/transport-og-reiseliv/artikler-og-publikasjoner/car-numbers-and-mileage-up`.

[14]   Carmeuse Systems. *Lithium Extraction and Refining Technology*. [Online; accessed 4. May 2024]. May 2024. URL: `https://systems.carmeuse.com/en/industries/lithium-extraction`.

[15]   Odne Stokke Burheim. *Engineering Energy Storage*. Academic Press Inc, 2017.

[16]   John Collins, Gerald Gourdin, and Deyang Qu. "Chapter 3.23 - Modern Applications of Green Chemistry: Renewable Energy". In: *Green Chemistry*. Ed. by Béla Török and Timothy Dransfield. Elsevier, 2018, pp. 771–860. ISBN: 978-0-12-809270-5. DOI: `https://doi.org/10.1016/B978-0-12-809270-5.00028-5`. URL: `https://www.sciencedirect.com/science/article/pii/B9780128092705000285`.

[17]   MIT Electric Vehicle Team. "A Guide to Understanding Battery Specifications". In: *MIT* (2008). URL: `https://web.mit.edu/evt/summary_battery_specifications.pdf`.

[18]   Sabine Piller, Marion Perrin, and Andreas Jossen. "Methods for state-of-charge determination and their applications". In: *Journal of power sources* 96.1 (2001), pp. 113–120.

[19]   Stefano Passerini et al. *Batteries: present and future energy storage challenges*. John Wiley & Sons, 2020.

[20]   Allan G Blackman. *Aylward and Finley´s Si Chemical Data 7th edition*. John Wiley and Sons Australia Ltd, 2014.

[21]   Arnulf Latz and Jochen Zausch. "Thermodynamic derivation of a Butler–Volmer model for intercalation in Li-ion batteries". In: *Electrochimica Acta* 110 (2013). ELECTROCHEMISTRY FOR ADVANCED MATERIALS, TECHNOLOGIES AND INSTRUMENTATION, pp. 358–362. ISSN: 0013-4686. DOI: `https://doi.org/10.1016/j.electacta.2013.06.043`. URL: `https://www.sciencedirect.com/science/article/pii/S0013468613011493`.

[22]   A. Chagnes et al. "Modeling viscosity and conductivity of lithium salts in y-butyrolactone". In: *Journal of Power Sources* 109.1 (2002), pp. 203–213. URL: `https://www.sciencedirect.com/science/article/pii/S0378775302000733`.

[23]   Michael S. Ding. "Electrolytic Conductivity and Glass Transition Temperature as Functions of Salt Content, Solvent Composition, or Temperature for LiPF6 in Propylene Carbonate + Diethyl Carbonate". In: *Journal of Chemical & Engineering Data* 48.3 (2003), pp. 519–528. URL: `https://doi.org/10.1021/je020219o`.

[24] M Menzinger and Re Wolfgang. "The meaning and use of the Arrhenius activation energy". In: *Angewandte Chemie International Edition in English* 8.6 (1969), pp. 438–444.

[25] Xingxing Wang et al. "Effects of Different Charging Currents and Temperatures on the Voltage Plateau Behavior of Li-Ion Batteries". In: *Batteries* 9.1 (2023). URL: `https://www.mdpi.com/2313-0105/9/1/42`.

[26] Gert Berckmans. "Cost Projection of State of the Art Lithium-Ion Batteries for Electric Vehicles Up to 2030". In: *Energies* 10 (Sept. 2017).

[27] John T. Warner. "Chapter 5 - The Cathodes". In: *Lithium-Ion Battery Chemistries*. Ed. by John T. Warner. Elsevier, 2019, pp. 99–114. ISBN: 978-0-12-814778-8. DOI: `https://doi.org/10.1016/B978-0-12-814778-8.00005-3`. URL: `https://www.sciencedirect.com/science/article/pii/B9780128147788000053`.

[28] Manh-Kien Tran et al. "Comparative Study of Equivalent Circuit Models Performance in Four Common Lithium-Ion Batteries: LFP, NMC, LMO, NCA". In: *Batteries* 7 (July 2021), p. 51. DOI: `10.3390/batteries7030051`.

[29] Royal Swedish Aca-emy of Sciences. *The Nobel Prize in Chemistry 2019*. 2019. URL: `https://www.nobelprize.org/prizes/chemistry/2019/summary`.

[30] Arumugam Manthiram. "A reflection on lithium-ion battery cathode chemistry". In: *Nature communications* 11.1 (2020), p. 1550.

[31] Hui Cheng et al. "Recent progress of advanced anode materials of lithium-ion batteries". In: *Journal of Energy Chemistry* 57 (2021), pp. 451–468.

[32] Francesca Pistorio et al. "Review on the Experimental Characterization of Fracture in Active Material for Lithium-Ion Batteries". In: *Energies* (2022).

[33] Kai Volgmann et al. "Solid-State NMR to Study Translational Li Ion Dynamics in Solids with Low-Dimensional Diffusion Pathways". In: *Zeitschrift für Physikalische Chemie* 231 (Jan. 2017).

[34] Silje Nornes Bryntesen et al. "Opportunities for the State-of-the-Art Production of LIB Electrodes—A Review". In: (2021). URL: `https://www.mdpi.com/1996-1073/14/5/1406`.

[35] Ali Davoodabadi et al. "Effect of calendering and temperature on electrolyte wetting in lithium-ion battery electrodes". In: *Journal of Energy Storage* 26 (2019), p. 101034.

[36] Ali Davoodabadi et al. "On electrolyte wetting through lithium-ion battery separators". In: *Extreme Mechanics Letters* 40 (2020), p. 100960.

[37] F Kong et al. "In situ studies of SEI formation". In: *Journal of power sources* 97 (2001), pp. 58–66.

[38]   David L Wood, Jianlin Li, and Seong Jin An. "Formation challenges of lithium-ion battery manufacturing". In: *Joule* 3.12 (2019), pp. 2884–2888.

[39]   Seong Jin An et al. "The state of understanding of the lithium-ion-battery graphite solid electrolyte interphase (SEI) and its relationship to formation cycling". In: *Carbon* 105 (2016), pp. 52–76.

[40]   John Collins et al. "Carbon surface functionalities and SEI formation during Li intercalation". In: *Carbon* 92 (2015), pp. 193–244.

[41]   Vivian Murray, David S. Hall, and J. R. Dahn. "A Guide to Full Coin Cell Making for Academic Researchers". In: *Journal of The Electrochemical Society* 166.2 (2019), A329. DOI: 10.1149/2.1171902jes. URL: https://dx.doi.org/10.1149/2.1171902jes.

[42]   Fang Dai and Mei Cai. "Best practices in lithium battery cell preparation and evaluation". In: *Communications Materials* 3.1 (2022), p. 64.

[43]   Brandon R Long et al. "Enabling high-energy, high-voltage lithium-ion cells: standardization of coin-cell assembly, electrochemical testing, and evaluation of full cells". In: *Journal of The Electrochemical Society* 163.14 (2016), A2999.

[44]   Yukun Sun et al. "Life-cycle evolution and failure mechanisms of metal-contaminant defects in lithium-ion batteries". In: *Journal of Power Sources* 557 (2023), p. 232591.

[45]   Kae E Fink et al. "Influence of metallic contaminants on the electrochemical and thermal behavior of Li-ion electrodes". In: *Journal of Power Sources* 518 (2022), p. 230760.

[46]   GD Wilcox and DR Gabe. "Faraday's laws of electrolysis". In: *Transactions of the IMF* 70.2 (1992), pp. 93–94.

[47]   G Nagasubramanian and D Doughty. "Improving the interfacial resistance in lithium cells with additives". In: *Journal of power sources* 96.1 (2001), pp. 29–32.

[48]   Won Mo Seong et al. "Abnormal self-discharge in lithium-ion batteries". In: *Energy & Environmental Science* 11.4 (2018), pp. 970–978.

[49]   Steven E Sloop, John B Kerr, and Kim Kinoshita. "The role of Li-ion battery electrolyte reactivity in performance decline and self-discharge". In: *Journal of power sources* 119 (2003), pp. 330–337.

[50]   Eduardo Redondo-Iglesias, Pascal Venet, and Serge Pelissier. "Global model for self-discharge and capacity fade in lithium-ion batteries based on the generalized eyring relationship". In: *IEEE Transactions on Vehicular Technology* 67.1 (2017), pp. 104–113.

[51]   Rachid Yazami and Yvan F Reynier. "Mechanism of self-discharge in graphite–lithium anode". In: *Electrochimica Acta* 47.8 (2002), pp. 1217–1223.

[52]   Takashi Utsunomiya et al. "Self-discharge behavior and its temperature dependence of carbon electrodes in lithium-ion batteries". In: *Journal of power sources* 196.20 (2011), pp. 8598–8603.

[53]   Albert H Zimmerman. "Self-discharge losses in lithium-ion cells". In: *IEEE Aerospace and Electronic Systems Magazine* 19.2 (2004), pp. 19–24.

[54]   Caiping Zhang et al. "A generalized SOC-OCV model for lithium-ion batteries and the SOC estimation for LNMCO battery". In: *Energies* 9.11 (2016), p. 900.

[55]   Qishui Zhong et al. "Experimental study on relationship between SOC and OCV of lithium-ion batteries". In: *International Journal of Smart Grid and Clean Energy* 3.2 (2014), pp. 149–153.

[56]   Cyril Truchot, Matthieu Dubarry, and Bor Yann Liaw. "State-of-charge estimation and uncertainty for lithium-ion battery strings". In: *Applied Energy* 119 (2014), pp. 218–227.

[57]   Andrew Weng, Jason B Siegel, and Anna Stefanopoulou. "Differential voltage analysis for battery manufacturing process control". In: *Frontiers in Energy Research* 11 (2023), p. 1087269.

[58]   Lena Spitthoff et al. "Incremental capacity analysis (dQ/dV) as a tool for analysing the effect of ambient temperature and mechanical clamping on degradation". In: *Journal of Electroanalytical Chemistry* 944 (2023), p. 117627.

[59]   David Anseán et al. "Lithium-ion battery degradation indicators via incremental capacity analysis". In: *IEEE Transactions on Industry Applications* 55.3 (2019), pp. 2992–3002.

[60]   Matthieu Dubarry and David Anseán. "Best practices for incremental capacity analysis". In: *Frontiers in Energy Research* 10 (2022), p. 1023555.

[61]   Linfeng Zheng et al. "Incremental capacity analysis and differential voltage analysis based state of charge and capacity estimation for lithium-ion batteries". In: *Energy* 150 (2018), pp. 759–769.

Appendix

A Project planing and progression

As the project runs over a single semester, careful considerations to time management were a key factor to success. The start of the semester focused on the preliminary work for this project, and can be found in attachment F. This preliminary work included cooperation agreements both internally, and externally for FREYR. An outline of the project tasks and goals also had to be made. This is done to tighten the project, and make it befitting of the timeline and scope of a bachelor's degree. In this work, considerations were made in terms of what could be standardized and what can be left for further work. This allowed the project to have a narrower scope and focus on how differential voltage analysis could be used to determine self discharge in LIBs. In relation to this work, a poster was made to give a brief, easily explained overview of the project. This poster can be found in attachment E. As the semester progressed, the problem formulation had to be changed to how analysis tools could be used to identify contamination in LIBs

A Gant chart was made to give a clear timetable of tasks and deadlines. For the students involved in this project, this allowed for better time management and a clear overview of work needed to be done to reach milestones. Another tool used to keep track of the practical part of the project was a battery Excel sheet, see attachment D. With this sheet, the students could keep track of the produced batteries, entering their type, weight, and noting irregularities. The sheet also calculated capacity and the amount of contamination needed in each battery. This documentation also goes a long way to prove the work and effort invested into the project for it to succeed.

For this, project a risk assessment was also central for work to begin. This assessment can be found in the preliminary project (F). The risk assessment gave way to important considerations in the lab work, as the most important thing in the lab is to stay safe. Even though the lab work itself was deemed safe and mostly low danger, there are many toxic products in the lab, and training on both equipment and handling of products had to be conducted. This battery production training lasted for 2–3 weeks before the attempt on batteries to use in the report were made.

B Datasheet LFP and NCM

The included datasheet contains information specifying cell characteristics. This includes cathode and anode compositions for LFP and NCM111 which has been refered to as NMC111 in the thesis. The datasheet sets the basis of cycling, specifying voltage range and capacity.

Cells information
LiFUN+

	Item	402035-S225290A	402035-S225290B
Cathode	Material	NCM111	LFP
	Active material ratio	96.4%	96.5%
	Press density (g/cc)	3.3	2.4
	Coating Weight (mg/cm2)	15	16
Anode	Material	AG	
	Active material ratio	95.7%	
	Press density (g/cc)	1.5	
	Coating Weight (mg/cm2)	7.7	

Cells information
LiFUN+

Item	402035-S225290A	402035-S225290B
Voltage range (V)	3.0~4.2v	2.5~3.65v
Capacity (mAh)	200	200
Electrolyte (g)	1.0	1.5
Assembly type	Winding structure	Winding structure
Formation	80 ± 5℃ & 1 MPa 1. Standing 3min 2. 0.2C, CC to 3.4V, 15min 3. Standing 3min 4. 0.5C, CC to 4.1V, 80min	55 ± 5℃ & 0.8 MPa 1. Standing 3min 2. 0.01C, CC to 3.2V, 5min 3. 0.05C, CC to 3.65V, 10min 4. 0.1C, CC to 3.65V, 30min 5. 0.5C, CC to 3.65V, 180min

C   Faulty electrolyte

During the course of the bachelor thesis, 130 non-working battery cells were created. The reason behind this was a non-working electrolyte that did not wett properly. Presented in Figure C.1 is the difference in wetting capability for the faulty electrolyte, on the right, and a working electrolyte, on the left. The fault in the electrolyte was discovered late in the thesis.
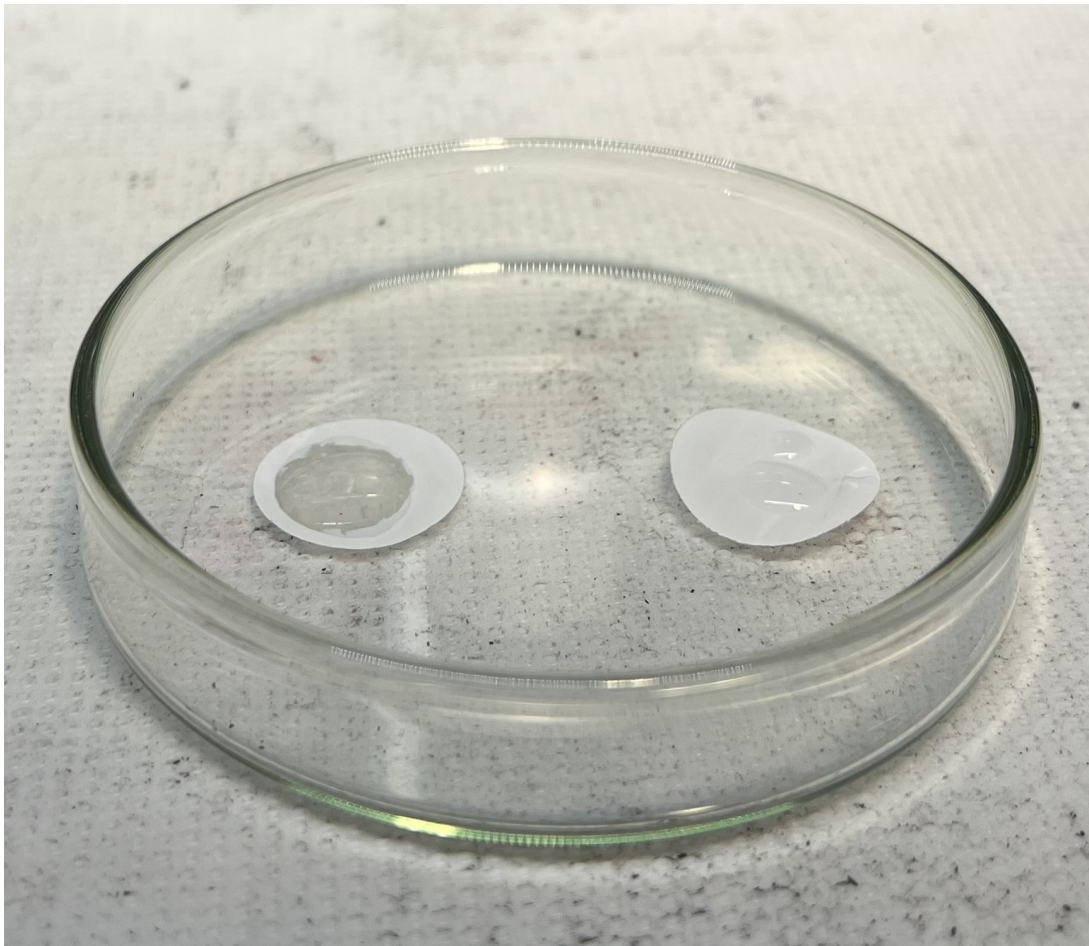

Figure C.1: *Picture taken of the different electrolytes in contact with separator. The right separator is applied with the electrolyte the group worked with from the start, while the left separator is applied a working electrolyte.*

D Battery documentation

Battery ID	Type	Cont.	1% cont. amt.	Channel	Date	Time	Succ. form.	Int. voltage (V)	Voltage A,W(V)	Weight AM	Weight (mg) [Cal]	Weight (mg) [An]	Cap (mAh) [Cal]	Cap (mAh) [An]	Note
0,7	LCO	Nei	0	5,3	03/05/2024	14:15	Ja		0	0	33,2	29	5,7768	5,046	Tester på nytt for å sjekke formation
0,7	LCO	Nei	0	5,5	29/2/2024		Ja				33,2	29	5,7768	5,046	
0,9	LCO	Nei	0	2,6	03/05/2024	14:13	Ja				33,2	29	5,7768	5,046	Tester på nytt for å sjekke formation
0,9	LCO	Nei	0	2,6	29/2/2024		Ja				33,2	29	5,7768	5,046	
1	LCO	Nei	0	5,3	03/08/2024	13:00	Nei			0,089	33,2	29	5,7768	5,046	
2	LCO	Nei	0	5,5	03/08/2024	13:00	Nei		1,34		33,2	29	5,7768	5,046	
3	LCO	Nei	0	4,1	03/08/2024	13:00	Nei		0,057		33,2	29	5,7768	5,046	
4	LCO	Nei	0	4,4	03/08/2024	13:00	Nei	-0,09	0,13		33,2	29,7	5,829	5,1678	
5	LCO	Nei	0	4,5	03/08/2024	13:00	Ja	0	0,066		33,2	29	5,7768	5,046	
6	LCO	Nei	0	2,5	03/08/2024	13:00	Ja	0	0,038		33,2	29	5,7768	5,046	
7	LCO	Nei	0										0	0	
101	LCO	Nei	0	2,2	03/08/2024	12:49	Nei	-0,08	0,057	0,0	33,5	28,4	5,829	4,9416	cathode side
102	LCO	Nei	0	2,6	03/08/2024	12:52	Nei	0	0	0,0	32,9	28,9	5,7246	5,0286	Use of 102 micro I on the anode side. Spilled som electrolyte because of separator rearrengement
103	LCO	Nei	0	2,2	03/04/2024	15:00	Nei	0,04	0,07	0,0	33,2	28,8	5,7768	5,0112	
104	LCO	Nei	0	2,6	03/04/2024	15:11	Nei	0,1	0,019	0,0	32,5	28,7	5,655	4,9938	Tester på nytt for å sjekke formation
105	LCO	Nei	0	2,6	03/08/2024	12:57	Nei	-0,99	0,05	0,0	34,1	29,3	5,9334	5,0982	
106	LCO	Nei	0	5,3	03/04/2024	15:19	Nei	0	0,04	0,0	33	29,1	5,742	5,0634	
107	LCO	Nei	0	5,5	03/04/2024	15:23	Nei	-0,09	0,07	0,0	33,5	29,7	5,829	5,1678	
201	LCO	Nei	0	2,2	03/11/2024	15:15	Nei	0	0,051	0,0	33,4	30,1	5,9856	5,2374	
202	LCO	Nei	0	2,5	03/11/2024	15:15	Nei	0	0	0,0	35	30,1	6,09	5,2374	
203	LCO	Nei	0	2,5	03/11/2024	15:15	Nei	0,08	0,019	0,0	34,7	30,4	6,0378	5,2896	
204	LCO	Nei	0	2,6	03/11/2024	15:15	Nei	0	0,008	0,0	34,2	30,7	5,9508	5,3418	
205	LCO	Nei	0	4,4	03/11/2024	15:15	Nei	0,03	0,075	0,0	34,4	30,1	5,9856	5,2374	
206	LCO	Nei	0	4,5	03/11/2024	15:15	Nei	-0,04	0,093	0,0	34,6	28,8	6,0204	5,0112	Skadet anode, flipped i prosessen, kan ha mistet elektrolytt
207	LCO	Nei	0	5,3	03/11/2024	15:15	Nei	0,04	0,003	0,0	34,2	29,5	5,9508	5,133	Skadet anode
nycelle005	LCO	Nei	0	2,2	03/05/2024	14:13	Ja	0,04	0,049	0,0	33,2	29	5,7768	5,046	Tester på nytt for å sjekke formation
nycelle005	LCO	Nei	0	5,3	29/2/2024		Ja			0,0	33,2	29	5,7768	5,046	
301	Lithium metal	Nei	0	2,2	18/03/2024	14:39	Nei	-2,7	1,300	0,0	27,7	26,8	0	5,0286	Lithium som katode :(
302	Lithium metal	Nei	0	2,6	18/03/2024	14:41	Nei	-2,7	1,280	0,0	28,4	26,8	0	5,2	Lithium som katode :(
303	Lithium metal	Nei	0	2,5	18/03/2024	14:43	Nei	-2,4	1,470	0,0	28,3	27,5	0	5,2	Lithium som katode :(
304	Lithium metal	Nei	0					-0,3		0,0	28,2	27,3	0	5,18	Lithium som katode :(
305	Lithium metal	Nei	0					-3,02		0,0	27,9	27,5	0		Lithium som katode :(
306	Lithium metal	Nei	0					-3,03		0,0	23	26,8	0		Lithium som katode :(
307	Lithium metal	Nei	0					-3,02		0,0	23	26,9	0		Lithium som katode :(
308	Lithium metal	Nei	0					-2,6		0,0	22,2	26,7	0		Lithium som katode :(
309	Lithium metal	Nei	0					-2,94		0,0	23,3	26,6	0		lithium som katode :(
310	Lithium metal	Nei	0					-2,94		0,0	23,1	27,2	0		lithium som katode :(
401	LFP	Nei	0	2,2	27/03/2024	14:00	Nei	0,04	0	28,5	34,2	26,4	6,84	5,28	
402	LFP	Nei	0					0,04	0,049	29,1	34,8	26	6,96	5,2	
403	LFP	Nei	0					0	0	30,8	36,6	25,9	7,32	5,18	
404	LFP	Nei	0	2,3	21/03/2024	14:00	Nei	0,12	0,26	31,5	37,3	25,8	7,46	5,16	Litt skadet med elektrolyttsøl
405	LFP	Nei	0					0	0	30,6	36,4	26	7,28	5,2	
406	LFP	Nei	0					0	0	30,8	36,6	25,9	7,32	5,18	
407	LFP	Nei	0	2,4	21/03/2024	14:00	Nei	0,08	0,17	30,3	36,1	26,4	7,22	5,28	
408	LFP	Nei	0					0	0	31,1	36,9	25,6	7,38	5,12	Litt skadet med elektrolyttsøl
501	Li×LCO	Nei	0	11,1	22/03/2024		Nei	3	1,82	0,0	36,1	24,2	6,2814	4,2108	Litt skadet med elektrolyttsøl
502	Li×LCO	Nei	0	11,2	22/03/2024		Nei	2,94	1,48	0,0	36,1	22,6	6,2814	3,9324	
503	Li×LCO	Nei	0	11,3	22/03/2024		Nei	0,83	1,32	0,0	35,7	29,1	6,0634	5,0634	
504	Li×LCO	Nei	0	11,4	22/03/2024		Nei	2,88	3,02	0,0	35,2	22,9	6,2118	3,9846	
505	Li×LCO	Nei	0	11,5	22/03/2024		Nei	3,09	3	0,0	35,7	21,6	6,2118	3,7584	
506	Li×LCO	Nei	0	11,7	22/03/2024		Nei	3	2,8	0,0	35,4	29,2	6,1596	5,0808	
507	Li×LCO	Nei	0	11,6	22/03/2024		Nei	2,85	2,03	0,0	34,1	27,2	5,9334	4,7328	
601	NMC	Nei	0	11,8	22/03/2024		Nei	0,08	0,127	27,2	32,9	26,3	6,58	5,26	
602	NMC	Nei	0				Nei	0	0	26,7	32,4	26,4	6,48	5,28	
603	NMC	Nei	0	12,1	22/03/2024		Nei	0,11	0,05	26,3	32	26,6	6,4	5,32	
604	NMC	Nei	0					0	0	26,5	32,2	26,4	6,44	5,28	
605	NMC	Nei	0					0	0	27,5	33,2	26,6	6,64	5,32	
606	NMC	Nei	0					0	0	27,1	32,8	26	6,56	5,2	
607	NMC	Nei	0					0,06	0,008	27,1	32,8	26,6	6,56	5,32	
608	NMC	Nei	0	12,3	22/03/2024		Nei	0	0,0012	27,0	32,7	26,7	6,54	5,34	
609	NMC	Nei	0	12,4	22/03/2024		0	0,05	0,084	27,5	33,2	27,3	6,64	5,46	

Prøve	Kjemi	Vasket	Li-verdi	Måling / Dato	Skadet	V1	V2	V3	V4	V5	V6	V7	Kommentar
610	NMC	Nei	0	12,5 22/03/2024		0,1	0,044	27,5	33,2	26,5	6,64	5,3	
611	NMC	Nei	0	12,6 22/03/2024		0	0	26,6	32,3	26,5	6,46	5,3	
612	NMC	Nei	0	12,7 22/03/2024		0	0	27,7	33,4	27,2	6,68	5,44	
613	NMC	Nei	0	12,6 22/03/2024	Nei	0,02	0,002	28,4	34,1	27,6	6,82	5,52	
614	NMC	Nei	0	12,7 22/03/2024	Nei	0,08	0,007	27,4	33,1	27,5	6,6	5,5	
615	NMC	Nei	0	12,8 22/03/2024	Nei	0,09	0,014	27,3	33	26	6,6	5,2	anode litt skadet på aktivt material siden
701	Li x LFP	Nei	0	11,1 24/03/2024		1,72	2,51	33,2	39,1	23,6	7,82	4,72	spring
702	Li x LFP	Nei	0	11,2 24/03/2024		3,1	1,52	30,0	35,8	23,2	7,16	4,64	Ingen spring
703	Li x LFP	Nei	0	11,3 24/03/2024		2,11	1,73	30,4	36,2	23,3	7,24	4,66	Ingen spring
704	Li x LFP	Nei	0	11,4 24/03/2024		2,18	2,1	29,9	35,7	27,5	7,14	5,5	Ingen spring
705	Li x LFP	Nei	0	11,5 24/03/2024		2,83	2,2	30,3	36,1	23,3	7,22	4,66	Ingen spring
706	Li x LFP	Nei	0	11,6 24/03/2024		2,18	1,06	30,4	36,2	23	7,24	4,6	Ingen spring
707	Li x LFP	Nei	0	11,7 24/03/2024		2,89	2,7	29,7	35,4	27,5	7,08	5,5	
708	Li x LFP	Nei	0	11,8 24/03/2024		1,44	0,79	29,7	35,4	22,3	7,08	5,5	
709	Li x LFP	Nei	0	12,1 24/03/2024		3,26	3,1	29,8	35,5	27,5	7,1	5,5	
801	LFP	Nei	0	12,2 25/03/2024		0,01	0,12	29,2	34,9	26,2	6,98	5,24	en spacer, en spring
802	LFP	Nei	0	12,3 25/03/2024		0,094	0,157	29,5	35,2	27,1	7,04	5,42	en spacer, en spring
803	LFP	Nei	0	12,4 25/03/2024		0,0059	0,1	29,6	35,3	26,7	7,06	5,34	en spacer, en spring
804	LFP	Nei	0	12,5 25/03/2024		0,005	0,05	29,9	35,6	26,6	7,12	5,32	en spacer, en spring
805	LFP	Nei	0	12,6 25/03/2024		0,0315	0,07	29,8	35,5	26,8	7,1	5,36	en spacer, en spring
901	Li x LFP	Nei	0	12,7 25/03/2024		3,14	3,2	29,5	35,2	22,2	7,04	4,44	en spacer, en spring
902	Li x LFP	Nei	0	12,8 25/03/2024		3,059	3,1	29,1	34,8	27,4	6,96	5,48	en spacer, en spring
903	Li x LFP	Nei	0	10,3 25/03/2024		3,25	3,25	29,1	34,8	22,9	6,96	4,58	en spacer, en spring
904	Li x LFP	Nei	0	10,4 25/03/2024		3,08	3,1	29,7	35,4	27,4	7,08	5,48	en spacer, en spring
905	Li x LFP	Nei	0	10,5 25/03/2024		3,18	3,2	29,7	35,4	27,1	7,08	5,42	en spacer, en spring
1001	Li x NMC	Nei	0	2,2 08/04/2024		2,2	1,6	27,8	33,5	27,4	6,7	5,48	en spacer, en spring
1002	Li x NMC	Nei	0	2,3 08/04/2024		2,3	2,1	27,0	32,7	27,5	6,54	5,5	en spacer, en spring
1003	Li x NMC	Nei	0	2,4 08/04/2024		2,4	3,1	27,1	32,8	22,4	6,56	4,48	Laget fra ferdig rengjort NMC ark
1004	Li x NMC	Nei	0	2,5 08/04/2024		2,5	3	27,8	33,5	22,8	6,7	4,56	Laget fra ferdig rengjort NMC ark
1005	Li x NMC	Nei	0	2,6 08/04/2024		2,6	1,7	27,5	33,2	23,4	6,64	4,68	Laget fra ferdig rengjort NMC ark
1006	Li x NMC	Nei	0	2,7 08/04/2024		2,7	2,8	27,8	33,5	27,9	6,7	4,56	Laget fra ferdig rengjort NMC ark
1007	Li x NMC	Nei	0	11,1 08/04/2024		3	3	27,2	32,9	27,8	6,58	5,56	Laget fra ferdig rengjort NMC ark
1008	Li x NMC	Nei	0	11,2 08/04/2024		3,1	2,8	22,8	33	22,5	6,56	4,5	Laget fra ferdig rengjort NMC ark
1009	Li x NMC	Nei	0,0441341	11,2 08/04/2024		3,1	3	33	33	28,2	6,6	5,64	Laget fra ferdig rengjort NMC ark
1010	Li x NMC	Nei	0	11,4 08/04/2024		11,3	3	27,1	32,8	23,6	6,56	5,48	Laget fra ferdig rengjort NMC ark
1101	Li x NMC	Ja	0,0441341	11,3 08/04/2024		2,8	3	27,3	33	23,1	6,6	4,62	Laget fra ferdig rengjort NMC ark
1102	Li x NMC	Ja	0,0441341	11,4 08/04/2024	Nei	3,1	3,1	27,3	33	23,1	6,6	4,56	Laget fra ferdig rengjort NMC ark
1103	Li x NMC	Ja	0,0441341	4,5 08/04/2024	Nei	3,1	3,1	27,3	33	23	6,6	4,6	Laget fra ferdig rengjort NMC ark
1104	Li x NMC	Ja	0,0441341	5,3 08/04/2024	Nei	3,1	3,1	27,3	33	22,8	6,56	4,56	Laget fra ferdig rengjort NMC ark
1105	Li x NMC	Ja	0,0441341	5,5 08/04/2024	Nei	3,1	3,1	27,3	33	23,1	6,6	4,62	Laget fra ferdig rengjort NMC ark
1106	Li x NMC	Ja	0,0441341	5,6 08/04/2024	Nei	1,7	1,7	27,5	33,2	22,4	6,64	4,48	Laget fra ferdig rengjort NMC ark
1107	Li x NMC	Ja	0,0441341	11,5 08/04/2024	Nei	3,1	3,1	27,0	32,7	22,5	6,54	4,5	Laget fra ferdig rengjort NMC ark
1108	Li x NMC	Ja	0,0441341	11,6 08/04/2024	Nei	3,1	3,1	26,9	32,6	27,8	6,52	5,56	Laget fra ferdig rengjort NMC ark
1109	Li x NMC	Ja	0,0441341	11,7 08/04/2024	Nei	3,1	3,1	26,9	32,6	22,5	6,52	4,5	Laget fra ferdig rengjort NMC ark
1110	Li x NMC	Ja	0,0441341	11,8 08/04/2024	Nei	3,1	3,1	26,5	32,2	27,8	6,44	5,56	Laget fra ferdig rengjort NMC ark
1201	Li x NMC	Nei	0,0441341	2,2		3,1		27,3	33	27,5	6,6	5,5	
1202	Li x NMC	Nei	0	2,3				27,6	33,3	23,4	6,66	4,68	
1203	Li x NMC	Nei	0	2,4				26,7	32,4	23,2	6,48	4,64	
1204	Li x NMC	Nei	0	2,5				26,8	32,5	27,8	6,5	5,56	
1205	Li x NMC	Nei	0	2,6				26,7	32,4	27,6	6,48	5,52	
1206	Li x NMC	Nei	0	2,7				26,4	32,1	23,8	6,42	4,76	
1207	Li x NMC	Nei	0	2,8				26,3	32	27,7	6,4	5,54	
1208	Li x NMC	Nei	0	5,3				26,9	32,6	28,2	6,52	5,64	
1209	Li x NMC	Nei	0	5,5				26,3	32	27,5	6,4	5,5	
1210	Li x NMC	Nei	0	5,6				26,5	32,2	23,1	6,44	4,62	
1301	Li x NMC	Ja	0,0441341	4,4				26,5	32,2	22,1	6,44	4,62	
1302	Li x NMC	Ja	0,0441341	4,5				26,8	32,5	22,5	6,5	4,5	
1303	Li x NMC	Ja	0,0441341	12,1				26,9	32,6	22,3	6,52	4,46	
1304	Li x NMC	Ja	0,0441341	12,2				26,8	32,5	22,3	6,5	4,46	
1305	Li x NMC	Ja	0,0441341	12,3				26,5	32,2	22,2	6,44	4,44	
1401	NMC	Nei	0	12,4				26,5	32,2	26,2	6,44	5,24	

E Poster

Predicting self-discharge in LIBs

Birk Lillebo, Lars Fredrik Hansen, Markus Hatlo

Internal supervisor: Professor Odne Stokke Burheim

External supervisor: Senior battery design engineer at FREYR Daniel Tevik Rogstad

Project description

Working title:

"Investigations on the accuracy of DVA anlysis as a measure for predicting self-discharge in LIBs"

This project is based upon how differential voltage analysis can be used as a measure for predicting self discharge.

To understand this connection, coin-cell batteries will be produced, and in a portion of the batteries metal powder will be introduced to heighten self-discharge. The recorded data from the formation process will be analyzed.

To verify our theoretical data predictions, the project will include a post storage test to inspect the practical self discharge.
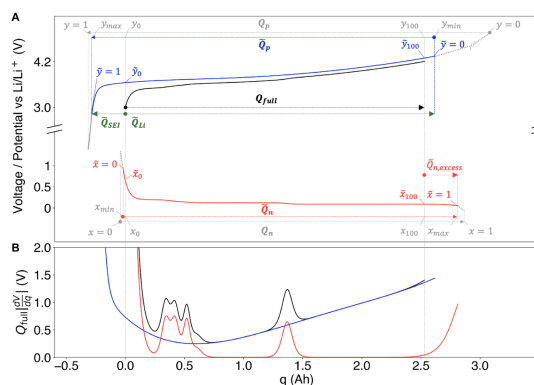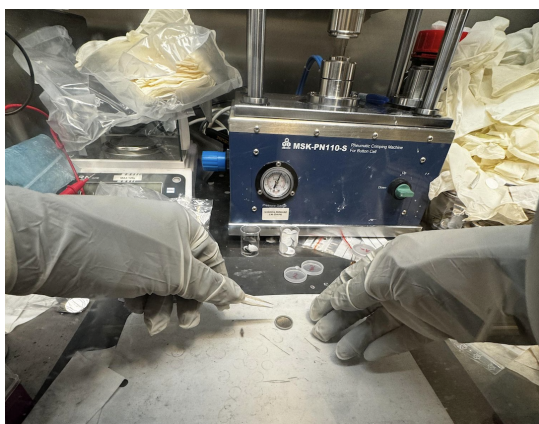
Goals

- Use of DVA to predict self discharge

- Shortened battery storage time

- Deeper understanding of LIB production

LIBLab

In the lithium ion battery lab, the group uses commercial electrodes as a base for button cells.

The electrodes are split into anode and cathode where the active material of one side is washed off.
Button cell sized leafs are punched out and assembled in the glove box.

FREYR

Freyr is a Norwegian battery company, with a focus on large scale sustainable battery production. Freyr are located in Mo i Rana and are opening a new factory in the USA. They work on energy storage systems and eletrical vehicles. Freyr also has a large portion dedicated to researching new technology

F   Preliminary project

FENT2900 - Bachelor´s Thesis,
Renewable Energy Engineering

Preliminary project

Birk Ferdinand Lillebo
Lars Fredrik H. Hansen
Markus Hatlo

Spring 2024

NTNU Norwegian University of Science and Technology
Department of Energy and Process Engineering

Preliminary project for bachelor thesis

The Thesis Working Title:	Field of Study
English:	Engineer, Renewable Energy
Investigations on the accuracy of DVA analysis as a measure for predicting self-discharge in LIBs	
Norwegian:	
Undersøkelser om nøyaktigheten av DVA-analyse som et vektøy for å forutsi selvutladning i LIBer	
Project Number	**Due Date**
24BIFOREN24-08	21.05.24
Group Participants	**Principal**
Birk Ferdinand Lillebo	FREYR
Lars Fredrik H. Hansen	
Markus Hatlo	
Internal Supervisor	**External Supervisor**
Odne Stokke Burheim	Daniel Tevik Rogstad
odne.s.burheim@ntnu.no	daniel.rogstad@freyrbattery.com
	454 64 006

Preface

This preliminary project lays the groundwork for a bachelor´s thesis. The bachelor´s thesis is made in spring 2024 by three third year students, forming the group 24BIFOREN-08 at NTNU. The students have backgrounds in renewable energy engineering and specializations in water and wind energy, and energy storage.

The preliminary project was prepared in january and february 2024. The goal of the preliminary project is to plan the work and execution of the bachelor project. The work has lead to discussions and started the groups work on defining the working title, problem definition, goals and progress plan.

The problem definition has been formulated and produced by the group members in collaboration with FREYR and the internal supervisor. A big thanks therefore goes to Daniel Tevik Rogstad at FREYR for providing the group with this opportunity. The group also wants to thank internal supervisor, professor Odne Stokke Burheim at the institute of energy and process engineering, and post doctorate Ejikeme Raphael Ezeigwe for providing direction, insight and interest in the project.

Contents

1 Introduction

This is the preliminary work for a bachelor's thesis and will present the contributors, the approach to the work and the aims of the thesis. The assignment is about improving the process of making lithium-ion batteries using DVA analysis. The client for this assignment is Freyr, and the supervisors are from the Department of Energy and Process Engineering at NTNU.

1.1 Background

Freyr is a battery company focusing on environmentally friendly, large-scale, and efficient production. During the production of batteries, the aging process is the most time consuming. It can take up to three weeks for a battery to complete aging. Additionally, an analysis of the batteries must conducted to determine parameters such as np-ratio, lithium consumption, and battery capacity. Often, these analysis methods can be destructive as it involves opening the cell. This presents an opportunity for optimization that Freyr is interested in. dV/dQ analysis, or Differential Voltage Analysis, is a non-destructive analysis method that can be performed during the formation stage of the battery. This analysis can provide us with both np-ratio, lithium consumption, and battery capacity. Furthermore, it is a mostly underutilized method in the battery industry. Freyr is keen to explore this analysis method, and if the bachelor's thesis concludes that the analysis is both accurate and time-saving, Freyr will consider adopting it.

1.2 Limitations and assumptions

It has been chosen to perform a mostly standard production and formation of the batteries. The analysis has been limited to only one anode materials and three cathode materials. In addition, the c-rate of the formation process has been limited to C/20. This is a compromise between speed and accuracy. The degradation has been limited to a maximum of 4 weeks. A longer degradation time will be to time consuming. These limitations have been set in order to complete the task within the time frame, as more variables will generate more data that takes longer to analyse. Additionally more variables will makes it more difficult to find decisive results.

1.3 Project members

Lars Fredrik Hansen (him)
Phone: 949 76 665
Email: lfhansen@ntnu.no
Third year at bachelor in renewable energy, with an immersion in wind and water energy.
Competence within renewable energy, electrical engineering, mathematics, physics, chemistry, electrical power systems, mechanics, thermodynamics, electrical machines and electromechanical energy conversion, heat and mass transfer, energy storage, fluid mechanics, wind energy, project managment, materials technology, and programming.

Birk Ferdinand Lillebo (him)

Phone: 949 84 030

Email: birk.lillebo@ntnu.no

Third year at bachelor in renewable energy, with an immersion in energy storage.

Competence within renewable energy, electrical engineering, mathematics, physics, chemistry, electrical power systems, mechanics, thermodynamics, electrical machines and electromechanical energy conversion, heat and mass transfer, energy storage, fluid mechanics, wind energy, control engineering, and programming.

Markus Hatlo (him)

Phone: 413 36 740

Email: markhat@stud.ntnu.no

Third year at bachelor in renewable energy, with an immersion in energy storage.

Competence within renewable energy, electrical engineering, mathematics, physics, chemistry, electrical power systems, mechanics, thermodynamics, electrical machines and electromechanical energy conversion, heat and mass transfer, energy storage, fluid mechanics, wind energy, control engineering, and programming.

1.4   Project contributers

Daniel Tevik Rogstad (Freyr)

Odne Stokke Burheim (NTNU)

Ejikeme Raphael Ezeigwe (NTNU)

2   Goals and framework

2.1   Orientation

This assignment was chosen because the group members wanted to work with lithium-ion batteries. After the subject was decided, next the group looked for companies to contact. FREYR came up quickly due to them being a leading battery company in Norway. The original assignment of investigating additives and determining a practical NP ratio came from FREYR and was inspired from the article, "Differential voltage analysis for battery manufacturing process control". Further the assignment was discussed between all participating members and Odne Burheim suggested to rather look at the self discharge of the batteries.

2.2   Problem definition

English:
This project is based upon how differential voltage analysis can be used as a measure for predicting self discharge. By such analysis, the thesis aims to shorten production and storage time. To understand this connection, coin-cell batteries will be produced, and in a portion of the batteries metal powder will be introduced to heighten self-discharge. The recorded data from the formation process will be analyzed. To verify our theoretical data predictions, the project will include a post storage test to inspect the practical self discharge. Further process improvements will consist of insuring accuracy and efficiency.

Norwegian:
Dette prosjektet er basert på hvordan differensialspenningsanalyse kan brukes for å forutsi selvutladning. Gjennom en slik analyse har oppgaven som mål å forkorte produksjons- og lagringstiden. For å forstå denne sammenhengen, vil knappcellebatterier bli produsert, og i en andel av batteriene vil det bli introdusert metal pulver for å øke mengde selvutladning. Dataene som er registrert under formasjonsprosessen vil bli analysert. For å bekrefte de teoretiske resultatene, vil prosjektet inkludere en test etter lagring for å inspisere den praktiske selvutladningen. Videre forbedringer i prosessen vil bestå av å sikre nøyaktighet og effektivitet.

2.3   Specifications

Instead of using complete pouch cell batteries, coin-cells will be produced from existing electrodes. This is both to increase the number of batteries and because coin-cells give more accurate results. LCO, LFP and lithium metal will be used as cathode materials. The metal powder will be used to make sure that some of the batteries have significantly higher self-discharge than the others, thus making them easier to differentiate.

2.4   Performance measures

The following sections defines the goals set for this bachelors thesis.

2.4.1   Result

The resulting discussion and conclusion concerning DVA-analysis will allow Freyr to consider the analysis method for usage on future batteries.

3

2.4.2   Process

The team will gain a greater understanding on how to create and analyze batteries, as well as a better understanding of batteries as a whole. Finally the process will teach the team how to work on similar tasks in the future.

2.4.3   Effect

The bachelor will give a greater understanding on the accuracy of DVA-analysis for predicting self-discharge. This in turn can shorten production and storage time for the battery production as a whole. Further, the cutting of storage time will result in a decrease of energy requirement per battery, and a reduction of storage area and cost.

2.5   Framework

This project requires the use of NTNUs battery lab. The research will use LCO and LFP batteries, which will be supplied by NTNU. The team will need time in the lab to practice making button cell batteries. After the button cell batteries are made, a storage time of two weeks and equipment to collect data is needed.

3 Approach

3.1 Phase 1: Startup

- Sign deal with Freyr, group members and supervisor
- Sign an internal cooperation agreement
- Read up on subject matter
- Define and limit the task
- HSE safety courses are carried out and a safety assessment is made.
- Lab tour with supervisor.

3.2 Phase 2: Preparations for data collection

- Group members practice making button cell batteries from pouch cell batteries. The most important factor is that the results are reproducible
- First draft of the code to process data is produced

3.3 Phase 3: Data collection and analysis

- Button cell batteries are produced
- During the formation, the voltage data is obtained
- The code to analyze the data is completed
- The batteries are stored for two weeks
- After two weeks, the self-discharge of the batteries is recorded
- The data from the formation process is analyzed in the form of DVA (DV/DQ).
- The data from DVA and self-discharge are compared and it is investigated whether there are connections that can predict which battery will self-discharge the most
- The statistical significance of the results are examined

3.4 Phase 4: Report writing

- Making discussion and conclusion
- Making first draft
- Proof reading
- Final thesis
- Making final presentation

3.5   Milestones

Official dates for different deliverables

What	When
Submission of agreement	22.12.2023
Submission of preliminary project	09.02.2024
Submission of poster	04.03.2024
First presentation	09.04.2024
Submission of the final report (via Inspera)	21.05.2024
Final presentation	23-24.05.2024

3.6   Quality assurance and reporting

It is important for the group that the result of the project is of a high quality. This is ensured by having regularly meetings with supervisors and contributors. Meetings with the supervisors happen on a weekly basis, where progress is discussed and any possible problems are addressed. About every third week there is a meeting with the supervisors and the outside contributors, where the progress is presented and feedback is given. The group also has internal meetings every week, to discuss what needs to be done, and resolve any conflicting opinions. Lastly the quality of the lab work is ensured through good training by the supervisors, and a practice period where the group members battery making skills are improved.

Appendix

A Gant chart

I

FENT2900 Bachelors Thesis Renewable Energy Engineering

Where	NTNU Trondheim
Start date for project:	01.01.2024

Description	Important deadlines	1	2	3	4	5	6	7	8	9	10	11	12	13	14	15	16	17	18	19	20	21	22
		January				February				March				April				May					
Phase 1: Start up																							
Sign data with FREYR, group members and supervisor	22.12.23																						
Sign internal cooperation contract																							
Read up on subject matter																							
Define and limit project																							
HSE safety course and risk assesment																							
Preliminary project	09.02.24																						
Phase 2: Preparation for data collection																							
Practise making button cell batteries																							
Produce draft for data processing code																							
Poster	04.03.24																						
Phase 3: Data collection and analysis																							
Complete code to analyse data																							
Produce button cell batteries and collect data																							
Store batteries and collect data from stored batteries																							
First presentation	09.04.24																						
The results are collected in a thesis																							
Phase 4: Report writing																							
Make discussion and conclusion																							
Draft	05.05.24																						
Proof reading																							
Final thesis	21.05.24																						
Make presentation																							
Presentation of bachelor's thesis	23-24.05.24																						

B   Risk assessment

NTNU

Organisatorisk enhet Institutt for energi og prosessteknikk (EPT)

Lokasjon Varmeteknisk battery lab

Utstyr / Aktivitet Glovebox, battery cycler, fume box

Dato 2024-02-09

Deltagere Birk Lillebo, Lars Fredrik Hansen, Markus Hatlo

Linjeleder Terese Løvås

Delaktivitet	Mulig uønsket hendelse	Eksisterende barrierer	Risikoverdi med eksisterende tiltak Menneske	Ytre miljø	Omdømme	Økonomi / materiell	Nye barrierer / risikoreduserende tiltak (handlingsplan)	Risikoverdi med nye tiltak Menneske	Ytre miljø	Omdømme	Økonomi / materiell	Ansvarlig	Dato	Status
The use NMP (N-Metyl-2-Pyrrolidon)	Get in the eye(s), Get on the	Using safety glasses	B2											
	Get on the skin	Use rubber gloves and lab coat	B2											
	Inhalation	Handling the substance under a fume hood	B2											
	Fire	Avoid heating it	B2											
	Get in the mouth and swallowing it	Do not touch face when handing substance	B1											
	Explosion	Avoid heating it	C1											
The use of Lithium iron phosphate (LiFePO4) and LCO (LiCoO2) extracted prefabricated electrodes	Get in the eye(s)	Using safety glasses	B2											
	Get on the skin	Use rubber gloves and lab coat	B2											
	Inhalation	Handling the substance under a fume hood	B2											
	Get in the mouth and swallowing it	Do not touch face when handing substance	B1											
	Fire		B2											
The glovebox	There is a leakage and the substance gets in the outside air. Also causing the atmosphere inside to be "infected".	All pressure gauges and indicators are functioning and are within acceptable ranges.	B1											
The use of the fume box	The ventilation is not working	Inspect prior to use, check if the ventilation is working.	B3											
Electrochemical characterization, battery cycling	Fire	Defined safety limits for the cycling of the batteries. Batteries tested inside fireproof cabinets.	B2			A2								
	Electrical shock	Avoid making contact with others electronic components of the machine	A2											
Battery (less than 10mAh)	Fire	Avoid opening, avoid overcharging and discharging	B2			A1								
Lithium metal	Fire	Only kept and used in glovebox	A1											
Electrolyte	exposure	Only kept and used in glovebox	A1											
LiPF6	exposure	Only kept and used in glovebox	A1											
EC ethylcarbonate	exposure	Only kept and used in glovebox	A1											
DMC dimethylcarbonate	exposure	Only kept and used in glovebox	A1											

Utstyr/aktivitet Glovebox, battery cycler, fume box
Dato 2024-02-09

MED EKSISTERENDE TILTAK

Menneske

		1		
5	3	10		
	1	1		

Ytre miljø

Omdømme

Økonomi / materiell

1				
	1			

ETTER NYE TILTAK

Menneske

Ytre miljø

Omdømme

Økonomi / materiell

III

C   Cooperation agreement

Cooperation Agreement

[Baklar Spring 2024]

Goals for Delivery, Well-Being and Learning

Delivery

1   We contribute to executing our areas of responsibility

We agree that everyone should contribute to the work of fulfilling our purpose and follow up on tasks from meetings. Everyone has a responsibility for their areas of responsibility and for updating each other and keeping group members informed about their work.

2   We arrive punctually and notify in case of abcense

Everyone arrives at the agreed time. If you are delayed, you inform the rest of the group in the chat. If more than 15 minutes late, the delayed member buys coffee/cocoa for the rest of the group. In case of recurring delays by an individual, the situation should be discussed collectively with the group.

3   We plan together and collaborate to achieve common goals

We start each office meeting by summarizing what has been done since the last meeting, where we go through the to-do list from the previous meeting and the upcoming calendar, before we plan and set goals for the coming week. After each meeting, we summarize the period since the last meeting and evaluate it. At the same time, we look at the major issues leading up to the next meeting. During the meetings, we can discuss any planned absences and ask each other for help with preparations and potentially stepping in for each other in case of excessive workload for any individual. The purpose is to ensure progress and encourage collaboration.

Well-Being

4   We work for a good atmosphere and give each other recognition

We want to have fun throughout this spring. It is easier and more motivating to work when there is a good atmosphere and energy in the group. We value laughter, good spirits, and give each other positive attention. We praise each other and strive for mutual trust.

5   We are open if we have a bad day, and we show consideration.

If one does not feel well on a day, we want them to notify, preferably at the beginning of the day. The group tries to consider the person having a bad day. The person experiencing a challenging day should also be mindful of their own behavior and demeanor in the work environment.

6   We set milestones and adhere to realistic deadlines.

Milestones are set at the beginning of the project, but we also work towards milestones established throughout the year. The purpose of this is to avoid excessive workload on each individual group member. It is important for the well-being of the group that everyone completes their part of the work on time.

2 av 3

V

7   Conflict resolution

In situations where we experience conflict within the group, it is important that we communicate before the irritation becomes too significant. We address this together. We act honestly, directly, and respectfully in the conflict. In the conflict, we listen to each other and try to interpret the others in the best possible way. In situations where it seems appropriate, a supervisor is included to have a neutral third party involved in the dialogue.

Learning

8   Constructive feedback

We provide each other with constructive feedback and evaluate the project collectively, allowing us to develop as much as possible. We communicate in a proper manner and facilitate an open dialogue in meetings. Most things can be communicated as long as it is done constructively and with good intentions.

9   We challenge ourselves, ask for help, and assist each other.

We will challenge each other to take on tasks we are not entirely comfortable with, in order to learn something new. Additionally, we will assist each other with the roles and responsibilities we have distributed among ourselves. This means both asking for help and offering help to others who are stuck, so that we can learn and support each other. This should be done in a low-threshold manner to help us achieve our common goals.

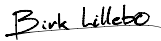## 10   We work for consensus and good compromises.

As far as possible, we will reach agreement on common decisions. In cases where we disagree, we will try to find good compromises and alternative solutions. We will be open to listening to each other's ideas and solutions. In disagreements, we will show consideration for each other, while distinguishing between the issue at hand and personal matters.

11   We evaluate the collaboration and revise the cooperation agreement.

We want to learn from the experiences we gain along the way. At the midpoint of the period, we evaluate the collaboration and the points in this collaboration agreement. Revision of the collaboration agreement can also be done if needed.

PLACE: TRONDHEIM   **DATE:** 09.02.2024

_____   _____
Birk F. Lillebo   **Lars Fredrik H. Hansen**

_____
Markus Hatlo

3 av 3

VI